

ผลของการตัดแปรสารอาหารต่อระดับลิพิดในไซยาโนแบคทีเรีย  
*Synechocystis* sp. PCC 6803 ที่มียีน *aas* แสดงออกเกินปกติ



บทคัดย่อและแฟ้มข้อมูลฉบับเต็มของวิทยานิพนธ์ตั้งแต่ปีการศึกษา 2554 ที่ให้บริการในคลังปัญญาจุฬาฯ (CUIR)  
เป็นแฟ้มข้อมูลของนิสิตเจ้าของวิทยานิพนธ์ ที่ส่งผ่านทางบัณฑิตวิทยาลัย

The abstract and full text of theses from the academic year 2011 in Chulalongkorn University Intellectual Repository (CUIR)  
are the thesis authors' files submitted through the University Graduate School.

วิทยานิพนธ์นี้เป็นส่วนหนึ่งของการศึกษาตามหลักสูตรปริญญาวิทยาศาสตรมหาบัณฑิต  
สาขาวิชาชีวเคมีและชีววิทยาโมเลกุล ภาควิชาชีวเคมี  
คณะวิทยาศาสตร์ จุฬาลงกรณ์มหาวิทยาลัย  
ปีการศึกษา 2558  
ลิขสิทธิ์ของจุฬาลงกรณ์มหาวิทยาลัย

EFFECT OF NUTRIENT MODIFICATION ON LIPID LEVEL  
IN CYANOBACTERIUM *Synechocystis* sp. PCC 6803 OVEREXPRESSING  
*aas* GENE

Miss Kamonchanock Eungrasamee



A Thesis Submitted in Partial Fulfillment of the Requirements  
for the Degree of Master of Science Program in Biochemistry and Molecular Biology

Department of Biochemistry

Faculty of Science

Chulalongkorn University

Academic Year 2015

Copyright of Chulalongkorn University



กมลชนก อึ้งรัศมี : ผลของการดัดแปรสารอาหารต่อระดับลิพิดในไซยาโนแบคทีเรีย *Synechocystis* sp. PCC 6803 ที่มียีน *aas* แสดงออกเกินปกติ (EFFECT OF NUTRIENT MODIFICATION ON LIPID LEVEL IN CYANOBACTERIUM *Synechocystis* sp. PCC 6803 OVEREXPRESSING *aas* GENE) อ.ที่ปรึกษา  
 วิทยานิพนธ์หลัก: ศศ. ดร. เสาวรัตน์ จันทะโร, อ.ที่ปรึกษาวิทยานิพนธ์ร่วม: ศศ. ดร. อรุณ อินเจริญศักดิ์, 141  
 หน้า.

ในการศึกษานี้ สายพันธุ์ *Synechocystis* sp. PCC 6803 ที่มีการแสดงออกเกินปกติของยีน *aas* (Ox-Aas) สร้างผ่านการเกิด single recombination โดย acyl-acyl carrier protein synthetase (AAS) เป็นเอนไซม์ที่สำคัญในกระบวนการนำกรดไขมันกลับมาใช้ ซึ่งเข้ารหัสโดยยีน *slr1609* หรือ *aas* ลำดับกรดอะมิโนของโปรตีน AAS ของ *Synechocystis* ประกอบด้วยสองบริเวณที่อนุรักษ์อย่างมากกับ acyl-ACP synthetase ของ *Arabidopsis thaliana* และ *Synechococcus* sp. PCC 7942 จากนั้นสืบค้นปัจจัยทางสรีรวิทยาที่รวมถึง การขาดสารอาหารและการเสริมอะซีเตตต่อระดับลิพิดรวมและลิพิดที่ไม่อิ่มตัวในสายพันธุ์ Ox-Aas และสายพันธุ์ปกติ (WT) ภายใต้สภาวะสูตรอาหาร BG<sub>11</sub> ปกติ พบว่าสายพันธุ์ Ox-Aas มีการเจริญและปริมาณรงควัตถุต่ำกว่า WT เพียงเล็กน้อย อย่างไรก็ตาม อัตราการเกิดออกซิเจนของ Ox-Aas สูงกว่า WT การค้นพบของเราแสดงการสะสมลิพิดของ Ox-Aas ที่สูงกว่าเมื่อเปรียบเทียบกับ WT ในทุกช่วงของการเจริญ ได้แก่ ระยะลือก (L), เลท-ลือก (LL) และระยะคงตัวช่วงเริ่มต้น (ES) ระดับลิพิดรวมของทั้งสองสายพันธุ์นั้นสูงสุดในระยะ L ของการเจริญ ประมาณ 15.3% และ 22.2% ของน้ำหนักแห้งของเซลล์ ใน WT และ Ox-Aas ตามลำดับ อย่างไรก็ตามระดับลิพิดที่ไม่อิ่มตัวของทั้ง WT และ Ox-Aas ทั้งคู่ไม่แตกต่างกันอย่างมีนัยสำคัญ ในอีกทางหนึ่ง พบว่าสภาวะการดัดแปรสารอาหารทั้งหมดที่รวมถึง BG<sub>11</sub>-N, BG<sub>11</sub>-P, BG<sub>11</sub>-N/P และ BG<sub>11</sub>+อะซีเตต ทำให้เกิดการลดลงเล็กน้อยของทั้งการเจริญและปริมาณรงควัตถุใน Ox-Aas และ WT ภายใต้สภาวะ BG<sub>11</sub>-P พบว่าระดับการสะสมของระดับลิพิดรวมของ Ox-Aas เพิ่มขึ้นถึง 27.3% ของน้ำหนักแห้งของเซลล์ ในระยะ L ของการเจริญ โดยเป็นที่น่าสนใจว่าปริมาณลิพิดที่ไม่อิ่มตัวของสายพันธุ์ Ox-Aas ถูกทำให้เพิ่มขึ้น 1.25 เท่า (ประมาณ 3.5% ของน้ำหนักแห้งของเซลล์) ภายใน 8 วันของการทดลองภายใต้สภาวะ BG<sub>11</sub>-N/P สำหรับการเสริมอะซีเตตที่ความเข้มข้น 20 มิลลิโมลาร์ และ 40 มิลลิโมลาร์นั้น พบว่าการเจริญและปริมาณรงควัตถุของ WT และ Ox-Aas ไม่แตกต่างกันในทางตรงกันข้าม พบว่าปริมาณลิพิดรวมและลิพิดที่ไม่อิ่มตัวนั้นลดลงอย่างมีนัยสำคัญตลอดเวลาที่ทดลองเมื่อความเข้มข้นของอะซีเตตนั้นเพิ่มขึ้น ในอีกทางหนึ่งพบว่าสายพันธุ์ Ox-Aas มีระดับการแสดงออกของ *plsX*, *aas* และ *phaA* ที่เพิ่มขึ้น ในขณะที่การแสดงออกของยีน *accA* ลดลงเมื่อเปรียบเทียบกับ WT ผลของการกระตุ้นด้วย BG<sub>11</sub>-P ถูกค้นพบใน WT ด้วยการแสดงออกที่เพิ่มขึ้นของทรานสคริปต์ *accA*, *aas* และ *plsX* ในขณะที่ผลเชิงยับยั้งของ BG<sub>11</sub>-P ถูกค้นพบในสายพันธุ์ Ox-Aas กับทรานสคริปต์ของยีนทั้งหมด ซึ่งได้รับอิทธิพลจากสมดุลของภาวะธำรงดุลภายในเซลล์ ดังนั้น การสะสมลิพิดที่เพิ่มขึ้นของ *Synechocystis* sp. PCC 6803 นั้นสำเร็จได้โดยการเพิ่มการแสดงออกเกินปกติของยีน *aas* และการเพิ่มขึ้นของปริมาณลิพิดในสายพันธุ์ที่มีการแสดงออกเกินปกติของยีนนี้ภายใต้สภาวะปกติ สามารถพบได้ด้วยเช่นกัน ภายใต้สภาวะขาดธาตุฟอสฟอรัส

ภาควิชา ชีวเคมี

สาขาวิชา ชีวเคมีและชีววิทยาโมเลกุล

ปีการศึกษา 2558

ลายมือชื่อนิสิต .....

ลายมือชื่อ อ.ที่ปรึกษาหลัก .....

ลายมือชื่อ อ.ที่ปรึกษาร่วม .....

# # 5671904023 : MAJOR BIOCHEMISTRY AND MOLECULAR BIOLOGY

KEYWORDS: LIPID CONTENT, SYNECHOCYSTIS SP. PCC 6803, ACYL-ACYL CARRIER PROTEIN SYNTHETASE, AAS, SLR1609

KAMONCHANOCK EUNGRASAMEE: EFFECT OF NUTRIENT MODIFICATION ON LIPID LEVEL IN CYANOBACTERIUM *Synechocystis* sp. PCC 6803 OVEREXPRESSING *aas* GENE. ADVISOR: ASST. PROF. SAOWARATH JANTARO, Ph.D., CO-ADVISOR: PROF. ARAN INCHAROENSAKDI, Ph.D., 141 pp.

In this study, *Synechocystis* sp. PCC 6803 strain overexpressing *aas* gene (Ox-Aas) was successfully constructed via single recombination. The putative acyl-acyl carrier protein synthetase (AAS) is a key enzyme in fatty acid recycling process encoded by *slr1609* or *aas* gene. The amino acid sequence of *Synechocystis* AAS contained two highly conserved regions similar to acyl-ACP synthetases of *Arabidopsis thaliana* and *Synechococcus* sp. PCC 7942. The effects of physiological factors including the nutrient deprivations and acetate supplementation on total lipid and unsaturated lipid levels in Ox-Aas and wild type (WT) were investigated. Under normal BG<sub>11</sub> condition, Ox-Aas growth and pigment contents were slightly lower than WT. However, the oxygen evolution rate of Ox-Aas cells was higher than that of WT. Our finding demonstrated the higher lipid accumulation of Ox-Aas compared to WT at all growth phases including log (L), late-log (LL) and early stationary (ES) phases. The highest level of total lipid of both strains was obtained under L-growth phase of about 15.3% and 22.2% of CDW in WT and Ox-Aas, respectively. Nevertheless, the unsaturated lipid levels of both WT and Ox-Aas strains were not significantly different. On the other hand, all nutrient-modified conditions including BG<sub>11</sub>-N, BG<sub>11</sub>-P, BG<sub>11</sub>-N/P and BG<sub>11</sub>+acetate, caused slight decreases of both cell growth and pigment contents in Ox-Aas and WT. Under BG<sub>11</sub>-P, the accumulation of total lipid level of Ox-Aas was increased to 27.3% of CDW at L-growth phase. Interestingly, the unsaturated lipid content of Ox-Aas strains was enhanced by 1.25 fold (about 3.5% of CDW) within 8 days of treatments under BG<sub>11</sub>-N/P condition. For acetate supplementation at both 20 mM and 40 mM concentrations, growth and pigment contents of WT and Ox-Aas showed no differences. In contrast, the total lipid and unsaturated lipid contents were significantly decreased with treatment time when the acetate concentration was increased. On the other hand, Ox-Aas strain had an increase in the expression of *plsX*, *aas* and *phaA* whereas the reduced expression of *accA* was observed when compared to those of WT. The BG<sub>11</sub>-P activating effect was found in WT with the increased expression of *accA*, *aas* and *plsX* whereas its inhibitory effect was found in Ox-Aas strain with all gene transcripts influenced by internal homeostasis balance. Altogether, the increased lipid accumulation of *Synechocystis* sp. PCC 6803 was achieved by overexpression of *aas* gene. The increase of lipid content in this overexpressing strain under normal growth condition was also observed under phosphorus-deprived condition.

Department: Biochemistry

Field of Study: Biochemistry and Molecular Biology

Academic Year: 2015

Student's Signature .....

Advisor's Signature .....

Co-Advisor's Signature .....

## ACKNOWLEDGEMENTS

First of all, I would like to express my deepest gratitude to my advisor Assistant professor Dr. Saowarath Jantaro and my co-advisor, Professor Dr. Aran Incharoensakdi, for their excellent guidance and counseling, instruction, kind support from beginning to the end of my master thesis. I also sincerely thank DPST for the opportunity to exchange and obtain the new experiences almost 6 months at Sweden. I really thank my advisor for the great advices of all stories that happened in my life. Not only giving the knowledge in this research but she also teaches the knowledge of life.

My sincere gratitude is also extended to Assistant, Professor Dr. Kanoktip Packdibumrung, Assistant Professor Dr. Rath Pichyangkura and Assistant Professor Dr. Wuttinun Raksajit for serving as the thesis committee, for their valuable comments and suggestions.

I would like to thank Professor Dr. Peter Lindblad for the advices, suggestion and taking care during my stay at Ångström Laboratories, Uppsala University, Sweden. I sincerely thank Ms. Rui Miao for her kind teaching and solving the problems of my research project. I am thankful to all staff members of Ångström Laboratories for the kindness and helpfulness.

Many thanks to all my dear staff members of Cyanobacteria group, Department of Biochemistry, Faculty of Science, Chulalongkorn University for their love, helping and kindness.

Thank you very much for the valuable support from Development and Promotion of Science and Technology Talents Project (DPST)'s scholarship for the foundation of tuition and expenses.

Last of all, the greatest indebtedness is expressed to my family for their love, unceasing hearten and great support throughout my life.

## CONTENTS

	Page
THAI ABSTRACT .....	iv
ENGLISH ABSTRACT.....	v
ACKNOWLEDGEMENTS .....	vi
CONTENTS.....	vii
LIST OF TABLES .....	xi
LIST OF FIGURES .....	xii
LIST OF ABBREVIATIONS.....	xvi
CHAPTER I INTRODUCTION.....	1
1.1 Environmental stresses .....	1
1.2 Lipid and fatty acid.....	4
1.3 Fatty acid and lipid biosynthesis.....	10
1.4 Phospholipid degradation .....	14
1.5 Acyl-acyl carrier protein synthetase .....	17
1.6 <i>Synechocystis</i> sp. PCC 6803 .....	18
1.7 Objectives .....	21
CHAPTER II MATERIALS AND METHODS.....	22
2.1 Materials .....	22
2.1.1 Equipments .....	22
2.1.2 Chemicals .....	23
2.1.3 Kits .....	25
2.1.4 Enzymes and restriction enzymes .....	25
2.1.5 Expression vector .....	26
2.1.6 Primers.....	27
2.1.7 Organisms.....	28
2.2 Construction and transformation of <i>aas</i> -overexpressing strain of <i>Synechocystis</i> sp. PCC 6803 .....	29
2.2.1 Gene information search and primer design.....	29

	Page
2.2.2 Amplification of <i>aas</i> gene fragment by polymerase chain reaction (PCR).....	31
2.2.3 Construction of recombinant plasmid .....	33
2.2.4 Natural transformation .....	35
2.3 Determinations of growth, pigment contents and oxygen evolution rate ....	36
2.3.1 Growth measurement .....	36
2.3.2 Determination of intracellular pigments.....	37
2.3.3 Determination of oxygen evolution rate.....	38
2.4 Determinations of lipid and unsaturated lipid contents .....	38
2.4.1 Quantitative screening by Sudan Black B staining .....	38
2.4.2 Determinations of total lipid contents .....	39
2.4.3 Determinations of total unsaturated lipid contents.....	39
2.5 Determination of expression levels of genes related to fatty acid biosynthesis .....	40
2.5.1 The extraction of total RNA.....	40
2.5.2 Preparation of extracted RNAs.....	41
2.5.3 Reverse transcription-polymerase chain reaction (RT-PCR).....	42
2.6 Sequence alignment and phylogenetic tree.....	42
CHAPTER III RESULTS .....	43
3.1 The <i>Synechocystis</i> sp. PCC 6803 construct with overexpressing <i>aas</i> gene. 43	
3.1.1 Construction of recombinant plasmid .....	43
3.1.2 Construction of <i>aas</i> -overexpressing strain of <i>Synechocystis</i> .....	46
3.2 Multiple alignment and phylogenetic analysis of acyl-ACP synthetase.....	51
3.3 Growth curve under normal and stress conditions.....	58
3.3.1 Cell growth under normal condition .....	58
3.3.2 Cell growth under nutrient deprived conditions.....	60
3.3.3 Cell growth under acetate addition.....	62
3.4 Intracellular pigment contents .....	64
3.4.1 Intracellular pigment contents under normal condition .....	64



	Page
3.4.2 Intracellular pigment contents under nutrient deprived conditions....	64
3.3.3 Intracellular pigment contents under acetate addition.....	70
3.5 Oxygen evolution rate of <i>Synechocystis</i> cells.....	74
3.5.1 Oxygen evolution rate under normal BG <sub>11</sub> condition .....	74
3.5.2 Oxygen evolution rate under phosphorus-deprived condition .....	74
3.5.3 Oxygen evolution rate under acetate addition.....	77
3.6 Sudan Black staining of <i>Synechocystis</i> cells.....	79
3.6.1 Total lipid screening by Sudan Black staining of <i>Synechocystis</i> cells under normal condition .....	79
3.6.2 Total lipid screening by Sudan Black B staining of <i>Synechocystis</i> cells under phosphorus-deprived condition .....	79
3.6.3 Total lipid screening by Sudan Black staining of <i>Synechocystis</i> sp. cells under acetate addition .....	84
3.7 Total lipid and unsaturated lipid contents.....	88
3.7.1 Total lipid contents of <i>Synechocystis</i> sp. PCC 6803 cells under normal condition.....	88
3.7.2 Total unsaturated lipid contents under normal condition.....	88
3.7.3 Total lipid contents under various nutrient deprived conditions.....	90
3.7.4 Total unsaturated lipid contents under various nutrient deprived conditions .....	92
3.7.5 Total lipid contents of the cells under the acetate addition .....	94
3.7.6 Total unsaturated lipid contents under acetate addition .....	96
3.8 The expression levels of genes related to fatty acid biosynthesis.....	98
3.8.1 The expression levels of <i>aas</i> transcript under normal condition.....	98
3.8.2 The expression levels of related genes under phosphorus-deprived condition.....	98
3.8.3 The expression levels of related genes under acetate addition.....	101
CHAPTER IV DISCUSSION.....	104
CHAPTER V CONCLUSION.....	115
REFERENCES .....	116

	Page
APPENDICE.....	130
APPENDIX A.....	131
APPENDIX B.....	133
APPENDIX C.....	134
APPENDIX D.....	135
APPENDIX E.....	136
APPENDIX F.....	137
APPENDIX G.....	138
APPENDIX H.....	139
APPENDIX I.....	140
VITA.....	141



## LIST OF TABLES

	Page
<b>Table 1.1</b> Naturally occurring fatty acids of saturated and unsaturated fatty acids structure and nomenclature. ....	7
<b>Table 2.1</b> Sequences of restriction sites onto pEERM vector.....	26
<b>Table 2.2</b> Sequence of the primers used in this study .....	27
<b>Table 2.3</b> Sequence of the primers for sequencing and determining the gene location.....	27
<b>Table 2.4</b> Sequence of the primers for RT-PCR .....	28
<b>Table 2.5</b> The components of PCR reaction .....	31
<b>Table 2.6</b> PCR condition used for <i>aas</i> amplification using genomic DNA as template.....	32
<b>Table 2.7</b> Primers that used to check the gene location in <i>aas</i> -overexpressed strains. ....	35
<b>Table 3.1</b> Gene codes, gene indexing names, organisms and sources in cyanobacteria and other species.....	56

## LIST OF FIGURES

	Page
<b>Figure 1.1</b> Some common types of storage and membrane lipids.. .....	6
<b>Figure 1.2</b> The structures of major glycerolipids in thylakoid membranes from plant and cyanobacteria.....	9
<b>Figure 1.3</b> Simplified overview of the fatty acid biosynthesis and some of the neighboring pathways in cyanobactrium <i>Synechocystis</i> sp. PCC 6803.....	11
<b>Figure 1.4</b> Cycles of fatty acyl chain elongation by type II fatty acid synthetase (FAS II).....	13
<b>Figure 1.5</b> The structure of phospholipid molecule. ....	16
<b>Figure 1.6</b> The position of digested phospholipid molecule by lipase enzymes... ..	16
<b>Figure 1.7</b> Representative electron micrographs of <i>Synechocystis</i> sp. PCC 6803 wild-type (WT) and circular genome map of <i>Synechocystis</i> . ....	20
<b>Figure 2.1</b> The <i>Aas</i> gene sequence and primer location.....	30
<b>Figure 3.1</b> Agarose gel electrophoresis of PCR product of <i>aas</i> gene fragment....	44
<b>Figure 3.2</b> Agarose gel electrophoresis of the digested products of pEERM vector and <i>aas</i> gene fragment restriction enzymes. ....	44
<b>Figure 3.3</b> Outlined construction map of recombinant plasmid Rc <i>Aas</i> and agarose gel electrophoresis of the digested recombinant plasmid with restriction enzymes.....	45

<b>Figure 3.4</b> The survived colonies appeared on BG <sub>11</sub> agar plates with antibiotic and diagrams of double and single homologous recombination in <i>aas-over</i> expressing strain of <i>Synechocystis</i> sp. PCC 6803. ....	47
<b>Figure 3.5</b> Confirmation of gene location using various pairs of primers .....	49
<b>Figure 3.6</b> Confirmation of gene location of single homologous recombination in Ox-Aas strain using various pairs of primers .....	50
<b>Figure 3.7</b> Clustal Mega amino acid alignment of fatty acid/phospholipid synthesis protein AAS in <i>Synechocystis</i> sp. PCC 6803 and other species.....	53
<b>Figure 3.8</b> Phylogenetic tree of acyl-ACP synthetase (AAS) or fatty-ACP ligase of organisms including cyanobacteria bacteria and other known species. ....	55
<b>Figure 3.9</b> Growth curves of <i>Synechocystis</i> sp. PCC 6803 wild type (WT), Control WT and Ox-Aas strains cells under normal BG <sub>11</sub> medium. ....	59
<b>Figure 3.10</b> Growth curves of WT, Control WT and Ox-Aas strains after adaptation to various nutrient deprivations.....	61
<b>Figure 3.11</b> Growth curves of WT, Control WT and Ox-Aas strains cultured in normal BG <sub>11</sub> medium containing different concentrations of acetate. ....	63
<b>Figure 3.12</b> Chlorophyll <i>a</i> and carotenoid contents of WT, Control WT and Ox-Aas strains grown for 15 days of cultivation. ....	66
<b>Figure 3.13</b> Chlorophyll <i>a</i> contents of WT, Control WT and Ox-Aas strains after adaptation to various nutrient deprivations.....	68
<b>Figure 3.14</b> Carotenoid contents of WT, Control WT and Ox-Aas strains after adaptation to various nutrient deprivations.....	69

<b>Figure 3.15</b> Chlorophyll a contents of WT, Control WT and Ox-Aas strains cultured in normal BG11 medium containing different concentrations of acetate. ....	71
<b>Figure 3.16</b> Carotenoid contents of WT, Control WT and Ox-Aas strains cultured in normal BG11 medium containing different concentrations of acetate. ....	73
<b>Figure 3.17</b> Oxygen evolution rates of WT and Ox-Aas in each growth stage. ...	75
<b>Figure 3.18</b> Oxygen evolution rates of WT, Control WT and Ox-Aas strains after adaptation to phosphorus-deprived BG11 medium. ....	76
<b>Figure 3.19</b> Oxygen evolution rates of WT, Control WT and Ox-Aas strains cultured in normal BG11 medium containing different concentrations of acetate. ....	78
<b>Figure 3.20</b> Microscopic images of Sudan black B stained cells including WT and Ox-Aas strains under normal condition. ....	80
<b>Figure 3.21</b> Microscopic images of Sudan black B stained cells including WT, Control WT and Ox-Aas strains after adaptation to phosphorus-deprived BG11 medium. ....	81
<b>Figure 3.22</b> Microscopic images of Sudan black B stained cells including WT, Control WT and Ox-Aas strains cultured in normal BG11 medium containing different concentrations of acetate. ....	85
<b>Figure 3.23</b> Total lipid and total unsaturated lipid contents of WT and Ox-Aas strains grown in each growth stage. ....	89

<b>Figure 3.24</b> Total lipid contents of WT, Control WT and Ox-Aas strains after adaptation to various nutrient deprivations.....	91
<b>Figure 3.25</b> Unsaturated lipid contents of WT, Control WT and Ox-Aas strains after adaptation to various nutrient deprivations. ....	93
<b>Figure 3.26</b> Total lipid contents of WT, Control WT and Ox-Aas strains cultured in normal BG11 medium containing different concentrations of acetate.....	95
<b>Figure 3.27</b> Total unsaturated lipid contents of WT, Control WT and Ox-Aas strains cultured in normal BG11 medium containing different concentrations of acetate. ....	97
<b>Figure 3.28</b> RT-PCR products of <i>16S</i> rRNA and <i>aas</i> transcripts in both strains under the normal BG <sub>11</sub> medium and the intensity ratio of <i>aas/16S</i> rRNA transcripts analyzed by GelQuant.NET program.....	99
<b>Figure 3.29</b> The transcript levels of <i>phaA</i> , <i>accA</i> , <i>aas</i> , <i>plsX</i> and <i>16S</i> rRNA genes of WT and Ox-Aas strains after adapted under the normal (BG <sub>11</sub> ) condition. The intensity ratios of <i>accA/16S</i> rRNA, <i>phaA/16S</i> rRNA, <i>aas/16S</i> rRNA and <i>plsX/16S</i> rRNA analyzed by GelQuant.NET program.....	100
<b>Figure 3.30</b> The transcript levels genes of WT and Ox-Aas after adapted under normal (BG <sub>11</sub> ) and phosphorus deprived medium (BG <sub>11</sub> -P) conditions and the intensity ratios of each gene/ <i>16S</i> rRNA analyzed by GelQuant.NET program...	102
<b>Figure 3.31</b> The transcript levels of genes of WT and Ox-Aas under normal (Normal) and the acetate addition and the intensity ratios of each gene/ <i>16S</i> rRNA transcripts analyzed by GelQuant.NET program.....	103

## LIST OF ABBREVIATIONS

AAS	Acyl-acyl carrier protein synthetase
ACP	Acyl carrier protein
FFA	Free fatty acid
K <sub>2</sub> Cr <sub>2</sub> O <sub>7</sub>	Potassium dichromate
SPV	Sulfo-phosphovanillin
H <sub>2</sub> SO <sub>4</sub>	Sulfuric acid
H <sub>3</sub> PO <sub>4</sub>	Phosphoric acid
EDTA	Ethylenediaminetetraacetic acid
LB	Luria broth
<i>cm<sup>r</sup></i>	Chloramphenicol resistance cassette gene
<i>Chl a</i>	Chlorophyll <i>a</i>
TAE	Tris-acetate-EDTA
Abs.	Absorbance
O.D.	Optical density
nm	Nanometer
bp	Base pair
Kb	Kilo base
°C	Degree Celsius
rpm	Revolutions per minute
min	Minute



hr	Hour
g	Gram
mg	Milligram
µg	Microgram
L	Liter
mL	Milliliter
µL	Microliter
mM	Millimolar
CDW	Cell dried weight
% w/w	Percentage of weight by weight
vol	Volume
PCR	Polymerase chain reaction
RT-PCR	Reverse transcription polymerase chain reaction

# CHAPTER I

## INTRODUCTION

### 1.1 Environmental stresses

The environmental stresses which influenced the physiological activities of living organisms are mainly divided into two types including biotic and abiotic stresses. Biotic stress is a stress damage caused by other living organisms, such as bacteria, viruses, fungi and parasites. While abiotic stress is the negative impact from non-living factors on organisms such as sunlight, wind, salinity, temperature, nutrients, pH and drought and affected on their growth and productivity. When the environmental stress exceeding a certain threshold level to cellular metabolism, it might effect on some enzymes by inhibiting or inducing their activities. Most environmental stresses which affected on fatty acid and lipid accumulations of plants and cyanobacteria are abiotic stress. The membrane lipids of organisms were found that dominantly responded to environmental stresses (Olie and Potts, 1986; Ritter and Yopp, 1993).

High temperature stress is one of abiotic stresses which induced thylakoid microdomain reorganization and thermal stabilization of photosynthesis by increasing the level of saturated monoglucosyldiacylglycerol (MGlcDG) in *Synechocystis* cells (Balogi *et al.*, 2005). Then, this compound interacted with the thylakoid-stabilizing small heat shock protein (Hsp) to prevent the damage of heat stress from the light. The highly saturated MGlcDG functioned as a heat shock lipid and played a role in thermotolerance of heat/light-primed cyanobacterial thylakoids (Balogi *et al.*, 2005). Moreover, the temperature and light effected on the growth and fatty acid profile of algae, *Nannochloropsis salina*. The specific growth rate was declined to less than 30%

of this maximum rate at 32.5 °C and 13.6 °C, respectively. The level of saturated fatty acids in cells was increased by high light treatment in order to prevent oxidative stress whereas the increased level of unsaturated fatty acids under the low light and low temperature induced the increase of membrane fluidity (Van Wagenen *et al.*, 2012). Cyanobacteria also respond to a decrease of ambient temperature by desaturating fatty acids of membrane lipids in order to compensate the decrease in membrane fluidity. Enzyme fatty acid desaturase played an important role during the process of cold acclimation of cyanobacteria which induced double bond into carbon chains of fatty acids (Murata and Nishida, 1987; Wada and Murata, 1990).

Nutrient availability is critical for cell division and intracellular metabolite cycling including fatty acids and lipids biosynthesis. Once nutrients such as N or P become depleted or limited in the medium, invariably, a steady decline in cellular reproduction rate ensued and most often limited growth. Once this occurs, the activated metabolic pathways responsible for biomass production were down-regulated and cells instead diverted and deposited much of the available C into lipid (Valenzuela *et al.*, 2013; Wang *et al.*, 2009). Under nitrogen starvation, the lipid yield of green algae *Scenedesmus quadricauda* cells was enhanced 2.27-fold (226 mg/L) when compared to that under nitrogen rich condition (99.33 mg/L). While its growth rate under N-deprived condition was lower than that under normal condition in algae (Anand and Arumugam, 2015). In contrast, non-nitrogen fixing marine cyanobacterium *Oscillatoria willei* BDU 130511 cells were grown under nitrogen-deprived stress which could decrease total lipid content (26.08 %g/DW) whereas the composition of fatty acids was changed, such as the newly synthesized C20:1 (18.47% of total fatty acids) presented under nitrogen starvation (Saha *et al.*, 2003).

Phosphorus (P) limitation resulted in increased lipid content, mainly TAG, in *Monodus subterraneus* (Eustigmatophyceae) (Khozin-Goldberg and Cohen, 2006), but decreased lipid content in *Nannochloris atomus* (Chlorophyceae) and *Tetraselmis* sp. (*Prasinophyceae*) (Reitan *et al.*, 1994). For marine species examined, increasing phosphorus deprivation was found to induce a higher relative content of 16:0 and 18:1 fatty acids and a lower relative content of 18:4  $\omega$ 3, 20:5  $\omega$ 3 and 22:6  $\omega$ 3 fatty acids in the green algae *Chlorella* sp. (Otsuka, 1961; Reitan *et al.*, 1994). P-deprivation or P-limitation effected on the growth reduction in marine cyanobacterium *Prochlorococcus* MED4 (Reistetter *et al.*, 2013). Also, the major membrane lipids of both *Prochlorococcus* and marine *Synechococcus* used sulfolipids as the predominant membrane lipids rather than phospholipids (Van Mooy *et al.*, 2009; Van Mooy *et al.*, 2006). Thus, sulfolipid production, the major component of cell membrane, was not solely correlated with P availability. This membrane structure was the reason why for adaptation of these strain in marine habitat (Reistetter *et al.*, 2013). Phosphorus deprivation mainly effected on the reductions of growth and pigment contents in cyanobacterium *Synechocystis* sp. PCC 6803 in short time treatment whereas phycobilisomes and pigment biosynthesis were unaffected after 6 days of P-depletion (Fuszard *et al.*, 2013). Under P-deprivation, the level of digalactosyldiacylglycerol, a major membrane lipid in the thylakoid membranes were increased in *Synechocystis* cells. The results suggested that DGDG may be required under phosphate limited conditions (Awai *et al.*, 2007).

Acetate addition in the culture media is the additional C source for many biosynthetic pathways including TCA cycle, PHB, fatty acid and lipid synthetic pathways. Acetate is converted to acetyl coenzyme A (CoA) via enzymatic acetyl-CoA

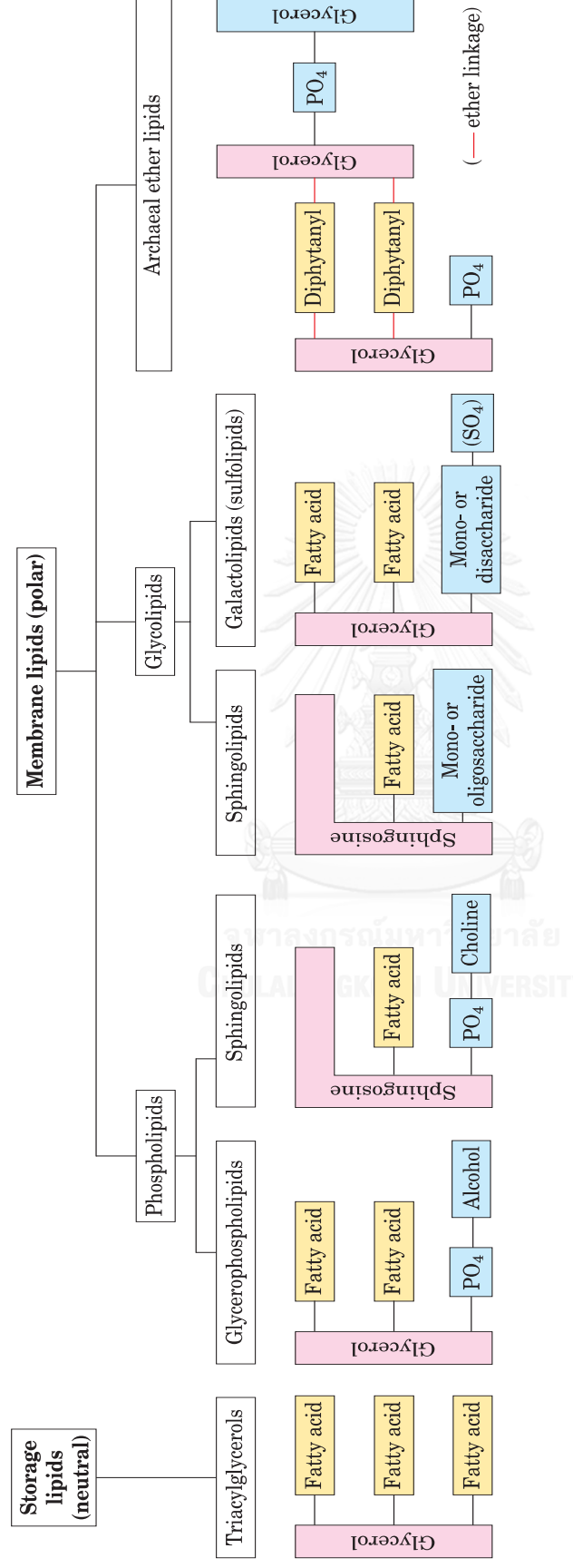
synthetase or acetate-CoA ligase (EC 6.2.1.1). The previous research reported that after treating with additional acetate (20 mM acetate) in term of sodium acetate (NaAc), the cell growth and the oxygen evolution rate of cyanobactrium *Synechocystis* sp. PCC 6803 were lower than normal BG<sub>11</sub> medium condition (0.114 and 0.129  $\mu\text{mol O}_2 / \mu\text{g chl } a/h$ , respectively). This study suggested that acetate addition enhanced PHB accumulation reaching to 11.0 % of the dry cellular weight in the presence of 20 mmol/L of acetate (Guifang *et al.*, 2002). In *Chlamydomonas reinhardtii* BafJ5, the enhanced lipid levels were obtained up to 30% (w/w DCW) by increasing acetate concentrations up to 50 mM of sodium acetate into culture medium. The mixotrophic state (50 mM acetate) under N sufficient and N limited conditions was the highest efficiency condition which effectively enhanced lipid accumulations in the cell up to 42% (w/w DCW) (Ramanan *et al.*, 2013).

## 1.2 Lipid and fatty acid

Lipid is one of the biomolecules which mainly contains carbon, hydrogen and oxygen atoms. Sometimes, it might contain nitrogen and phosphorus atoms. The common forms are fat, oil and waxes. Lipid is classified by the solubility property. Mostly, lipids can be dissolved in organic solvents such as ether, alcohol, chloroform and carbon tetrachloride. Thus, in order to separate or extract the lipids from the cells or tissues of the organisms, solvent extraction method is suitable to perform. The lipid is classified into two types including complex lipid and simple lipid. The complex lipid reacts with base solution to generate soap and glycerol via saponification. There are 4 types of complex compounds including acylglycerol, phosphoglyceride, sphingolipid and waxes whereas the simple lipid, including 3 types of terpene, steroid and

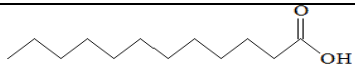
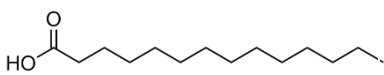
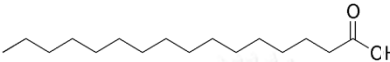


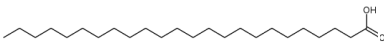

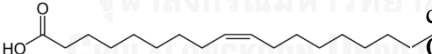
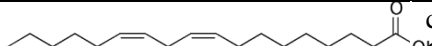
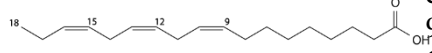
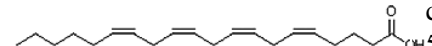
prostaglandin, could not react with base. From the chemical structure of lipids existing in many organisms, they are divided into 3 groups including (1) storage lipids which used as energy sources and played a role in the metabolism such as triacylglyceride, (2) membrane lipid, such as phosphoglyceride and sphingolipid, and (3) the other which important for living such as prostaglandin and steroid (Figure 1.1).

Fatty acid is an organic molecule which contains long-chain hydrocarbon structure linked with carboxylic acid group. A part of hydrocarbon compound is called acyl group. In the natural, most free fatty acids in the cells were formed with other compounds to the complex lipid. Fatty acids are classified into two groups consisting of saturated and unsaturated fatty acids. The saturated lipid structure is hydrocarbon compound which each of carbon atom in the chain attached to each other with single bond whereas the unsaturated fatty acid is hydrocarbon compound which some carbon atoms connected to one another with double bond. The fatty acid contained one of double bond is named as monounsaturated fatty acid whereas the one contained more than one of double bonds is named as polyunsaturated fatty acid. The general structures of saturated and unsaturated fatty acids are shown in Table 1.1.



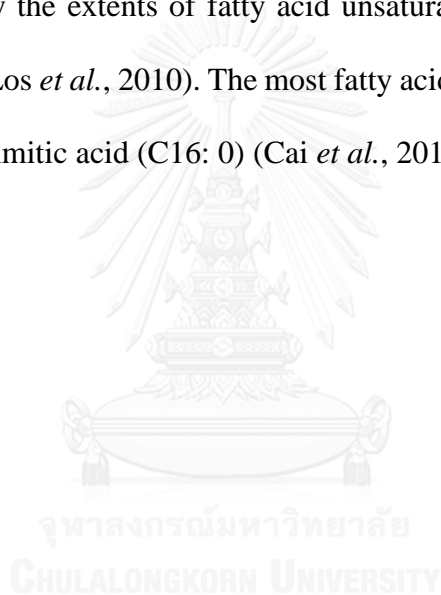
**Figure 1.1** Some common types of storage and membrane lipids. The lipid types shown glycerol or sphingosine as the backbone (pink screen), which attach one or more long chain alkyl groups (yellow screen) and a polar head group (blue color). The alkyl groups are fatty acids in ester linkage (Nelson and Cox, 2008).

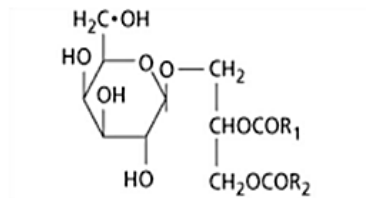
**Table 1.1** Naturally occurring fatty acids of saturated and unsaturated fatty acids structure and nomenclature (Nelson and Cox, 2008).

Carbon skeleton	Structure	Systematic name	Common name
12:0		Dodecanoic acid	Lauric acid
14:0		Tetradecanoic acid	Myristic acid
16:0		Hexadecanoic acid	Palmitic acid
18:0		Octadecanoic acid	Stearic acid
20:0		Eicosanoic acid	Arachidic acid
24:0		Tetracosanoic acid	Lignoceric acid
16:1 ( $\Delta^9$ )		cis-9-Hexadecenoic acid	Palmitoleic acid
18:1 ( $\Delta^9$ )		cis-9-Octadecenoic acid	Oleic acid
18:2 ( $\Delta^{9,12}$ )		cis-,cis-9,12-Octadecadienoic acid	Linoleic acid
18:3 ( $\Delta^{9,12,15}$ )		cis-,cis-,cis-9,12,15-Octadecatrienoic acid	$\alpha$ -Linolenic acid
20:4 ( $\Delta^{5,8,11,14}$ )		cis-,cis-,cis-,cis-5,8,11,14-Icosatetraenoic acid	Arachidonic acid

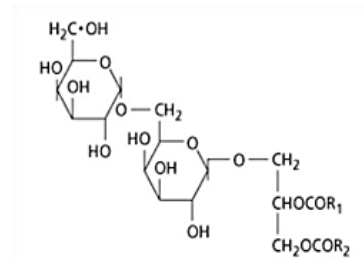


Cyanobacteria generally contain considerable amounts of lipids, which are mainly present in the thylakoid membranes (Quintana *et al.*, 2011). The membranes in cyanobacteria are mainly located on the cytoplasmic (plasma) membrane and thylakoid membranes. Both membranes contain four major glycerolipids include monogalactosyldiacylglycerol (MGDG), digalactosyldiacylglycerol (DGDG), sulfoquinovosyldiacylglycerol (SQDG) and phosphatidylglycerol (PG) whose structures shown in Figure 1.2. The molecular motion of these glycerolipids is determined mainly by the extents of fatty acid unsaturation that are esterified to the glycerol backbones (Los *et al.*, 2010). The most fatty acid composition of total lipids in cyanobacteria was palmitic acid (C16: 0) (Cai *et al.*, 2013; Maslova *et al.*, 2004).

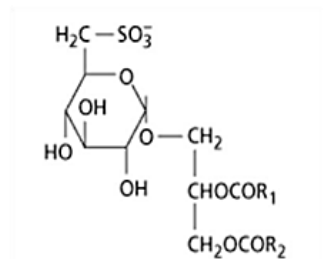




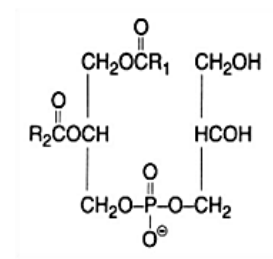
Monogalactosyl diacylglycerol (MGDG)



Digalactosyl diacylglycerol (DGDG)



Sulfoquinovosyl diacylglycerol (SQDG)

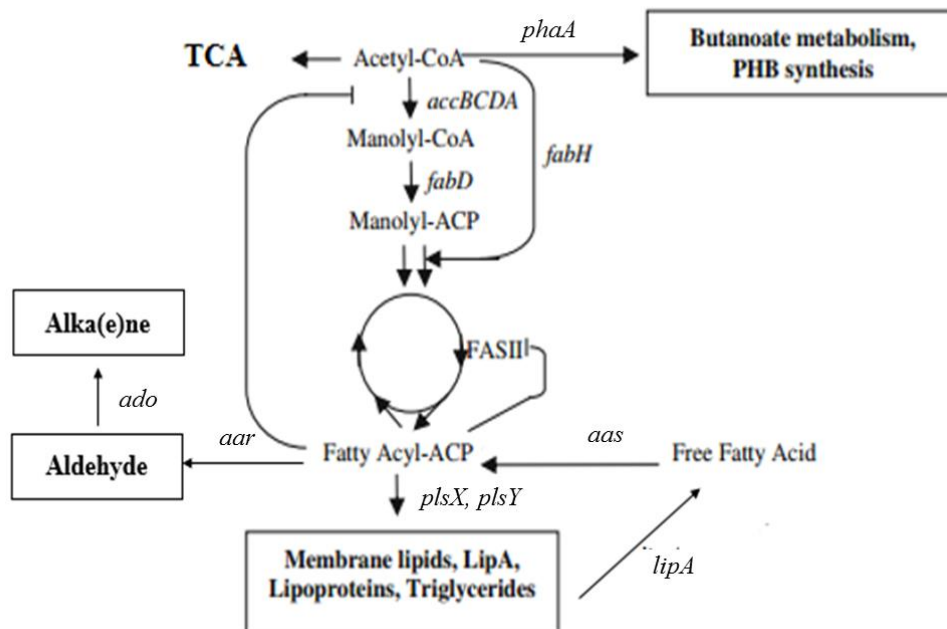


Phosphatidylglycerol (PG)

**Figure 1.2** The structures of major glycerolipids in thylakoid membranes are monogalactosyl diacylglycerol (MGDG), digalactosyl diacylglycerol (DGDG), sulfoquinovosyl diacylglycerol (SQDG) and phosphatidylglycerol (PG) from plant and cyanobacteria.

### 1.3 Fatty acid and lipid biosynthesis

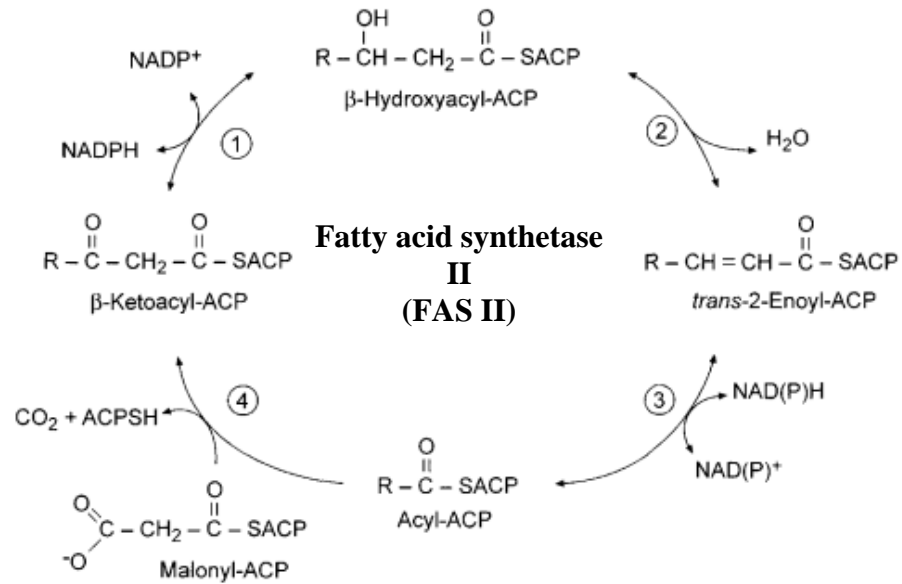
In Figure 1.3, there are many reaction steps and enzymes involved in fatty acid and lipid productions. The first step towards the fatty acid synthesis is acetyl-CoA can be converted to malonyl-CoA in a rate limiting reaction catalyzed by a multi-subunit acetyl coenzyme A carboxylase or ACCase (encoded by *accA*, *accB*, *accC*, and *accD*) (Davis *et al.*, 2000). Then, malonyl-CoA is converted to malonyl-ACP by ACP transferase (encoded by *fabD*) with the catalysis of  $\beta$ -ketoacyl synthase (encoded by *fabH*). After that, the fatty acyl-ACP synthesis from malonyl-ACP involves four different reactions catalyzed in most prokaryotes by type II fatty acid synthase (FAS II) system or the cycles of fatty acyl chain elongation while the fatty acid reaction in eukaryote is composed of a single multifunctional enzymatic entity or type I fatty acid synthase (FAS I). FAS II reactions are shown in Figure 1.4 (Heath *et al.*, 2002). First of all,  $\beta$ -ketoacyl-ACP synthase III (encoded by *fabB*) is the enzyme of the initial condensation reaction that converted malonyl-ACP to  $\beta$ -ketoacyl-ACP and catalyzed a reduction step yielding  $\beta$ -hydroxyacyl-ACP by  $\beta$ -ketoacyl-ACP reductase (FabG encoded by *fabG*). Then,  $\beta$ -hydroxyacyl-ACP is dehydration to produce trans-2-enoyl-ACP by  $\beta$ -hydroxyacyl-ACP dehydrase (FabZ encoded by *fabZ*) and it catalyzed a reduction reaction by trans-2-enoyl-ACP reductase (FabI encoded by *fabI*) resulting in fatty acyl-ACP. These condensation, reduction, dehydration and reduction reactions cycle are repeated by adding two-carbon units to the growing chain until the terminal process when the fatty acid or acyl reached to 16 (palmitic acid) or 18 (stearic acid) carbons in length using malonyl-CoA as substrate, in order to produce a saturated fatty acid of the desired length. The two reduction reactions in FAS II require NADPH oxidation to NADP<sup>+</sup> (Heath *et al.*, 2002; Quintana *et al.*, 2011).



**Figure 1.3** Simplified overview of the fatty acid biosynthesis and some of the neighboring pathways in cyanobacterium *Synechocystis* sp. PCC 6803 (modified from Quintana *et al.*, 2011). Key enzyme genes in those pathways are indicated PHB, poly- $\beta$ -hydroxybutyrate; acyl-ACP, fatty acyl- acyl carrier protein; alkane (alkene); *pha A*, polyhydroxyalkanoates pecific beta-ketothiolase gene; *accBCDA*, multi-subunit acetyl-CoA carboxylase gene; *lip A*, lipolytic enzyme gene; *aas*, acyl-ACP synthetase gene; *aar*, acyl-ACP reductase gene; *ado*, aldehyde-deformylating oxygenase; *plsX* and *plsY*, putative phosphate acyl-transferases.

Previous researches reported that the fatty acyl-ACPs, the end products, can be controlled on fatty acid synthesis by inhibiting the rate-limiting step of ACCase enzymatic activity in both bacterial *Escherichia coli* and plant, *Brassica napus* (Andre *et al.*, 2012; Davis and Cronan, 2001). Cyanobacteria are the evolutionary ancestors of plant plastids, therefore FAS machineries of both are similar (Vothknecht and Westhoff, 2001). Thus, the demand of *de novo* fatty acids is signaled by a variety of signals, including acyl-ACP and acyl-CoA. These metabolites allosterically inhibit fatty acid biosynthetic enzymes and the production of malonyl-CoA, which used in fatty acid synthesis could be decreased on gene expression for the entire biosynthetic pathway. In addition, acyl-ACPs also inhibited  $\beta$ -ketoacyl synthase (encoded by *fabH*) and trans-2-enoyl-ACP reductase (FabI encoded by *fabI*) activities resulting the decreases on fatty acid biosynthesis (Heath and Rock, 1996).

Acyl-ACPs products from FAS system are directed to the membrane lipid biosynthesis including monogalactosyl diacylglycerol (MGDG), digalactosyl diacylglycerol (DGDG) sulfoquinovosyl diacylglycerol (Anand and Arumugam, 2015)(SQDG) and phosphatidylglycerol (PG) (Weier *et al.*, 2005). The previous study, Zhang and Rock (2008) reported that two enzymes, PlsX and PlsY involved in membrane lipid synthesis. Firstly, acyl-ACP chain is added by phosphate using PlsX or phosphate acyl transferase (encoded by *plsX*) and then transferred to glycerolaldehyde-3-phosphate (G3P) which is catalyzed by PlsY. Moreover, fatty acyl-ACPs might not come from *de novo* fatty acid synthesis, it can be synthesized from intracellular free fatty acids (FFAs) catalyzed by acyl-acyl carrier protein synthetase (encoded by *aas* gene) (Quintana *et al.*, 2011).



**Figure 1.4** Cycles of fatty acyl chain elongation by type II fatty acid synthetase (FAS II). All intermediates in fatty acid synthesis of thioesters of the acyl carrier protein (ACP) include (1)  $\beta$ -ketoacyl-ACP reductase (FabG encoded by *fabG*), (2)  $\beta$ -Hydroxyacyl-ACP dehydrase (FabZ encoded by *fabZ*), (3) *trans*-2-enoyl-ACP reductase (FabI encoded by *fabI*) and (4)  $\beta$ -ketoacyl-ACP synthase I or II (FabB or FabF encoded by *fabB* or *fabF*) (Heath *et al.*, 2002).

Recently, Kaczmarzyk and Fulda (2010) reported that acyl-ACP synthetase, encoded by *aas* gene in cyanobacterium *Synechocystis* sp. PCC 6803, is the key enzyme in fatty acid recycling process by incorporating intracellular free fatty acids into acyl-acyl carrier protein. Then, the acyl-acyl carrier protein further functions as a substrate for many biosynthetic processes, such as poly- $\beta$ -hydroxybutyrate (PHB), lipid, alkene/alkane and fatty alcohol productions (Gao *et al.*, 2012; Wang *et al.*, 2013). However, naturally producing lipid contents in living cells are limited by biochemical homeostasis mechanism.

#### 1.4 Phospholipid degradation

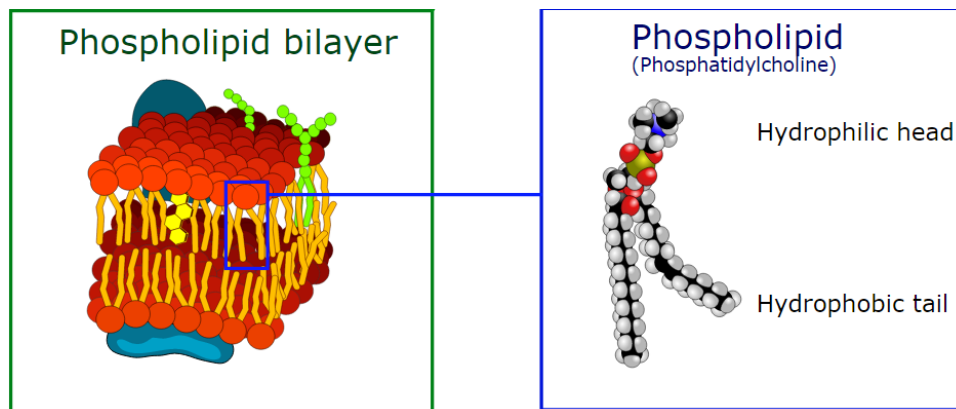
Phospholipid or phosphoglyceride are membered to a class of lipids which contains a molecule of glycerol as backbone linked with two molecules of fatty acids and a molecule of phosphoric acid by ester bond. The structure of the phospholipid molecule generally consists of hydrophobic and hydrophilic parts. Thus, they can form lipid bilayers (Figure 1.5) due to their amphiphilic property. In the nature, there are major components of all cell membranes. Phospholipid is degraded by the activity of special lipase enzymes (Figure 1.6). The enzymes are classified as phospholipases A<sub>1</sub>, A<sub>2</sub>, A<sub>3</sub>, C or D depending on the site of hydrolysis including

1. Lipase A<sub>1</sub> enzyme; the ester bond between fatty acid molecule and carbon atom at the position 1 of glycerol digested by lipase A<sub>1</sub>.
2. Lipase A<sub>2</sub> enzyme; the ester bond between fatty acid molecule and carbon atom at the position 2 of glycerol digested by lipase A<sub>2</sub>.
3. Lipase B enzyme; the ester bonds between fatty acid molecules and glycerol digested by lipase B.

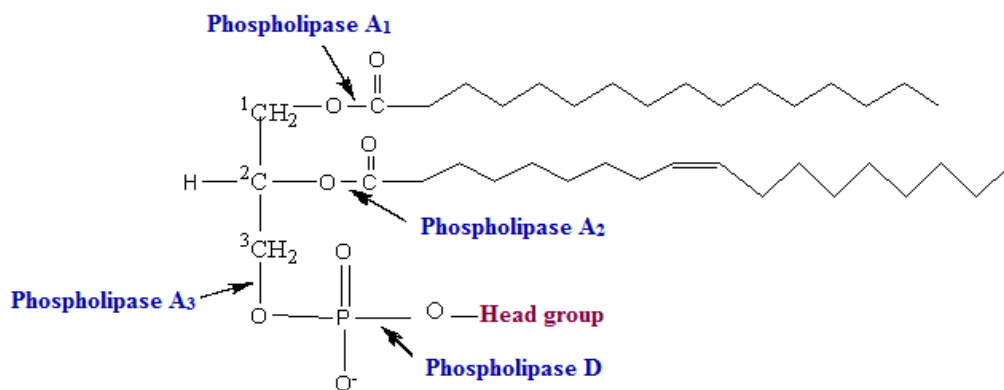
4. Lipase C enzyme; the phosphodiester bond between phosphoric acid molecule and glycerol digested by lipase C.
5. Lipase D enzyme; the chemical bonds between alcohol molecule and phosphoric acid digested by lipase D.

After degradation pathway, lipids are broken down into glycerol and fatty acids. The hydrolytic products of catalysis depend on the specific enzyme and substrate including free fatty acids, lysosphospholipids, diacylglycerol, phosphatidic acid and phosphorylated or free base (e.g. choline, ethanolamine, serine and inositol) (Fisher and Jain, 2001). In prokaryote *Escherichia coli* (*E. coli*), it contains 10 enzymatic activities by degrading phospholipids, intermediates in the phospholipid biosynthetic pathway, or triacylglycerol (Heath *et al.*, 2002). *Arabidopsis thaliana* is popular model used for studies in the higher plant. It contains three lipase genes and encodes three lipase enzymes which specific to differential substrates (Padham *et al.*, 2007). In cyanobacterial *Synechocystis* sp. PCC 6803 and *Synechococcus* sp. PCC 7942, the products like free fatty acids can turn to acyl-acyl carrier protein (ACP) via esterification to ACP by acyl-acyl carrier protein synthetase enzymatic activity, and then acyl-ACP can be used as the precursor for membrane lipid biosynthesis (Kaczmarzyk and Fulda, 2010). In addition, living cells also synthesizes the acetyl-CoA via  $\beta$ -oxidation pathway which used as the substrate for both fatty acid synthesis and TCA cycle (Figure 1.3) (Heath *et al.*, 2002).





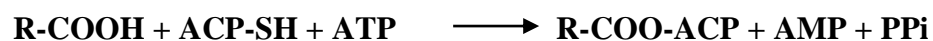
**Figure 1.5** The structure of phospholipid molecule which generally consists of two hydrophobic fatty acid "tails" and a hydrophilic "head", joined together by a glycerol molecule (Source: <https://en.wikipedia.org/wiki/Phospholipid>).



**Figure 1.6** The position of digested phospholipid molecule by lipase enzymes.

### 1.5 Acyl-acyl carrier protein synthetase

Acyl-acyl carrier protein (ACP) synthetase is the fatty acid activating enzyme involved in fatty acid and lipid recycling biosynthesis. Previous study reported that long chain fatty acids exogenously supplied were becoming incorporated into acyl-ACP by the direct activity of acyl-ACP synthetase in *Escherichia coli* (Ray and Cronan, 1976). The enzyme commission name for this enzyme is fatty acids ACP ligase. The intracellular free fatty acids might be raised from two sources, either by hydrolytic turnover of phospholipid fatty acids or by thioesterase mediated cleavage of acyl-CoA molecules formed to free fatty acids during transport of extracellular fatty acids via  $\beta$ -oxidation process (Barnes and Wakil, 1968; Bonner and Bloch, 1972). Acyl-ACP compound which is the substrate in membrane lipid synthesis can be synthesized by fatty acid synthetase from various plant tissues (Jaworski and Stumpf, 1974). Moreover, Ray and Cronan (1976) reported that acyl-ACP synthetase permits the synthesis of a much wider variety of acyl-ACP derivatives than does the plant system and the formation of acyl-ACP requires ATP, ACP-SH (acyl carrier protein-SH) and  $Mg^{2+}$  and  $Ca^{2+}$  as cofactors. This enzyme catalyzes the following reaction:



The activities of acyl-ACP synthetase and acyl-CoA synthetase (encoded by *fabD*) are dependent. Koo and coworkers (2005) reported that AAE15 protein of *Arabidopsis thaliana* was recently described as acyl-ACP synthetase. The conclusions were based on the comparison of enzymatic activity that the results demonstrate that plants possess a mechanism for direct activation of free fatty acid to ACP in the plastid

via an acyl-ACP synthetase encoded by *at4g14070* (Koo *et al.*, 2005). In cyanobacteria, the fatty acid activating enzymes are annotated as acyl-CoA synthetase due to their similar protein sequences with the plants. The motif sequence of amino acids was identified as the member of superfamily of AMP-binding proteins. Recently, Kaczmarzyk and Fulda (2010) suggested that fatty acid activating enzyme in cyanobacteria *Synechocystis* sp. PCC 6803 and *Synechococcus elongatus* PCC 7942 were acyl-ACP synthetase which catalyzed the incorporation of exogenous fatty acid into acyl-ACPs, the intermediate substrates in various pathways of lipid, poly- $\beta$ -hydroxybutyrate (PHB), alkene/alkane and fatty alcohol productions (Gao *et al.*, 2012; Kaczmarzyk and Fulda, 2010; Wang *et al.*, 2013).

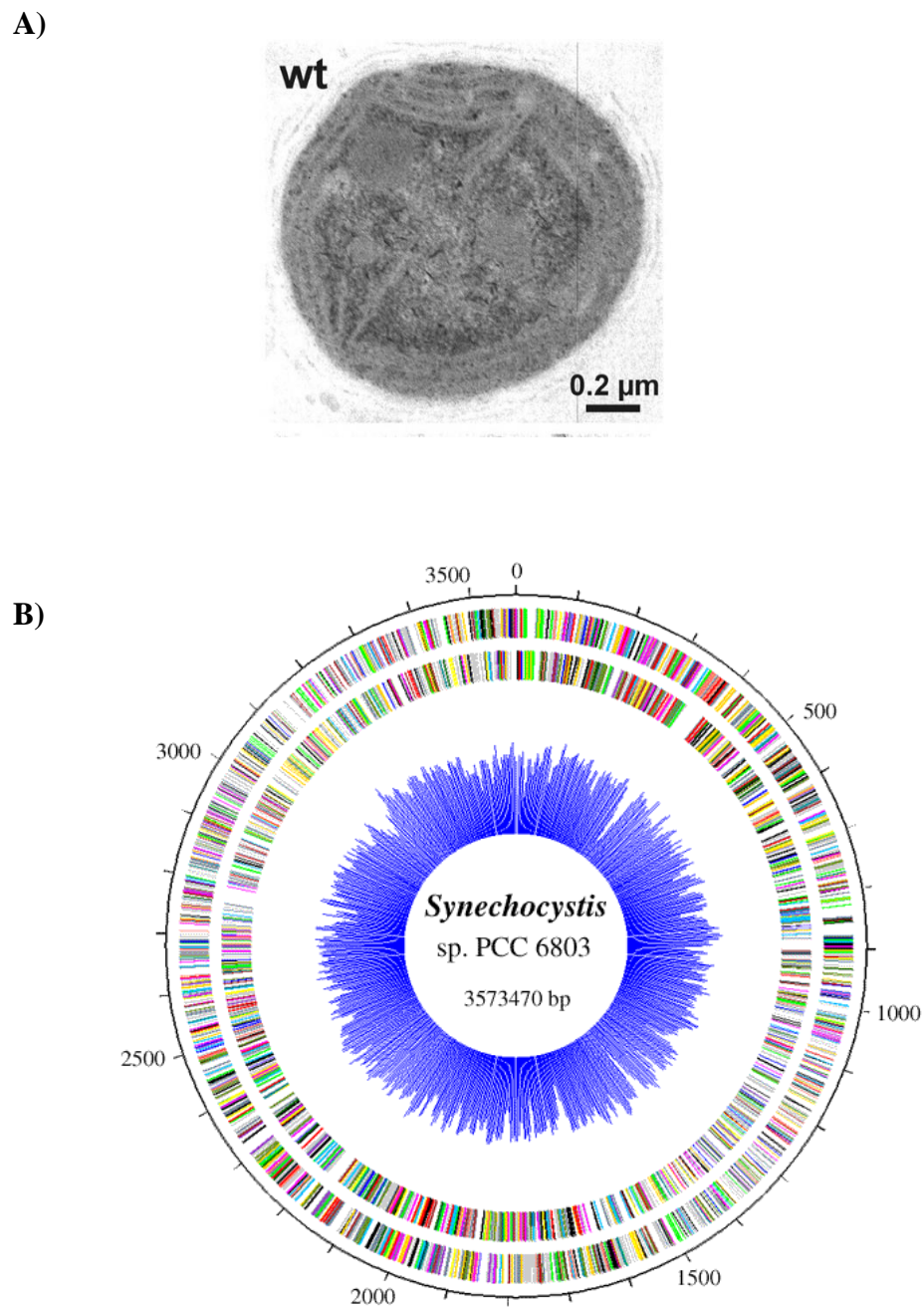
In *Synechocystis* sp. PCC 6803 which was the model of this study, the acyl-ACP synthetase (Meene *et al.*) is encoded by *slr1906* gene which contains 696 amino acids (2,091 bp). This enzyme catalyzes the ATP-dependent esterification of fatty acids to the fatty acyl-ACP and plays a role in recycling of fatty acids from the membrane lipid degradation. In previous report, *aas* mutant strain of *Synechocystis* cells gave the pool of free fatty acids which were secreted into the culture medium whereas the wild-type (WT) cells were kept inside the cells (Kaczmarzyk and Fulda, 2010).

### **1.6 *Synechocystis* sp. PCC 6803**

Cyanobacteria, formerly known as blue-green algae, are photoautotrophic organisms capable of oxygen-producing photosynthesis (Kaneko and Tabata, 1997). They generally use chlorophyll *a* pigment and phycobilisomes which embedded on the outer surface of cyanobacterial thylakoid membrane as the light harvesting in photosynthetic process (Montgomery, 2014). Additionally, the sunlight, H<sub>2</sub>O and CO<sub>2</sub>

were critically incorporated for synthesizing their energy storage components, such as carbohydrates, lipids and proteins. These energy storage components form a potential feedstock which can be converted into bioenergy (Quintana *et al.*, 2011). Thus, the practical advantage of cyanobacteria is the reduction of greenhouse gas CO<sub>2</sub> in the atmosphere towards to carbon source biosynthesis, the key factor for valuable productions including renewable biofuels and natural chemicals (Kaneko *et al.*, 1996). Cyanobacteria are commonly grown in various habitats such as lakes, ponds, springs, wetlands, streams, and rivers. They play a major role adaptation responded to the nitrogen, carbon, and oxygen dynamics of many aquatic environments (Vincent, 2009).

A cyanobacterium *Synechocystis* sp. PCC 6803 was used as the model for this research. It is a unicellular non-nitrogen (N<sub>2</sub>)-fixing cyanobacterium which ubiquitously grown in fresh water. In Figure 1.7A, *Synechocystis* 6803 are spherical cells of approximately 1.5 to 2.0 μm in diameter studied by electron microscopy. Consequently, their intracellular organization is well characterized (Liberton *et al.*, 2006; Meene *et al.*, 2006). The advantages of this strain are the complete genome sequences and known intracellular structure. Moreover, the total length of the circular genome was deduced as 3,573,470 bp long (Figure 1.7B) with the average GC content of 47.7% (Kaneko *et al.*, 1996). It possesses a photosynthesis process like the higher plants. Then, *Synechocystis* sp. PCC 6803 is one of the most popular organisms for genetic engineering and physiological studies serving as a model of higher plant involved the photosynthesis system (Ikeuchi and Tabata, 2001).



**Figure 1.7** Representative electron micrographs (A) of *Synechocystis* sp. PCC 6803 wild-type (WT) (Fuhrmann *et al.*, 2009). Circular genome map (B) of *Synechocystis* sp. PCC 6803 by Dr. Satoshi Tabata and coworkers at the Kazusa DNA Research Institute in 1996. (Source: <http://www.kazusa.or.jp/cyano/Synechocystis/map/click/cmap.html>).

The previous research suggested that *Synechocystis* cells were easily engineered because the foreign DNA could be likely transformed and integrated into their genomic DNA by homologous recombination (Grigorieva and Shestakov, 1982; Zhang and Rock, 2008). *Synechocystis* was also used as the model for studying the mechanism network and the effect of environmental stress and adapted conditions on the biosynthesis mechanism (Jantaro *et al.*, 2003) such as the nutrient availability (nitrogen, phosphorus and carbon sources) and cultivated condition (Schopf *et al.*, 1996; Yu *et al.*, 2013).

### 1.7 Objectives

1. To construct *Synechocystis* sp. PCC 6803 with overexpressing *aas* gene
2. To investigate the effects of nutrient modifications on lipid levels in wild type and overexpressing strains

## CHAPTER II

### MATERIALS AND METHODS

#### 2.1 Materials

##### 2.1.1 Equipments

<b>Equipments</b>	<b>Models and Company</b>
Autoclave	Model HA-30, Hirayama Manufacturing Corporation, Japan
Centrifuge	Mikro 220 R Hettich, Germany 5417C Eppendorf, Germany
Gel documentation	Syngene <sup>®</sup> Gel Documentation
Gel Electrophoresis System	Gibthai, Thailand
Fume Hood	Science Technology Protection Laboratory Hood, USA
Laminar flow	Boss Tech Scientific Instruments, Thailand
Microscope	Olympus BX51
Microwave	Sharp, Thailand
Oxygraph system	Clark-type oxygen electrode, Hansatech Instruments, England
PCR apparatus	Master Cycler Gradient Eppendorf, Germany
PH meter	Metter Toledo, USA

<b>Equipments</b>	<b>Models and Company</b>
Power supply	Power PAC 1000 BIO-RAD, USA
Spectrophotometer	Biomate 3 Thermo Scientific, USA
Vortex	Model 232 Touch mixer Fischer Scientific, USA
Water bath	Hangzhou Bioer Technology, China

### 2.1.2 Chemicals

<b>Chemicals</b>	<b>Companies</b>
Acetic acid	Scharlau Chemie S.A., Spain
Agarose	Invitrogen, USA
Ammonium ferric citrate	Ajax Finechem, Australia
Ammonium persulfate (APS)	Merck, Germany
Boric acid	Scharlau Chemie S.A., Spain
Bromophenol blue	Sigma, USA
Calcium chloride dehydrate	Ajax Finechem, Australia
Citric acid	Ajax Finechem, Australia
Chloroform	Merck, Germany
Coomassie blue G-250	Fluka, USA
Copper (II) sulfate	Carlo Erba Reagents, France
Dimethylformamide	Lab Scan, Ireland
Dithiothreitol (DTT)	Sigma, USA
EDTA	Ajax Finechem, Australia



**Chemicals****Companies**

Ethanol	Burdick & Jackson <sup>®</sup> , Australia
Ethidium bromide	Sigma, USA
Glycerol	Ajax Finechem, Australia
Glycine	Ajax Finechem, Australia
HEPES	Calbiochem <sup>®</sup> , Germany
Isoamylalcohol	Sigma, USA
Isopropanol	Sigma, USA
Magnesium chloride	Ajax Finechem, Australia
Magnesium sulfate heptahydrate	Ajax Finechem, Australia
Mercaptoethanol	Sigma, USA
Methanol	Burdick & Jackson <sup>®</sup> , Australia
<i>Ortho</i> -Phosphoric acid	Merck, Germany
Phenol	Merck, Germany
Potassium acetate	Rankem, India
Potassium dichromate	Sigma, USA
Potassium sodium tartrate	Merck, Germany
Safranin O Dye	Sigma, USA
Sodium acetate	Ajax Finechem, Australia
Sodium chloride	Ajax Finechem, Australia
Sodium hydroxide	Ajax Finechem, Australia
Sodium nitrate	Ajax Finechem, Australia
Sudan Black B	Sigma, USA

**Chemicals**

Sulfuric acid

Tris (hydroxymethyl)-aminomethane

Trizol<sup>®</sup> reagent

Vanillin

**Companies**QR&C<sup>®</sup>, New Zealand

USB Corporation, USA

Invitrogen, USA

Sigma, USA

**2.1.3 Kits****Kits**GeneRuler<sup>™</sup> 100 bp DNA LadderGeneRuler<sup>™</sup> 1 kb DNA Ladder

Plasmid extraction kit

SuperScrip<sup>™</sup> III First-strand Synthesis System**Companies**

Fermentas, Canada

Fermentas, Canada

Invitrogen, USA

Invitrogen, USA

**2.1.4 Enzymes and restriction enzymes****Enzymes and restriction enzymes***Xba*I*Spe*I

RNase-Free DNase

T4 DNA ligase

*Phusion* DNA polymerase*Tag* DNA polymerase**Companies**

Fermentas, Canada

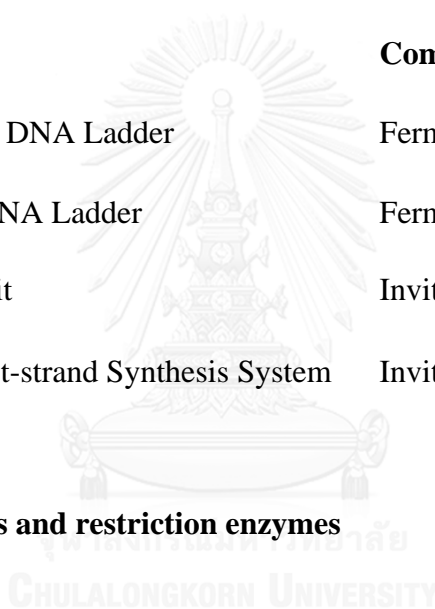
Fermentas, Canada

Fermentas, Canada

Fermentas, Canada

Invitrogen, USA

Invitrogen, USA



### 2.1.5 Expression vector

The expression vector, namely pEERM vector (Appendix B) was used in this experiments. This pEERM vector is a plasmid which provided by Prof. Peter Lindblad, Ph.D. from Department of Chemistry – Ångström Laboratory, Uppsala University, Sweden. It has 3,595 nucleotide sequences which contained PsbA2 promoter site, multiple cloning sites of *Xba*I, *Spe*I and *Pst*I and chloramphenicol resistance cassette as selective marker, respectively. The sequences of restriction sites onto pEERM vector are shown in Table 2.1.

**Table 2.1** Sequences of restriction sites onto pEERM vector.

Restriction enzymes	Sequence
<i>Xba</i> I	5'...T↓C T A G A...3' 3'...A G A T C↑T...5
<i>Spe</i> I	5'...A↓C T A G T...3' 3'...T G A T C↑A...
<i>Pst</i> I	5'...C T G C A↓G...3' 3'...G↑A C G T C...5'

### 2.1.6 Primers

**Table 2.2** Sequence of the primers used in this study

Target			PCR
gene	Name	Primers	product size (bp)
<i>aas</i>	Aas_Forward 3	5'-AGACAATCTAGAGTGGACAGTGGCCAT-3'	2,091
<i>aas</i>	Aas_Reverse 3	5'-ATAAACACTAGTTTAAAACATTTTCGTC-3'	
<i>cm<sup>R</sup></i>	Cm_Forward	5'-GAGTTGATCGGGCACGTAAG-3'	800
<i>cm<sup>R</sup></i>	Cm_Reverse	5'-CTCGAGGCTTGGATTCTCAC-3'	

**Table 2.3** Sequence of the primers for sequencing and determining the gene location

Name	Sequences
UUSPsbA2_SF	5'-GTGATGCCTGTCAGCAAAACAACCTT-3'
Aas_F3	5'-AGACAATCTAGAGTGGACAGTGGCCAT-3'
Aas_R5	5'-GGAGATGGTTCAAGCTCAGG-3'
Aas_F4	5'-ACTCCCTAGAAAGAAGCGCC-3'
Aas_R6	5'-ATAAACACTAGTTTAAAACATTTTCGTC-3'
Aas_SR	5'-GGCTATTCCAATGGATTTGAGGTTG-3'
Cm_SF	5'-GGCAGAATGCTTAATGAATTACAACAG-3'
Cm_SR	5'-CTGAAATGCCTCAAATGTTCTTTACG-3'
UUSF_Aas	5'-GCGATCGCCGTCAATTTTCGATCAG-3'

**Table 2.4** Sequence of the primers for RT-PCR

Target		PCR product	
gene	Name	Primers	size (bp)
<i>16s</i>	16s_F	5'-AGTTCTGACGGTACCTGATGA-3'	521
<i>16s</i>	16s_R	5'-GTCAAGCCTTGGTAAGGTTAT-3'	
<i>plsX</i>	PlsX_F	5'-AAGGGGTGGTGGAAATGGAA-3'	488
<i>plsX</i>	PlsX_R	5'- AAGTAGGTCCCTTCCTTCGG-3'	
<i>accA</i>	AccA_F	5'-ATGCACGGCGATCGAGGAGGT-3'	428
<i>accA</i>	AccA_R	5'-TGGAGTAGCCACGGTGTACAC-3'	
<i>aas</i>	Aas_F_RT	5'-CCCATTGAAGATGCCTGTTT-3'	304
<i>aas</i>	Aas_R_RT	5'-GTGCTGGGATAAAACGGAAA-3'	
<i>phaA</i>	PhaA_F	5'-TCAGCCGGATAGAATTGGACGAAGT-3'	432
<i>phaA</i>	PhaA_R	5'-CAAACAAGTCAAAATCTGCCAGGGTT-3'	

### 2.1.7 Organisms

*Synechocystis* sp. PCC 6803 wild type strain was provided from Department of Chemistry - Ångström Laboratory, Uppsala University, Sweden.

*Escherichia coli* (DH5 $\alpha$ ) strain was used as a host for plasmid propagation.

## 2.2 Construction and transformation of *aas*-overexpressing strain of *Synechocystis* sp. PCC 6803

### 2.2.1 Gene information search and primer design

The information of *aas* gene was obtained from Cyanobase database (<http://genome.microbedb.jp/cyanobase/Synechocystis>). It reports that *aas* gene or *slr1609* encoding Acyl-acyl ACP synthetase enzyme plays a role in fatty acid and lipid production in *Synechocystis* sp. PCC6803. The *aas* gene starts its sequence from 487,287 to 489,377. This gene has 2,091 nucleotide sequences or 696 amino acid sequences (Appendix B.).

In order to design primer which contained restriction sites of the both ends of *aas* gene fragment by sites of *Xba*I and *Spe*I sequences, respectively using genomic DNA as template (Figure 2.1).

Aas\_F3 as Forward primer---→

5'-AGACAATCTAGAGTGGACAGTGGCCATGGCGCTCAATC-3'

GTGGACAGTGGCCATGGCGCTCAATCCAGGATAAAGCTTGGTCAGACTGGGTATAAACTGTCA  
 ACATATTTCTGCAAGAGTGGGCCAATTGGGAAAATCAACCTCAAATCCATTGGAATAGCCTTTTTCAACCGTAAAAA  
 TCCAACCTTTCTCTCTTCCCTTCTTCCATCTGATTATGGTTACGCCAATTAACCTACCATTCCATCCATTGCCTGGCG  
 GATATCTGGGCTATCACCGGAGAAAATTTGCCGATATTGTGGCCCTCAACGATCGCCATAGTCATCCCCCGTAAC  
 TTTAACCTATGCCAATTGCGGGAAGAAATTACAGCTTTTGGCGCTGGCCTACAGAGTTTAGGAGTTACCCCCATCA  
 ACACCTGGCCATTTTCCGCGACAACAGCCCCGGTGGTTTATCGCCGATCAAGGCAGTATGTTGGCTGGAGCCGTC  
 AACGCCGTCCGTTCTGCCAAGCAGAGCGCCAGGAATTACTCTACATCCTAGAAGACAGCAACAGCCGTACTIONAAT  
 CGCAGAAAATCGGCAAACCCTAAGCAAATGGCCCTAGATGGCGAAACCATTGACCTGAAACTAATCATCTCCTCA  
 CCGATGAAGAAGTGGCAGAGGACAGCGCCATTCCCCAATATAACTTTGCCAGGTCATGGCCCTAGGGGCCGGCA  
 AAATCCCCACTCCCGTCCCCGCCAGGAAGAAGATTTAGCCACCCTGATCTACACCTCCGGCACCCACAGGACAACC  
 CAAAGGGGTGATGCTCAGCCACGGTAATTTATTGCACCAAGTACGGGAATTGGATTGCGTATTATCCCCGCCCGG  
 GCGATCAGGTGTTGAGCATTGTTGCCCTGTTGGCACTCCCTAGAAAGAAGCGCCGAATATTTCTTCTTCCCGGGGCT  
 GCACGATGAACTACACCAGCATTCCGCATTTCAAGGGGGATGTGAAGGACATTAAACCCCATCACATTGTCGGTGTG  
 CCCCCGCTGTGGGAATCCCTCTACGAAGGGGTACAAAAACGTTCCGGGAAAAGTCCCTGGGCAACAAAAGCTA  
 ATTAATTTCTTTTTCGGCATTTCCCAAAAATATATTTGGCCAAACGCATTGCCAATAACCTGAGCTTGAACCATCTCCA  
 CGCTTCGGCGATCGCCAGGTTGGTGGCCCCGGTCCAAGCCTTGGTGTAGTCTCCTCCTACCTCGGGGACAAA  
 ATTGTCTACCATAAGGTACGCCAGGCCGCTGGGGGCGACTGGAACTCTCATTTCGGGAGGAGGGGCGTTAGCTA  
 GACATTTAGATGATTTTTACGAAATCACCAGCATTCCCGTCTGGTGGGCTATGGCTTAACGGAAACGGCCCCAGTA  
 ACTAATGCCAGGTGCATAAACATAATTTGCGCTATTCTCTGGCCGCCCATTCCTTTACAGAAAATTCGATTGTTG  
 ACATGAAAACCAAGGAGGATTTGCCCCCGAAACCCAAGGTCTTGTGCTAATCCGTGGTCCCCAGGTGATGCAGGG  
 CTATTACAACAAGCCGGAAGCCACCGCCAAAGTTTTAGACCAGGAAGGCTGGTTCCGACAGCGGTGACTTAGGCTGG  
 GTAACGCCCAAAATGATTTGATTCTACCGGTCCGGCCAAGGACACCATTGTGCTCAGTAACGGGGAAAATGTGG  
 AACCCCAACCCATTGAAGATGCCTGTTTACGCAGTGCCTACATTGACCAGATTATGCTGGTGGGCCAGGATCAAAAA  
 TCCTTGGGGCTTTGATTGTGCCAACTTCGATGCATTGCAAAAATGGGCAGAGACGAAAATTTACAAATCACCGTG  
 CCGGAACCGTCCGGCTAGCAGTGAAGGGATGCAGGCTAGTGGTTGTATGACCCCCAAGTGGTGGGGTTAATGCGG  
 TCGGAGTTGCATCGGGAAGTGCAGGATCGCCCTGGCTACCGAGCCGATGACCAGATTAAGGATTTCCGTTTTATCC  
 CAGCACCATTTCCCTGGAAAACGGCATGATGACCCAAACCTGAAGCTCAAACGACCAGTGGTAACCCAAACTTAT  
 CAACATTAATTGACGAAATGTTTTAA

3'-CTGCTTTACAAAATTTGATCAAAAATA-5'

←---Aas\_R3 as Reverse primer

**Figure 2.1** The *aas* gene sequence and primer location. The yellow and blue highlight represented the annealing sequences and the restriction sequences including *Xba*I site for Aas\_F3 forward and *Spe*I site for Aas\_R3 reverse primer, respectively.

### 2.2.2 Amplification of *aas* gene fragment by polymerase chain reaction (PCR)

To amplify *aas* gene fragments using genomic DNA of *Synechocystis* cells as template, the components in each reaction as the Table 2.5 below was used and the Aas\_F3 and Aas\_R3 primers were used as forward and reverse primers, respectively.

**Table 2.5** The components of PCR reaction

Reagents	Volume ( $\mu\text{L}$ )
1. Distill water	31
2. 5xGC buffer	10
3. 10 mM dNTP mix	1
4. 10 mM Forward_ Primer	2.5
5. 10 mM Reverse_ Primer	2.5
6. DNA template	2.5
7. DNA polymerase	0.5
Total volume	50

After that, all reagents were mixed by vortexing and then amplified the *aas* gene fragment by PCR with this condition as detailed in the Table 2.6 below. From the PCR condition, the steps 2 to 4 were repeated for 29 cycles.

After the PCR product of *aas* gene fragments were obtained, it was purified by GeneJet PCR purification kit as described in following. The 1X DNA binding buffer



was added into the PCR product and mixed by vortexing. After that the solution was transferred to column and centrifuged at 12,000 rpm (21,009  $x g$ ), for 1 min. Then, the flow through fraction was discarded and added by 700  $\mu\text{L}$  of washing buffer and immediately centrifuged for 1 min. The next, the flow through fraction was discarded and centrifuged at 12,000 rpm (21,009  $x g$ ), for 1 min (to completely remove buffer). After that, the column was transferred to a new 1.5 mL tube and 50  $\mu\text{L}$  of the elution buffer was added into the column and centrifuged after that for 1 min, at 12,000 rpm (21,009  $x g$ ). Then, the quantitative of PCR product was checked using 1% agarose gel electrophoresis and compared its size with the DNA marker.

**Table 2.6** PCR condition used for *aas* amplification using genomic DNA as template.

PCR condition steps	Temperature and time
1. Initial denaturation	98°C, 1 min
2. Denaturation	98°C, 10 s
3. Annealing	44°C, 30s
4. Extension	72°C, 1 min
5. Final extension	72°C, 5 min
6. Hold on	4°C

### 2.2.3 Construction of recombinant plasmid

To construct recombinant plasmid (namely, RcAas), *aas* gene fragment and pEERM vector were digested with the same restriction enzymes of *Xba*I and *Spe*I. The *aas* gene fragment and pEERM vector were separately added with 10X Fast digestion buffer. After that, the restriction enzymes (1 000 ng sample: 1  $\mu$ L restriction enzyme) including *Xba*I and *Spe*I were added and adjusted with distilled water to final reaction volume. Then, those solutions were incubated in 37°C for 30 min. Next, the digested product were purified by DNA clean purification kit.

The ligation between digested *aas* gene fragment and digested pEERM vector was then conducted by 9  $\mu$ L of digested *aas* gene fragment was added into the 1  $\mu$ L of digested pEERM vector. Then, 2  $\mu$ L of 2X ligation buffer, 7  $\mu$ L of distilled water and 1  $\mu$ L of T4 ligase enzyme were sequentially added into the solution. After that, the solution was mixed by vortexing and incubated at room temperature for 1 hr. The ligated solution was stored in -20°C before used.

After the recombinant plasmid RcAas was successfully constructed, it was transformed into the competent cell *E. coli* DH5 $\alpha$ . Firstly, 10  $\mu$ L of RcAas plasmids were added into 90  $\mu$ L of competent cells. Then, the reaction was chilled on ice for 30 min. After that, the mixture was incubated in 42°C for 1 min and immediately chilled on ice for 5 min. Next, 900  $\mu$ L of LB medium was added into the reaction and then incubated in 37°C, 250 rpm for an hour. After that, the reaction was centrifuged 1 min, at 12,000 rpm (21,009  $\times$  g) and 900  $\mu$ L of the supernatant was discarded. The cell pellets were resuspended by pipetting and further spreaded by spreader on LB agar plate containing antibiotic chloramphenicol (35 $\mu$ g/mL) for selection of the positive colony. Lastly, the LB agar plate was incubated in 37°C for overnight.

The next step is the selection of the positive colony containing *RcAas* plasmid by Colony PCR using a specific pair of primer including Aas\_F3 and Aas\_R3 primers as in Table 2.5. Then, the positive colony was selected and cultivated in LB media containing antibiotic chloramphenicol and later incubated at 37°C for overnight. After that, *RcAas* plasmids were extracted by plasmid extraction kit and completely digested with restriction enzymes including *Xba*I and *Spe*I for agarose gel electrophoresis. Moreover, the *RcAas* plasmids were also confirmed by sequencing.



### 2.2.4 Natural transformation

After the obtained RcAas plasmid was correctly confirmed, it was transformed into *Synechocystis* sp. PCC 6803 cells by natural transformation method. First of all, The *Synechocystis* cells were cultivated until O.D.730 reaching about 0.5. Then, 10 µg of the recombinant plasmid RcAas was added into 1 mL of condensed *Synechocystis* cells and incubated at 28°C for 6 hrs by inverting the mixture tube every 2 hrs. After that, the transformed *Synechocystis* cells were spread on BG<sub>11</sub> agar plate containing 35 µg/mL chloramphenicol and cultivated at 28°C for 2-3 weeks. Later, the grown colonies were randomly selected and identified as the positive colony by Colony PCR using specific pair of primers shown in Table 2.7 in order to confirm gene location and segregation of *Synechocystis* transformants with overexpressing *aas* gene (Ox-Aas).

**Table 2.7** Primers that used to check the gene location in *aas*-overexpressed strains.

Pair no.	Forward primer	Reverse primer	Annealing temperature (°C)	Expected PCR product sizes (Kb)
1	UUSF_PsbA2	Cm_SR	55	2.5
2	pE_SF	pE_SR	55	0.35
3	Cm_SF	Aas_SR	55	2.5
4	Aas_F6	Cm_SR	55	1.4
5	UUSF_Aas	Cm_sR	55	2.5

Moreover, the empty pEERM vector was also transformed into *Synechocystis* cells in order to construct the control WT strains of *Synechocystis* cell containing pEERM vector. The control WT strain was performed from the same natural transformation process and could be cultivated on BG<sub>11</sub> agar medium containing antibiotic chloramphenicol. The survived colonies were randomly selected and checked as the positive colony by Colony PCR using UUSF\_PsbA2 and Cm\_SR as primers. The annealing temperature was at 55°C and its expected PCR product size was 500 bp.

## **2.3 Determinations of growth, pigment contents and oxygen evolution rate**

### **2.3.1 Growth measurement**

Wild type (WT), control WT and *aas*-overexpressing (Ox-Aas) strains were cultivated on BG<sub>11</sub> agar plate. After that, they were transferred into liquid BG<sub>11</sub> medium. For both control WT and overexpressing strains, BG<sub>11</sub> medium used was added 35µL/mL of antibiotic chloramphenicol and cultivated until the O.D. 730 nm was about 0.5 which used as the starter before transferring into new BG<sub>11</sub> medium. The beginning of cultivation, *Synechocystis* cell culture was harvested and measured its O.D. 730 nm using spectrophotometer every 24 hours for 15 days.

For nutrient modified conditions, the BG<sub>11</sub> medium was modified including nitrogen-deprived (BG<sub>11</sub>-N), phosphorus-deprived (BG<sub>11</sub>-P) and nitrogen/phosphorus-deprived (BG<sub>11</sub>-N/P) conditions. Firstly, all strains studied were cultivated under normal BG<sub>11</sub> medium until reaching to log phase of cell growth. Then, the log phase growing cells were harvested by centrifugation at 6,000 rpm (4,025  $\times$  g) speed and transferred to the new media including normal BG<sub>11</sub> medium, BG<sub>11</sub>-N, BG<sub>11</sub>-P and

BG<sub>11</sub>-N/P conditions. After that, the treated cells were harvested and measured its O.D. 730 nm every 24 hours for 8 days.

For the condition of acetate addition, BG<sub>11</sub> medium was modified by adding various concentrations of acetate including 20 mM and 40 mM. In this treatment, cells were cultivated under these acetate conditions compared with the normal BG<sub>11</sub> medium (0 mM acetate). The initial O.D. 730 nm was about 0.150 as the start of cultivation. After that, the treated cells were harvested and measured its O.D. 730 nm every 24 hours for 15 days.

### 2.3.2 Determination of intracellular pigments

Cultured cells were harvested and measured for their intracellular pigment contents. One mL of cell cultures were centrifuged for 10 min at 12,000 rpm (21,009  $\times$  g). Then, the liquid phase was discarded and added 1 ml of DMF (dimethyl formamide) in order to extract the pellets. After that, the mixture was vortexed and centrifuged for 10 min at 12,000 rpm (21,009  $\times$  g). Finally, the extracted solution was measured its absorbance at 461, 625 and 664 nm, respectively, using spectrophotometer. And then, the results were calculated by following equations;

$$\text{Chlorophyll } a \text{ contents } (\mu\text{g} / \text{cell}) = [(12.1 \times \text{OD}_{664}) - (0.17 \times \text{OD}_{625})] / \text{Total cells}$$

(Moran, 1980)

$$\text{Carotenoid contents } (\mu\text{g} / \text{cell}) = [(\text{OD}_{461} - (0.046 \times \text{OD}_{664})) \times 4] / \text{Total cells}$$

(Chamovitz, 1993)

$$\text{Total cells (cells / mL)} = (\text{OD}_{730} / 0.25) \times 10^8$$

(Jantaro *et al.*, 2003)

### 2.3.3 Determination of oxygen evolution rate

The oxygen evolution rate is normally represented the photosynthetic efficiency of cyanobacteria cells. Firstly, five mL of cell cultures were centrifuged  $5,000 \times g$ , for 10 min at  $25^{\circ}\text{C}$ . Then, the aqueous phase was discarded and the cell pellets were resuspended by adding 2 mL of BG<sub>11</sub> medium. After that, the solution was incubated under darkness for 30 min and measured for the oxygen evolution by Clark type oxygen electrode. The data are shown in the relative of O<sub>2</sub> content which produced during the photosynthesis process by calculating as following equation;

$$\text{Oxygen evolution } (\mu\text{mol/mL/min/mg chl } a) = \frac{\text{slope } (\mu\text{mol})}{\text{Total sample (mL)}} \times \frac{\text{mL}}{\text{mg Chl } a} \times \frac{60 \text{ min}}{1 \text{ hr}}$$

The data in term of the relative O<sub>2</sub> evolution rate were represented as  $\mu\text{mol/mg Chl } a/\text{hr}$ .

## 2.4 Determinations of lipid and unsaturated lipid contents

### 2.4.1 Quantitative screening by Sudan Black B staining

The Sudan Black B staining was dyed on polar lipids onto the membrane. One mL of cell cultures was collected by centrifugation at 12,000 rpm ( $21,009 \times g$  for 10 min. After that, the cell pellets were smeared on the glass slide and left for 10 min to evaporate the solution. Then, Sudan Black B staining solution was dropped onto to the pellets and left for 5 min. The excessed Sudan Black B solution was removed by safanin solution and left for 10 min. Next, the sample was destained using distilled water. Finally, the glass cover was put on the top of stained cells and observed visually under the light microscope.

#### 2.4.2 Determinations of total lipid contents

The acid-dichromate oxidation reaction method (Fales, 1971) was used to determine for total lipid contents. Five mL of cell cultures was collected by centrifugation at 6,000 rpm ( $4,025 \times g$ ) for 10 min. After that, 2 mL of  $H_2SO_4$  was added into the pellet and mixed by vortexing to disrupt the cells. Then, 2 mL of  $K_2CrO_7$  solution was added into the mixture and put the tube in boiled water located on the hot plate for 30 min. Next, the mixture was cooled down to the room temperature and then 2 mL of distilled water was added and mixed together. Finally, lipid contents were determined by measuring its absorbance at 600 nm with spectrophotometer and further calculated the lipid contents using the standard curve of lipid contents in Appendix H. The reaction mixture without  $K_2CrO_7$  solution was also measured its absorbance which used as the background measurement of this reaction.

#### 2.4.3 Determinations of total unsaturated lipid contents

The colorimetric sulfo-phosphovanillin (SPV) method (Cheng *et al.*, 2011) was used to determine total unsaturated lipid contents. Five mL of cell cultures was collected by centrifugation at 6000 rpm ( $4,025 \times g$ ) for 10 min. After that, 2 mL of  $H_2SO_4$  was added into the pellet tube and mixed by vortexing to disrupt the cells. Next, the mixture was boiled on the hot plate for 30 min and left it cooled down to the room temperature and then 2 mL of  $H_3PO_4$ : vanillin (1:1) was added and mixed together. Finally, the unsaturated lipid content was determined by measuring its absorbance at 540 nm with spectrophotometer and normalization with the standard curve of unsaturated lipid contents in Appendix I. The reaction solution without  $H_3PO_4$ : vanillin



solution was also measured for the absorbance which used as the background measurement of this reaction.

The levels of lipid and unsaturated lipid contents were represented as a percentage of lipid contents per milligram (mg) of cell dry weight (%w/w CDW). Cell dry weight was performed as following procedures. About 2-5 mL of cell cultures was harvested by centrifuging at 6,000 rpm ( $4,025 \times g$ ) for 10 min. Then, the cell pellets were dried in 80°C oven for overnight. After that, the constant weight of the cells in term of mg were measured by the digital balance.

## **2.5 Determination of expression levels of genes related to fatty acid biosynthesis**

### **2.5.1 The extraction of total RNA**

Extraction of total RNA and reverse transcription polymerase chain reaction (RT-PCR) technique were used for the determination of gene expression levels. Firstly, 10 mL of both Ox-Aas and WT cell cultures (O.D.<sub>730</sub> of about 0.3-0.5) were harvested centrifuging at 6,000 rpm ( $4,025 \times g$ ) for 5 min. The obtained pellets were resuspended in 250  $\mu$ L of DEPC-treated water and 750  $\mu$ L of Trizol<sup>®</sup> reagent mixing with 0.2 g of acid washed-glass beads. After that, the mixture was incubated at 65°C for 5 min. Then, the cells were immediately disrupted by vortexing for 2-3 times until the cells was broken and left the reaction tube at room temperature for 1 min. Next, 200  $\mu$ L of CHCl<sub>3</sub> was added into the mixture and left it at room temperature for 5 min, then centrifuged at 4°C with 12,000 rpm ( $21,009 \times g$ ) for 15 min. After that, 400  $\mu$ L of supernatant was transferred to a screw tube and RNA was precipitated by adding 500  $\mu$ L of isopropanol and incubated at room temperature for 10 min. The pellets of RNA were obtained by

centrifuging at 4°C with 12,000 rpm (21,009  $\times$  g) for 15 min and washing by an addition of 1 mL of cold 75% ethanol solution and collected by centrifuging at 4°C with 12,000 rpm (21,009  $\times$  g) for 5 min, then the RNA pellets were dried at room temperature. Finally, 20  $\mu$ L of DEPC-treated water was used to dissolve the RNA pellets and incubated at 55°C for 10 min, subsequently stored it in -20°C refrigerator until used.

### 2.5.2 Preparation of extracted RNAs

RT-PCR was performed for cDNA synthesis using RNA as the template. The contaminated DNA was removed by treating with 2.5  $\mu$ L of DNase enzyme and 2.5  $\mu$ L of DNase buffer (to final volume of 25  $\mu$ L). The enzyme activity was activated by incubating at 37°C for 20 min followed by inactivating DNase by heating at 75°C for 10 min, and subsequently added 2.5  $\mu$ L of 50 mM EDTA. Next, 2  $\mu$ L of RNA solution was diluted (50 fold) by adding 98  $\mu$ L of DEPC-treated water. After that, RNA concentration was measured its absorbance at 280 and 260 nm using spectrophotometer, and later calculated the concentration of RNA by following formula:

RNA concentration ( $\mu$ g/ $\mu$ l) =  $OD_{260} \times 0.04 \mu$ g/ $\mu$ L of RNA  $\times$  dilution factor.

Then, 2  $\mu$ g of RNA was added and adjusted with DEPC-treated water until reaching the final volume of 16  $\mu$ L. After that, 5  $\mu$ L of the RNA solution was checked by running 1% agarose gel electrophoresis.

### 2.5.3 Reverse transcription-polymerase chain reaction (RT-PCR)

Firstly, 8  $\mu\text{L}$  of total RNA (1  $\mu\text{g}$ ), 1  $\mu\text{L}$  of 10 mM dNTP and 1  $\mu\text{L}$  of hexamer as primer were mixed and adjusted the volume with DEPC-treated water (to final volume of 10  $\mu\text{L}$ ). The solution was incubated at 65°C for 5 min and chilled on ice for 1 min. After that, 2  $\mu\text{L}$  of 10x RT buffer, 4  $\mu\text{L}$  of 25 mM  $\text{MgCl}_2$ , 2  $\mu\text{L}$  of DTT, 1  $\mu\text{L}$  of RNaseOUT™ (40U/  $\mu\text{L}$ ) and 1  $\mu\text{L}$  of SuperScript™III RT (200U/ $\mu\text{L}$ ) were sequentially added to each RNA tube (10  $\mu\text{L}$ ). Next, cDNA synthesis mixture was incubated at 25°C for 10 min, 50°C for 50 min and 85°C for 5 min using PCR machine for synthesized cDNA. And then, cDNA tube was chilled on ice and 1  $\mu\text{L}$  of RNaseH was added into the solution, sequentially activated the enzyme by incubated at 37°C for 20 min in order to remove contaminated RNA. After that, cDNA was stored at -20°C before use. Finally, cDNA was used as the template in PCR reaction using various specific pairs of primers. The PCR product was checked by agarose gel electrophoresis. The band intensity was measured by Gel Documentation system.

### 2.6 Sequence alignment and phylogenetic tree

The amino acid sequences of *aas* gene in *Synechocystis* sp. PCC 6803 were obtained from Cyanobase (<http://genome.kazusa.or.jp/caynabase>) database. Then, the sequence was aligned to other species and organisms using Blast program from NCBI database (<http://blast.ncbi.nlm.nih.gov/Blast.cgi>). After that, the sequences of *aas* from other organisms were aligned by Multiple alignment and phylogenetic tree of full-length of *aas* genes were performed using Clustal Omega program.

## CHAPTER III

### RESULTS

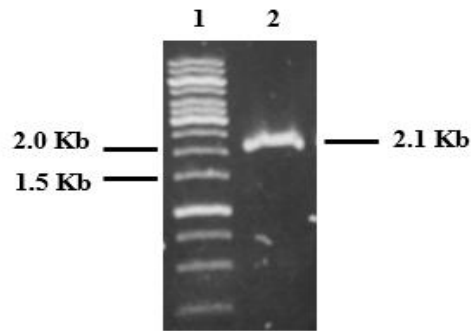
#### 3.1 The *Synechocystis* sp. PCC 6803 construct with overexpressing *aas* gene

##### 3.1.1 Construction of recombinant plasmid

Genomic DNA of cyanobacterium *Synechocystis* sp. PCC 6803 was used as the template for amplification of whole *aas* gene sequence. In Figure 3.1, agarose gel electrophoresis showed an amplified fragment of *aas* gene. From this experiment, the temperature of annealing step was 44°C, the PCR product size was about 2.1 Kb when compared with marker sizes. This band size was corresponding to the expected size of 2.1 Kb which reported in Cyanobase database.

In the next step before ligation, both pEERM vector and *aas* gene fragment were digested with the same restriction enzymes including *Xba*I and *Spe*I and analyzed by 1% agarose gel electrophoresis. In Figure 3.2A, pEERM vector was completely digested and shown only one band with the size of 3.6 Kb whereas the digested *aas* gene fragment (Figure 3.2B) was shown with a band size of about 2.1 Kb.

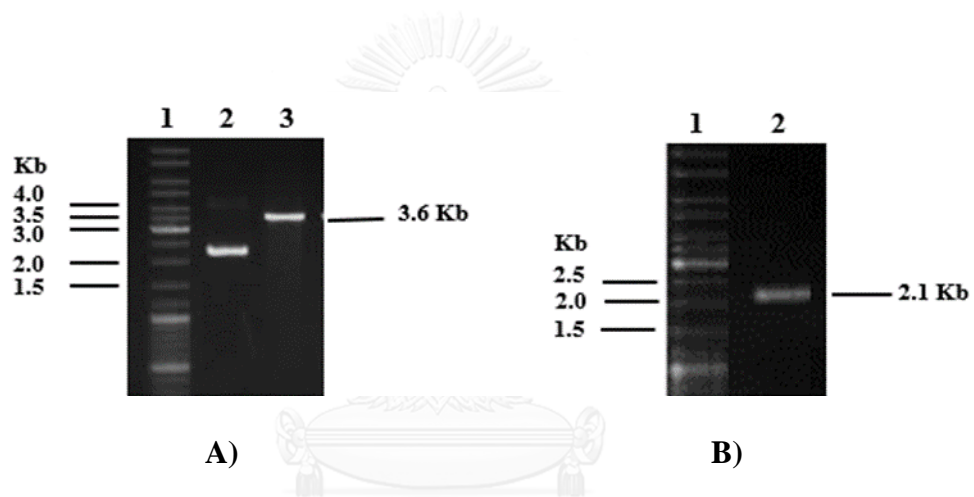
After the selection of recombinant clone, the extracted recombinant plasmid RcAas from each clone was digested by *Xba*I and *Spe*I restriction enzymes to confirm its correct size (Figure 3.3B). This result showed that RcAas from clones No.1 and 4 digested by these restriction enzymes gave 2 fragments with their sizes of about 3.5 and 2.1 Kb, respectively.



**Figure 3.1** Agarose gel electrophoresis of PCR product of *aas* gene fragment:

lane 1) DNA marker

lane 2) PCR product of *aas* gene fragment (2.1 Kb)



**Figure 3.2** Agarose gel electrophoresis of the digested products of (A) pEERM vector and (B) *aas* gene fragment by *Xba*I and *Spe*I restriction enzymes.

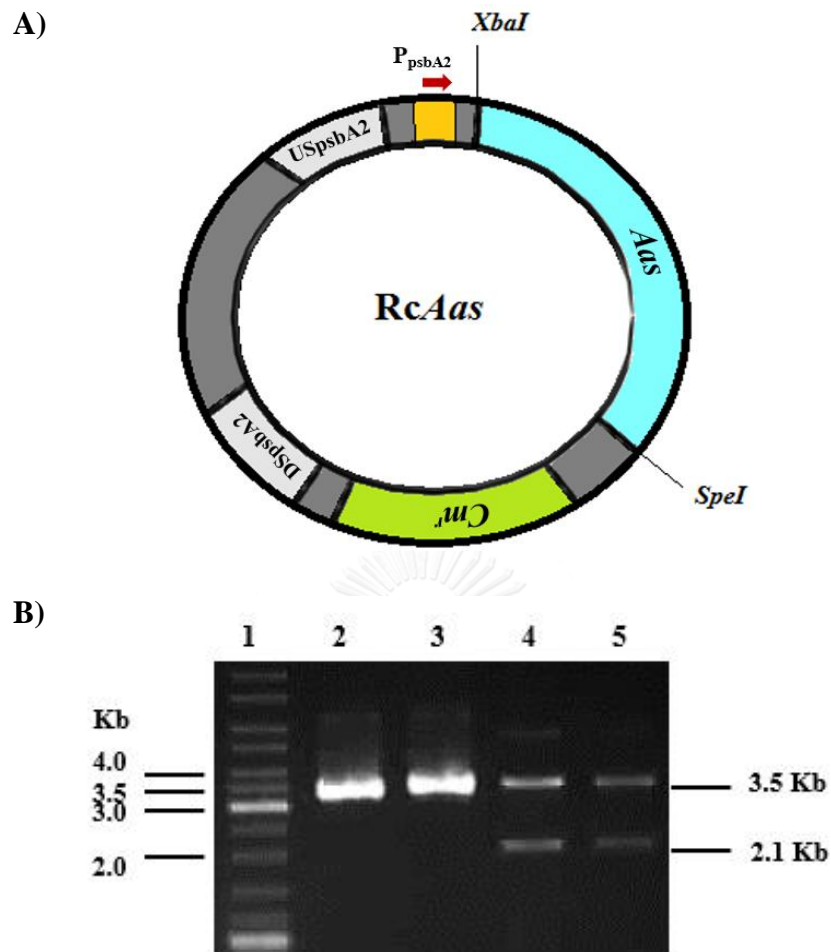
**A)** lane 1) DNA marker,

lane 2) Uncut pEERM vector

lane 3) Digested pEERM vector (3.6 Kb)

**B)** lane 1) DNA marker

lane 2) Digested *aas* gene (2.1 Kb)



**Figure 3.3** Outlined construction map of recombinant plasmid *RcAas* (A) and agarose gel electrophoresis of the digested recombinant plasmid with restriction enzymes *XbaI* and *SpeI* (B):

lane 1) DNA marker

lane 2) Recombinant plasmid *RcAas* containing *Aas* gene from clone no.1

lane 3) *RcAas* from colony no.4

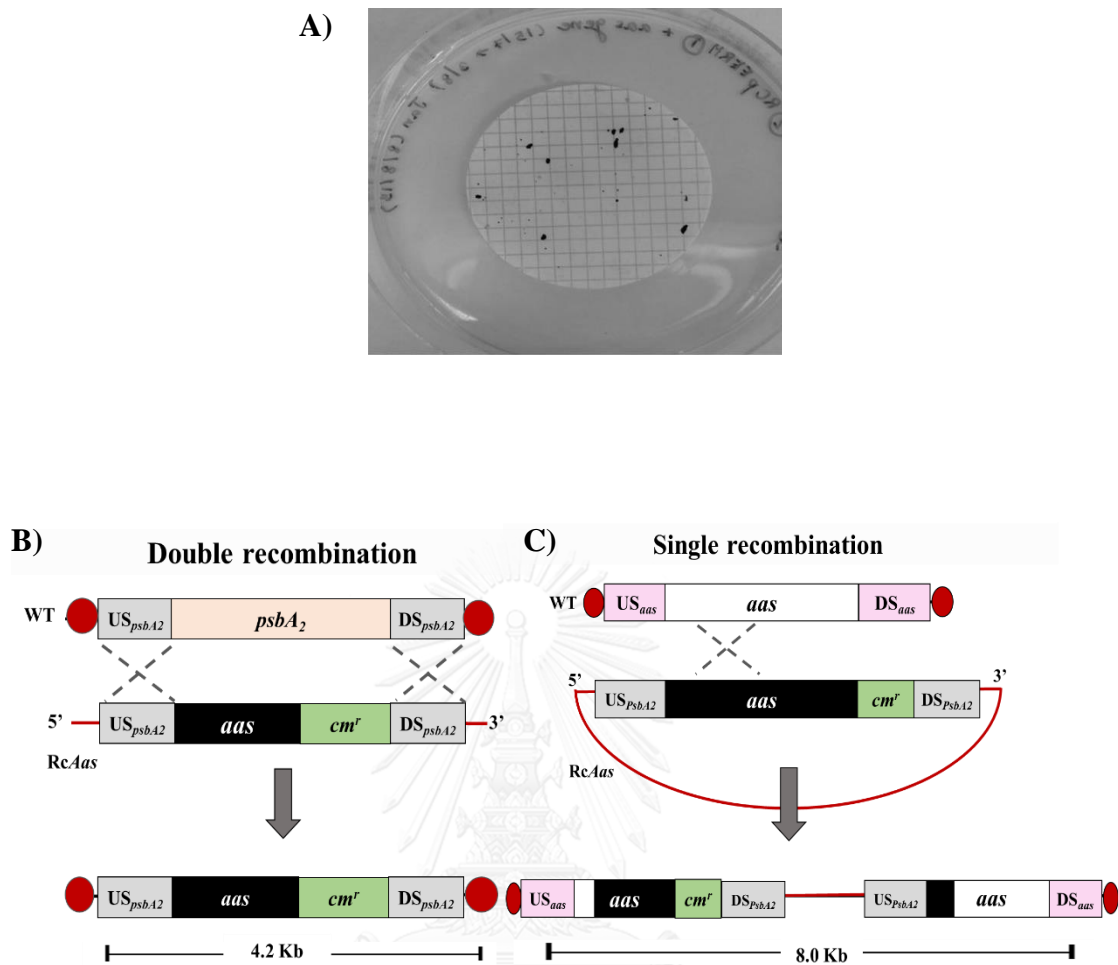
lane 4) Double-digested *RcAas* from clone no.1

lane 5) Double-digested *RcAas* from clone no.4

Later, the RcAas from clones No.1 and 4 were confirmed by sequencing using 6 primers (PsbA2\_F, Aas\_F3, Aas\_R5, Aas\_F6, Aas\_R3 and Cm\_SR) and analyzed the alignment results using EMBOSS WATER program. The recombinant plasmid containing *aas* gene, namely RcAas was successfully obtained.

### 3.1.2 Construction of *aas*-overexpressing strain of *Synechocystis*

The RcAas plasmid was transformed into *Synechocystis* sp. PCC 6803 cells by natural transformation process, then screened and selected on the BG<sub>11</sub> agar media containing antibiotic chloramphenicol (Cm). After 3-4 weeks, the survived cells were appeared as colonies on the membrane (Figure 3.4A). After that, the survived colonies were randomly picked and confirmed the gene location by PCR technique using various pairs of primers. The expected overexpression was outlined in Figures 3.4B and 3.4C corresponding to its homologous recombination. In nature, double homologous recombination was usually happened by crossing over between the sequence homologous or flanking region on each side to replace the gene fragment. In this study, *psbA2* gene was replaced by *aas* gene and its construction was efficiently targeted for *psbA2* gene disruption (Figure 3.4B). Another process is the single recombination which can rarely occurred by the foreign gene which has similarly sequences with the target gene, was inserted into the target by crossing over to generate 2 hybrids of the genes as in Figure 3.4C. Firstly, the Up-up stream of *psbA2* gene using UUSF\_PsbA2 as forward primer and Cm\_SR as reverse primer were used to check double homologous recombination. The optimum temperature of annealing step was 55°C. The expected PCR product should be 3.0 Kb. The result after using this primer pair was



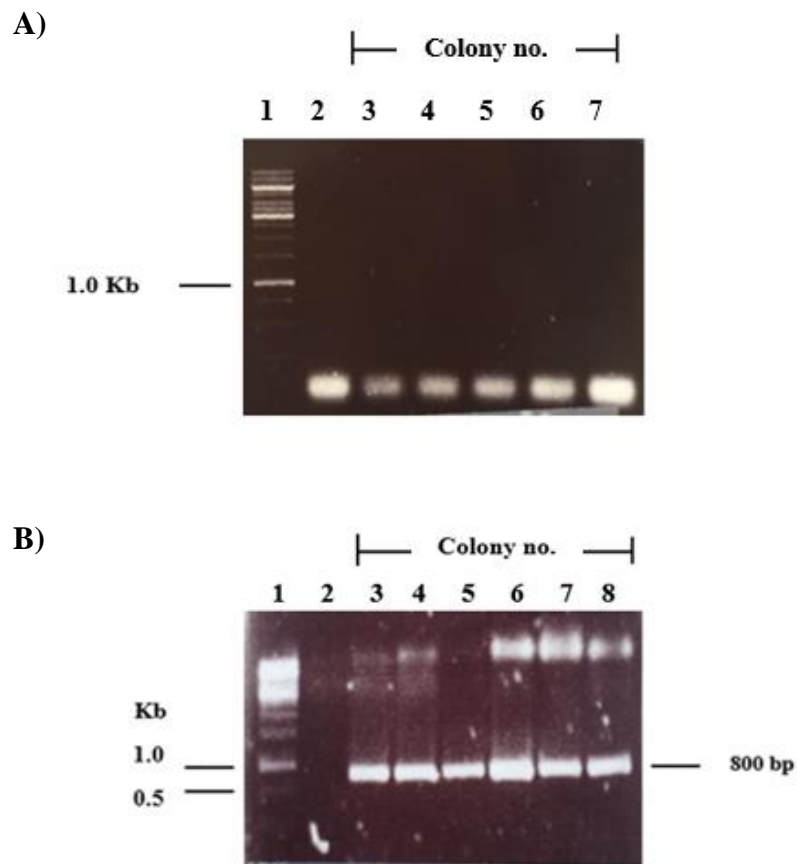
**Figure 3.4** The survived colonies appeared on BG<sub>11</sub> agar plates with 35  $\mu$ L/mL chloramphenicol after 3-4 weeks (A). Diagrams of double homologous recombination (B) and single recombination (C) in *aas*-over expressing strain of *Synechocystis* sp. PCC 6803.



shown in Figure 3.5A, the expected gene fragment size of 3.0 Kb after PCR using UUSF\_PsbA2 primer was not appeared in all samples. To check whether it was a single recombination overexpressing strain, we designed many specific pairs of primer as in Table 2.3 and the results shown in Figure 3.6.

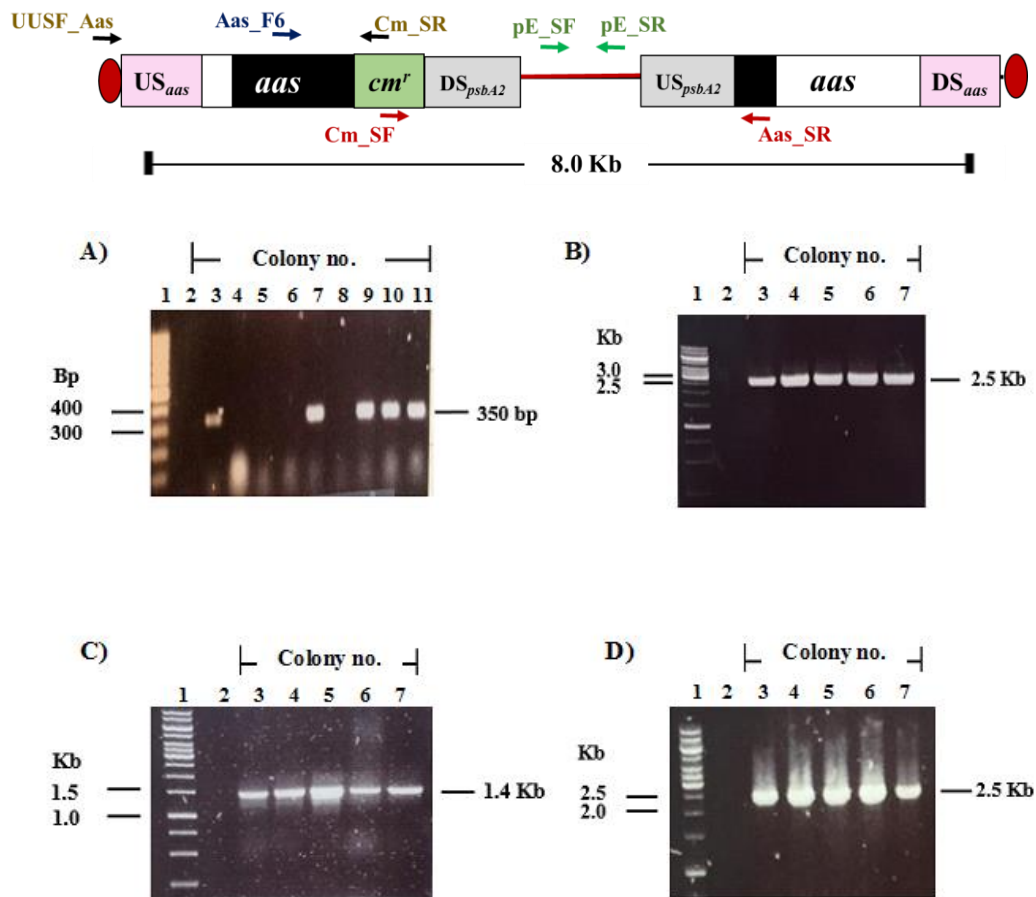
The empty pEERM vector was also transformed into *Synechocystis* sp. PCC 6803 cells in order to generate the Control WT strain. The cells were screened and selected on the BG<sub>11</sub> agar media containing antibiotic chloramphenicol (Cm). After 3-4 weeks, the survived cells were appeared on the membrane and randomly picked and sequentially confirmed the gene location by PCR technique using UUSF\_PsbA2 as forward primer and Cm\_SR as reverse primer. The expected size was 800 bp. In Figure 3.5B, this expected fragment size of 800 bp was found in all randomized colonies, the strain, namely Control WT, was successfully constructed by homologous recombination. Control WT strain was used for comparison between WT and overexpressing strains.

From the results of PCR using various pairs of primer, in Figure 3.6A, the pE\_SF and pE\_SR primers with the expected size of 350 bp were used for checking that backbone structure of pEERM vector which integrated into the genomic DNA of WT. The expected PCR transformants were found in 5 colonies. After that, these colonies were amplified by different pairs of primers. In Figure 3.6B, the use of Cm\_SF and Aas\_SR primers with the expected size of 2.5 Kb, was found in all colonies which suggested that *aas* gene located after *cm* resistance cassette gene. In Figure 3.6C, the use of Aas\_F6 and Cm\_SR primers with the expected size of 1.4 Kb, was also found in all colonies which suggested that *aas* gene located before *cm* resistance cassette gene



**Figure 3.5** Confirmation of gene location using UUS\_PsbA2 and Cm\_SR as forward and reverse primers, respectively in (A) Ox-Aas strain (3.0 Kb) and (B) Control WT (800 bp).

- |           |  |           |  |
|-----------|--|-----------|--|
| <b>A)</b> | Ox-Aas strain as temple                        | <b>B)</b> | Control WT strain as temple                    |
|           | lane 1) DNA marker                             |           | lane 1) DNA marker                             |
|           | Lane 2) Negative control                       |           | Lane 2) Negative control                       |
|           | (using WT as the template)                     |           | (using WT as the template)                     |
|           | lane 3-7) PCR product of each colony (3.0 Kb). |           | lane 3-7) PCR product of each colony (800 bp). |



**Figure 3.6** Confirmation of gene location of single homologous recombination in Ox-Aas strain using various pairs of primers:

- |   |   |
|---|---|
| <p><b>A)</b> pE_SF and pE_SR primers<br/>(the expected size of 350 bp)<br/>lane 1) DNA marker<br/><br/>Lane 2) Negative control<br/>(using WT as the template)<br/>lane 3-11) PCR product of each colony</p>  | <p><b>B)</b> Cm_SF and Aas_SR primers<br/>(the expected size of 2.5 Kb):<br/>lane 1) DNA marker<br/><br/>Lane 2) Negative control<br/>(using WT as the template)<br/>lane 3-7) PCR product of each colony</p>   |
| <p><b>C)</b> Aas_F6 and Cm_SR primers<br/>(the expected size of 1.4 Kb):<br/>lane 1) DNA marker<br/><br/>Lane 2) Negative control<br/>(using WT as the template)<br/>lane 3-7) PCR product of each colony</p> | <p><b>D)</b> UUSF_Aas and Cm_SR primers<br/>(the expected size of 2.5 Kb):<br/>lane 1) DNA marker<br/><br/>Lane 2) Negative control<br/>(using WT as the template)<br/>lane 3-7) PCR product of each colony</p> |

In Figure 3.6D, the use of UUSF\_Aas and Cm\_SR primers with the expected size of 2.5 Kb suggested that whole *aas* gene located before *cm* resistance cassette gene in all colonies. Consequently, the results confirmed that the obtained Ox-Aas transformant was successfully constructed by single recombination which generated two hybrid of *aas* gene. The first, *aas* gene fragment was located after the *aas* promoter site and the second, *aas* gene fragment was located after *cm* resistance cassette gene and *PsbA2* promoter site which come from pEERM vector (Figure 3.6).

### 3.2 Multiple alignment and phylogenetic analysis of acyl-ACP synthetase

The result of multiple alignment and phylogenetic tree from *Synechocystis* sp. PCC 6803 and other know species were performed by multiple sequence alignment, Clustal Omega program (1.2.1) and the phylogenetic tree was constructed by Tree View software. From the database of Cyanobase reported that *aas* gene (*slr1906*) encodes a protein related to fatty acid/phospholipid synthesis, namely Acyl-acyl carrier protein (ACP) synthetase which was functioned to incorporate free fatty acids into fatty-acyl ACP, the substrates of complex lipid synthesis (Kaczmarzyk and Fulda, 2010). The amino acid multiple alignment of *Synechocystis* AAS with known other species was shown in Figure 3.7. The identity percentage of *Synechocystis* sp. PCC 6803 AAS protein to AAS protein of unicellular cyanobacterium *Synechococcus elongatus* sp. PCC 7942, YP\_399935 encoded Acyl-ACP synthetase shared highly conserved sequence with 55%. When aligned it with the higher plant, the identity percentages of *Arabidopsis thaliana* NP\_193143 gene encoded putative acyl-ACP synthetase/ligase (AtAAE15) shared 39% whereas the identity percentage with *Escherichia coli* strain K-12 MG1655, EG11679 encoded 2-acylglycerophosphoethanolamine acyltransferase/

acyl-ACP synthetase was 25%. Moreover, the putative amino acid residues were potentially predicted as coded acyl-ACP synthetase protein presented in *Arabidopsis thaliana*, *Synechocystis* sp. PCC 6803 and *Synechococcus* sp. PCC 7942. The phylogenetic relationships of AAS proteins of *Synechocystis* and known other organisms were shown in Figure 3.8. The nucleotide sequence of *Synechocystis* PCC 6803 AAS was closely grouped in the same clade with bacteria *Bacillus subtilis* strain BEST 7613, cyanobacterium *Synechocystis* sp. PCC 6714, bacteria *Nocardia brasiliensis* ATCC 700358 and *Aeromonas veronii* strain B565, respectively.





```

E.coli          ---YRIVP---ELVYD-----RSCTVLFGTSTFLGHYARF-----A-----
Arabidopsis    PNYIVSVPLVYETLYSGIQKQISASSAGRKFLALTLIKVSMAYMEMKRIYEGMCLTKEQK
SynPCC6803    PHHIVGVPRLWESLYEGVQKTFREKSPGQKLNFFFGISQKYILAKRIANNLSLNHLHA
SynPCC7942    PQFMVSVLRLWESIYEGVQKQFREQPAKKRRLIDTFFGLSQRVYLARRRWQGLDLLALNQ
                *   *   :*.
                : :   :

E.coli          -----NPDY-----FY-----RLRYVVAGAEKIQESTKQ
Arabidopsis    PPMYIVAFVDWLWARVIAALLWPLHMLAKKLIYKKIHSSIG-ISKAGISGGGSLPIH-VD
SynPCC6803    SAI-----ARLVARCQALVLSPLHYLGDKIVYHKVRQAAGGRLETLISGGGALARH-LD
SynPCC7942    SPA-----QRLAEGVRMLALAPLHKLGDRLVYGKVRREATGGRIRQVISGGGSLALH-LD
                * . : . : : * . :

E.coli          LWQDKFGLRLILEGYGVTECAPVVSINVPMAPGTGVRILPGMDARLLSVPG-----IEE
Arabidopsis    KFFEAIQVILQNGYGLTETSPVVCARTLSCNVLGSAGHPMHGTEFKIVDPETNNVLPPTS
SynPCC6803    DFYEITSIPVLVGYGLTETAPVTNARVHKHNLRYSSGRPIPFTEIRIVDMETKEDLPPE
SynPCC7942    TFFEIVGVDLLVGYGLTETSPVLTGRRPWHNLRGSAGQPIPGTAIRIVDPETKENRPSGD
                : : . : : * : * : * . : * : : * : :

E.coli          GGRLQLKGNINMGYLRVEKPGVLEVPVTAENVRGEMERGWDYDGDIVRFDEQ-----
Arabidopsis    KGIKVRGPPQVMKGYKPNPSTT-----KQVLNESGWFNTGDTGWIAPHHSKGRSRH
SynPCC6803    QGLVLRGPPQVMQGYYNKPEAT-----AKVLDQEGWFDSDGLGWVTPQ-----
SynPCC7942    RGLVLAQGPQIMQGYFNKPEAT-----AKAIDAEGWFDGDLGYIVGE-----
                * : : * : * : * . : * : * : * .

E.coli          --GFVQIQGRAKRAFAKI--AGEMVSLMVEQLALGVSPDKVHATAIKSDASKGEALVLF
Arabidopsis    CGGVIVLEGRAKDTIVLSTGENVE-----PLEIEEAAMRS-----
SynPCC6803    --NDLILTGRAKDTIVLSNGENVE-----PQPIEDACLRS-----
SynPCC7942    --GNLVLTRAKDTIVLTNGENIE-----PQPIEDACLRS-----
                : : * * * : : * * : . * : . : : * *

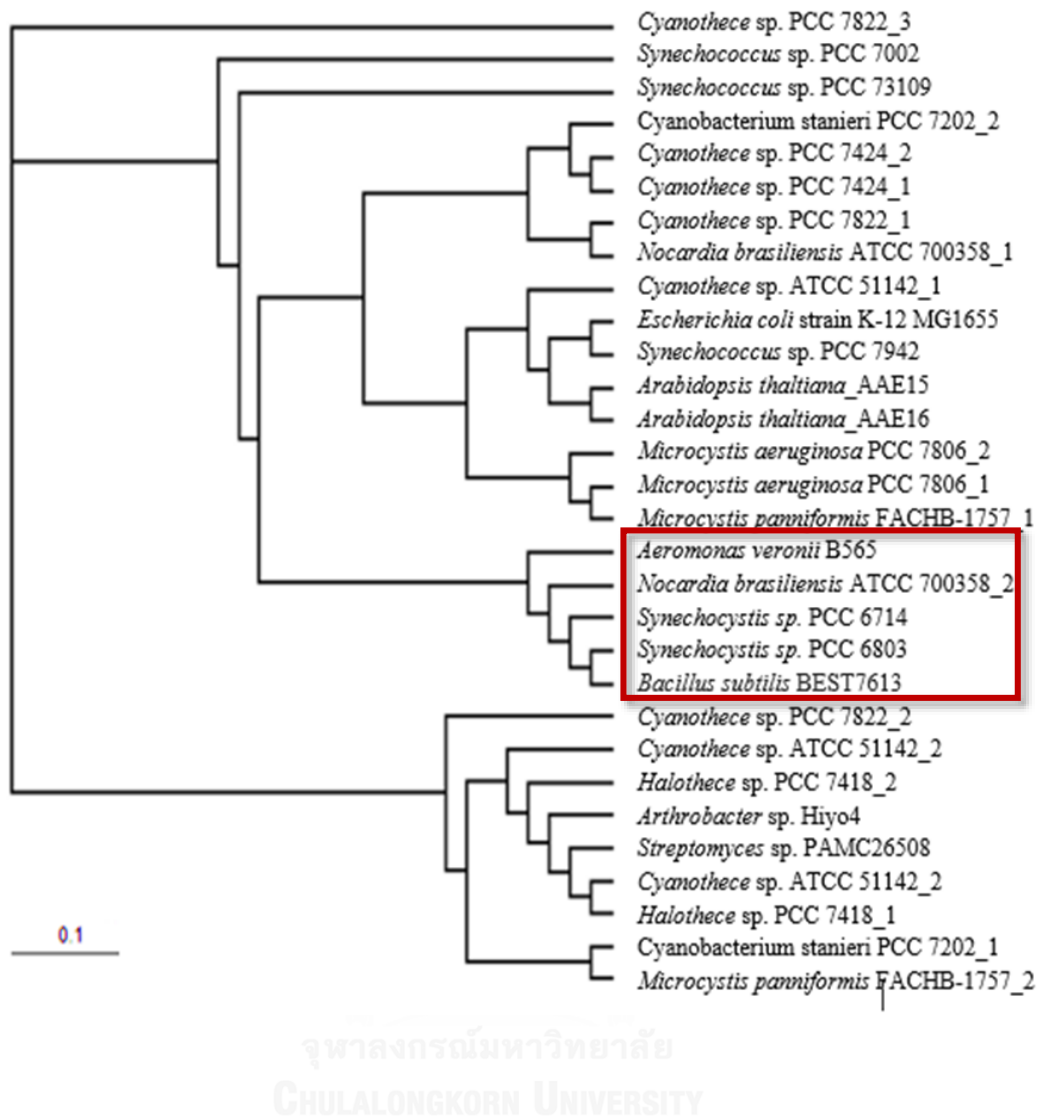
E.coli          DNELTRDKLQQYAREHGVPELAVPRDIRYLKQMPLLGSGK-----PDFVTLKSWVDE
Arabidopsis    -----RVIEQIVVIGQD RRRRLGAI I I PNKEEAQRVDPE
SynPCC6803    -----AYIDQIMLVGQD QKSLGALIVPNFDALQKWAET
SynPCC7942    -----SYISQIMLVGQD RKSLGALIVPNQEAIALWASE
                : * : : * : : * :

E.coli          AEQHD-----
Arabidopsis    TSK-----E-----TLKSLVYQEL---RK-WTSECSFQVGPVLIVDDP
SynPCC6803    KNLQITVPEPSASSEGMQASGLYDPQVVGLMRSELHREVRDRPGYRADDQIKDFRFI PAP
SynPCC7942    QGISQTD-----IQGVVQKLIREELNREVRDRPGYRIDDRIGPFRLIEEP

E.coli          -----
Arabidopsis    FTIDNGLMTPMKIRRDMMVAVKYKEEIDQLYS---
SynPCC6803    FSLENGMMTQTTLKLRPVVTQTYQHLLIDEMF----
SynPCC7942    FSMENGQLTQTTLKIRRNVAEHYAAMIDGMFESAS

```

**Figure 3.7** (Continue) Clustal Mega amino acid alignment of fatty acid/phospholipid synthesis protein AAS in *Synechocystis* sp. PCC 6803 and *Synechococcus* sp. PCC 7492 from cyanobase and other species including *Arabidopsis thaliana* (a gene encoding encoded putative acyl-ACP synthetase/ligase (AtAAE15)) and *Escherichia coli* strain K-12 (a gene encoding 2-acylglycerophosphoethanolamine acyltransferase/acyl-ACP synthetase). The specific putative amino acid residues for AAS proteins are indicated by yellow highlight.



**Figure 3.8** Phylogenetic tree of acyl-ACP synthetase (AAS) or fatty-ACP ligase of organisms including cyanobacteria bacteria and other known species from NCBI database The branch lengths of tree are proportional to calculated divergence.



**Table 3.1** Gene codes, gene indexing names, organisms and sources in cyanobacteria and other species.

ID/name	Organisms	Encoded Protein	Source
<b>Cyanobacteria</b>			
<b>Aas/Slr1906</b>	<i>Synechocystis</i> sp. PCC 6803	Acyl-acyl carrier protein (ACP) synthetase	Cyanobase
<b>Synpcc7942_0918</b>	<i>Synechococcus elongatus</i> PCC 7942	Acyl-acyl carrier protein (ACP) synthetase	
<b>gb CP007542.1</b>	<i>Synechocystis</i> sp. PCC 6714	Acyl-acyl carrier protein (ACP) synthetase	NCBI
<b>gb CP013998.1</b>	<i>Synechococcus</i> sp. PCC 73109	Acyl-acyl carrier protein (ACP) synthetase	
<b>gb CP000951.1</b>	<i>Synechococcus</i> sp. PCC 7002	Acyl-acyl carrier protein (ACP) synthetase	
<b>gb CP001291.1</b>	<i>Cyanothece</i> sp. PCC 7424	Acyl-acyl carrier protein (ACP) synthetase	
<b>gb CP000806.1</b>	<i>Cyanothece</i> sp. ATCC 51142	Acyl-acyl carrier protein (ACP) synthetase	
<b>gb CP001701.1</b>	<i>Cyanothece</i> sp. PCC 8802	Acyl-acyl carrier protein (ACP) synthetase	
<b>gb CP001287.1</b>	<i>Cyanothece</i> sp. PCC 8801	Acyl-acyl carrier protein (ACP) synthetase	
<b>gb CP002198.1</b>	<i>Cyanothece</i> sp. PCC 7822	Acyl-acyl carrier protein (ACP) synthetase	
<b>gb CP011304.1</b>	<i>Microcystis aeruginosa</i> NIES-2549	Acyl-acyl carrier protein (ACP) synthetase	
<b>AM778958.1</b>	<i>Microcystis aeruginosa</i> PCC 7806	Acyl-acyl carrier protein (ACP) synthetase	
<b>dbj AP009552.1</b>	<i>Microcystis aeruginosa</i> NIES-843	Acyl-acyl carrier protein (ACP) synthetase	
<b>gb CP011339.1</b>	<i>Microcystis panniformis</i> FACHB-1757	Acyl-acyl carrier protein (ACP) synthetase	
<b>gb CP003946.1</b>	<i>Leptolyngbya</i> sp. PCC 7376	Acyl-acyl carrier protein (ACP) synthetase	

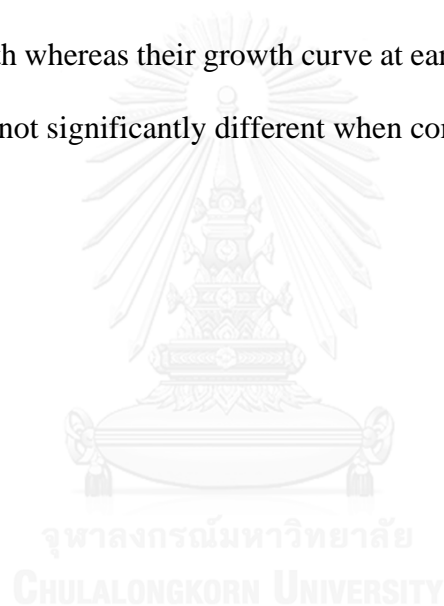
**Table 3.1** (Continue) Gene codes, gene indexing names, organisms and sources in cyanobacteria and other species.

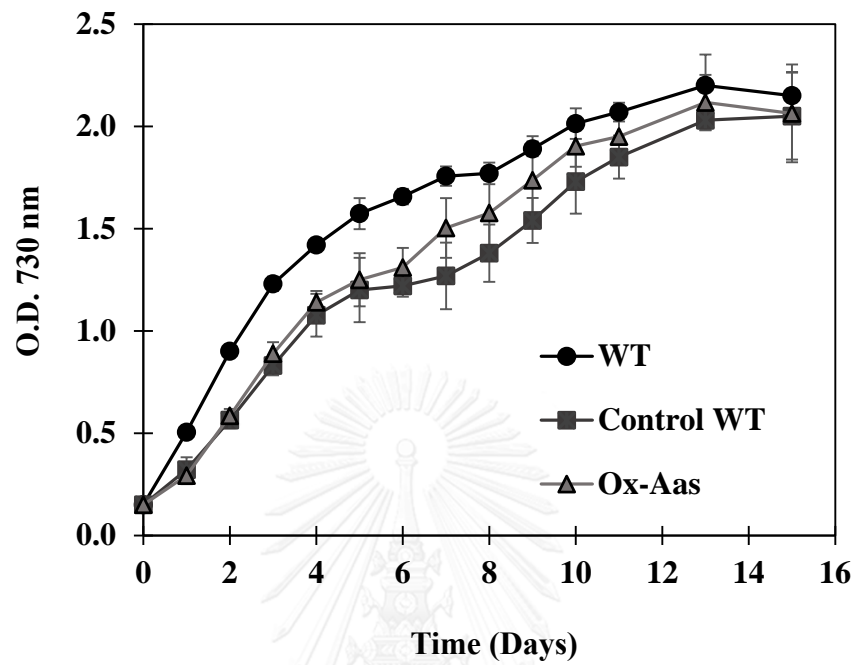
ID/name	Organisms	Encoded Protein	Source
<b>Cyanobacteria</b>			
<b>gb CP003945.1</b>	<i>Halotheca</i> sp. PCC 7418	Acyl-acyl carrier protein (ACP) synthetase	NCBI
<b><u>gb CP003940.1</u></b>	Cyanobacterium stanieri PCC 7202	Acyl-acyl carrier protein (ACP) synthetase	
<b>Bacteria</b>			
<b>dbj AP012495.1</b>	<i>Bacillus subtilis</i> BEST7613	2-acylglycerophosphoethanolamine acyltransferase	NCBI
<b>gb CP002607.1</b>	<i>Aeromonas veronii</i> B565	Acyl-acyl carrier protein (ACP) synthetase	
<b>gb CP003876.1</b>	<i>Nocardia brasiliensis</i> ATCC 700358	Acyl-acyl carrier protein (ACP) synthetase	
<b>Aas</b>	<i>Escherichia coli</i> strain K-12 MG1655	Acyl-acyl carrier protein (ACP) synthetase	
<b>gb CP003990.1</b>	<i>Streptomyces</i> sp. PAMC26508	Acyl-acyl carrier protein (ACP) synthetase	
<b>dbj AP014718.1</b>	<i>Arthrobacter</i> sp. Hiyo4	Acyl-acyl carrier protein (ACP) synthetase	
<b>Plants</b>			
<b>NP_193143</b>	<i>Arabidopsis thaliana</i>	Acyl-acyl carrier protein (ACP) synthetase	NCBI

### 3.3 Growth curve under normal and stress conditions

#### 3.3.1 Cell growth under normal condition

Those WT, Control WT and Ox-Aas cells were grown under the normal BG<sub>11</sub> condition for 15 days. In Figure 3.9, the growth pattern of all strains studied were mainly divided into 3 phases including log (L) (day 0 to 4), late log (LL) (day 5 to 10) and early stationary (ES) (day 11 to 15), respectively. The growth curve of both Control WT and Ox-Aas strains was significantly lower than WT during log and late log phases (day 1 to 10) of growth whereas their growth curve at early stationary phase of Ox-Aas and Control WT was not significantly different when compared with WT.

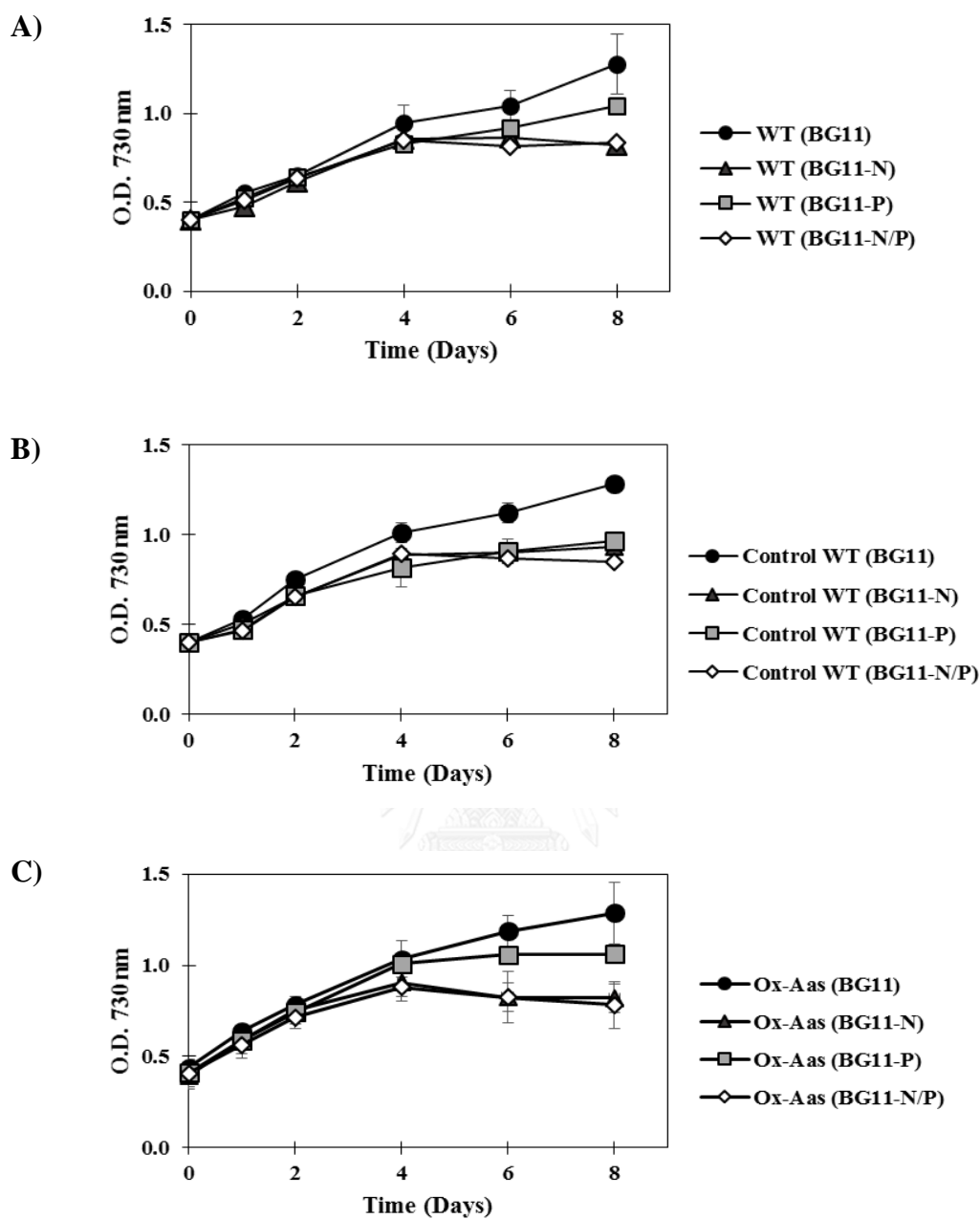




**Figure 3.9** Growth curves of *Synechocystis* sp. PCC 6803 wild type (WT), Control WT and Ox-Aas strains cells under normal BG<sub>11</sub> medium condition for 15 days. Data represented as Mean  $\pm$  S.D, (n=3).

### 3.3.2 Cell growth under nutrient deprived conditions

After all strains were grown to log phase, cells were harvested and transferred into new media including normal BG<sub>11</sub> medium, nitrogen-deprived BG<sub>11</sub> medium (BG<sub>11</sub>-N), phosphorus-deprived BG<sub>11</sub> medium (BG<sub>11</sub>-P) and nitrogen/phosphorus-deprived BG<sub>11</sub> medium (BG<sub>11</sub>-N/P), respectively. Growth curves of all strains studied were showed in Figure 3.10. In Figure 3.10A, growth of WT cells under BG<sub>11</sub>-N medium at the start of treatment (from log phase cells at day 0 to 3) were not different from normal BG<sub>11</sub> condition. After the cells were adapted in BG<sub>11</sub>-N for 4 days, the growth of WT was significantly decreased when compared with that under normal BG<sub>11</sub> medium along 8 day-treatment. On the other hand, growth of WT under BG<sub>11</sub>-P medium at the beginning of treatment at day 0 to 2 were not different with normal BG<sub>11</sub> condition. And after the adaptation in BG<sub>11</sub>-P for 4 days, the growth tendency of WT was significantly lowered than that under normal BG<sub>11</sub> condition. Likewise, WT cell growth under BG<sub>11</sub>-N/P medium at the beginning of treatment at day 0 to 3 were not different with normal BG<sub>11</sub> condition but started to decrease after 4 day-treatment. In Figure 3.10B, cell growth of Control WT under BG<sub>11</sub>-N medium showed a significant decrease after 4 day-treatment and a constant level in day 6 and day 8 of treatment. For BG<sub>11</sub>-P condition, it also decreased cell growth of Control WT strain after 4 day-treatment and kept gradually increases in day 6-8 of treatment. Similarly, it was found in BG<sub>11</sub>-N/P condition that Control WT strain was decreased on its cell growth starting from day 4 of treatment. However, the constant level of Control WT growth was observed at day 6 and day 8 of treatment. In Figure 3.10C, growth of Ox-Aas cells under BG<sub>11</sub>-N medium at the beginning of treatment at day 0 to 2 were not different with normal BG<sub>11</sub> condition. After the cells were adapted with BG<sub>11</sub>-N

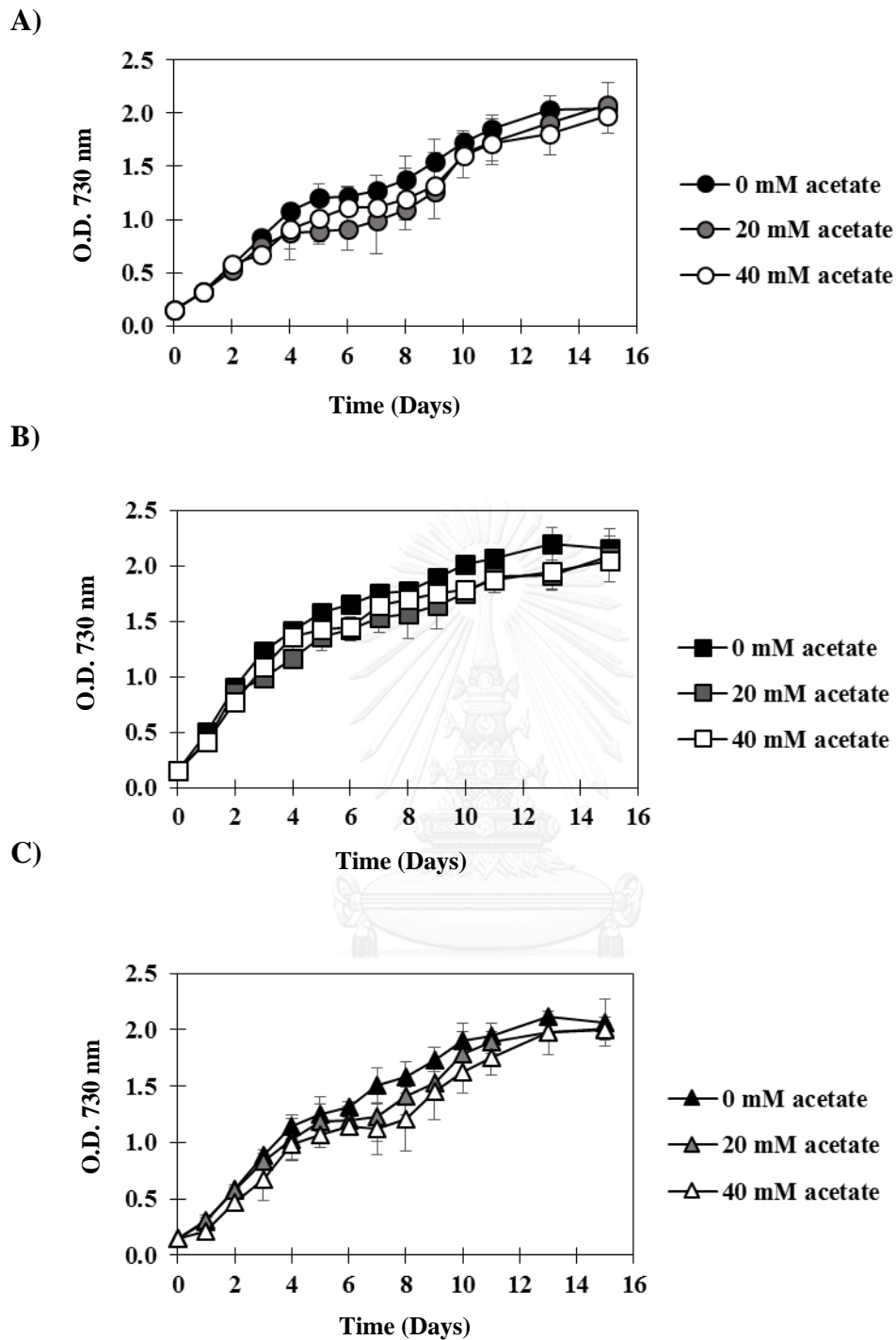


**Figure 3.10** Growth curves of WT (A), Control WT (B) and Ox-Aas (C) strains after adaptation to various nutrient deprivations, including nitrogen-deprived BG<sub>11</sub> medium (BG<sub>11</sub>-N), phosphorus-deprived BG<sub>11</sub> medium (BG<sub>11</sub>-P) and nitrogen/phosphorus-deprived BG<sub>11</sub> medium (BG<sub>11</sub>-N/P), compared with normal BG<sub>11</sub> medium (BG<sub>11</sub>). Data represented as Mean  $\pm$  S.D, (n=3).

for 4 days, the growth tendency of Ox-Aas was significantly lowered than that under normal BG<sub>11</sub> medium, and tended to decrease along day 8-treatment. On the other hand, Ox-Aas growth under BG<sub>11</sub>-P medium after adaptation for 6 days was slightly lowered when compared to normal condition. In contrast, Ox-Aas growth was decreased significantly by BG<sub>11</sub>-N/P condition when compared to normal BG<sub>11</sub> condition, and decreasing tendency was observed until day 8-treatment.

### 3.3.3 Cell growth under acetate addition

Those WT, Control WT and Ox-Aas cells were grown with their starter of O.D.730 nm at 0.150 in the various concentrations of acetate, including normal BG<sub>11</sub> medium (0 mM acetate) as control condition, normal BG<sub>11</sub> medium with 20 mM and 40 mM of acetate addition, respectively. Growth curves of all strains studied were showed in Figure 3.11. In Figure 3.11A, the growth pattern of WT studied under normal and acetate addition was not different during log (day 0-4) and early stationary (day 10 to 15) phases whereas it showed gradual decreases at late log phase (day 5-9) of growth when the amount of acetate was increased compared with control BG<sub>11</sub> condition. In Figure 3.11B, the growth pattern of Control WT studied under normal and acetate addition was not different during log (day 0-4) and late-log (day 5 to 9) phases whereas it was slightly lowered at early stationary phase (day 10-15) of growth when the amount of acetate was increased compared with control condition. In Figure 3.11C, the increase of acetate concentration of 20 and 40 mM slightly decreased on Ox-Aas cell growth when compared to control BG<sub>11</sub> condition. The decrease pattern could be observed during late-log and early stationary phases of growth.



**Figure 3.11** Growth curves of WT (A), Control WT (B) and Ox-Aas (C) strains cultured in normal BG<sub>11</sub> medium containing different concentrations of acetate including 0 mM, 20 mM and 40 mM, respectively. Data represented as Mean  $\pm$  S.D, (n=3).



### **3.4 Intracellular pigment contents**

#### **3.4.1 Intracellular pigment contents under normal condition**

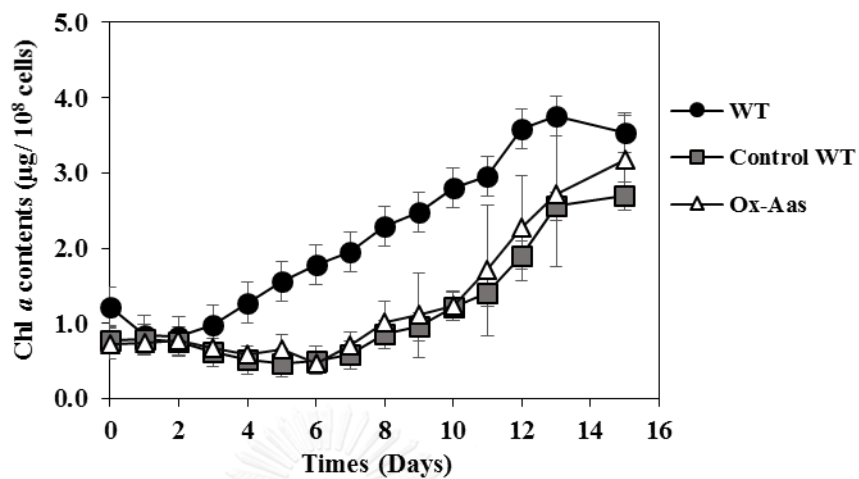
Those WT, Control WT and Ox-Aas cells were grown under normal BG<sub>11</sub> condition. The chlorophyll *a* (Figure 3.12A) and carotenoid contents (Figure 3.12B) were determined. During day 1 to 2 of cell growth, the chlorophyll *a* contents in all strains studied were not different. And then, the chlorophyll *a* contents of Control WT and Ox-Aas cells were significantly decreased after day 2-cultivation compared to WT. The carotenoid contents of all strain cells were not different during day 1-4 of cell growth and then the carotenoid contents of both Control WT and Ox-Aas strains were significantly reduced when compared to WT after day 4 of cultivation. Interestingly, the carotenoid content of Ox-Aas cells at day 15 was not different with WT. The intracellular pigment contents of both Control WT and Ox-Aas strains were not significantly different in all growth stages.

#### **3.4.2 Intracellular pigment contents under nutrient deprived conditions**

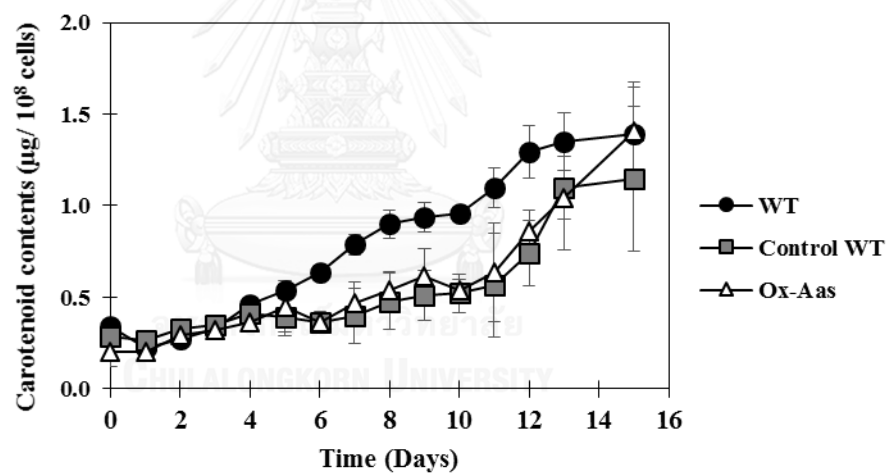
After log phase growing, WT, Control WT and Ox-Aas cells were transferred to treatments under the nutrient deprived conditions, including normal BG<sub>11</sub> medium, BG<sub>11</sub>-N, BG<sub>11</sub>-P and BG<sub>11</sub>-N/P. All strains studied were determined for the Chl *a* and carotenoid contents as shown in Figures 3.13 and 3.14. In Figure 3.13A, the Chl *a* content of WT cells under normal BG<sub>11</sub> medium tended to increase during treatment from day 1 to 8. Under a treatment of BG<sub>11</sub>-N medium, that Chl *a* content of WT shown a gradual decrease in first 4-6 days of treatment. After WT cells were treated under P-deprived condition. We found that their Chl *a* contents after 2 - 4 days of treatment

were not significantly different from normal BG<sub>11</sub> condition but it was slightly decreased after 6 days of treatment. Moreover, after 2 days of treatment under BG<sub>11</sub>-N/P condition, the Chl *a* content in WT cell was lowest among normal condition and other treatments. In Figure 3.13B, that Chl *a* content of Control WT cell under normal BG<sub>11</sub> medium was increased during treatment. Under BG<sub>11</sub>-N condition, that Chl *a* contents of Control WT were not different along 2-6 days of treatment and after that it was significantly decreased when compared to normal condition. After Control WT cells were treated by P-deprived condition, the Chl *a* content was decreased comparing to normal BG<sub>11</sub> condition. For BG<sub>11</sub>-N/P condition, their Chl *a* content in Control WT cells was not different at first 0-2 days of treatment with its cultivation under normal condition but significantly decreased after 2 days of treatment. On the other hand, Ox-Aas strain showed its Chl *a* level under BG<sub>11</sub>-N/P as similar as under BG<sub>11</sub>-N condition. In contrast, the BG<sub>11</sub>- P treatment obviously decreased its Chl *a* accumulation along 8 days of treatment (Figure 3.13C).

A)

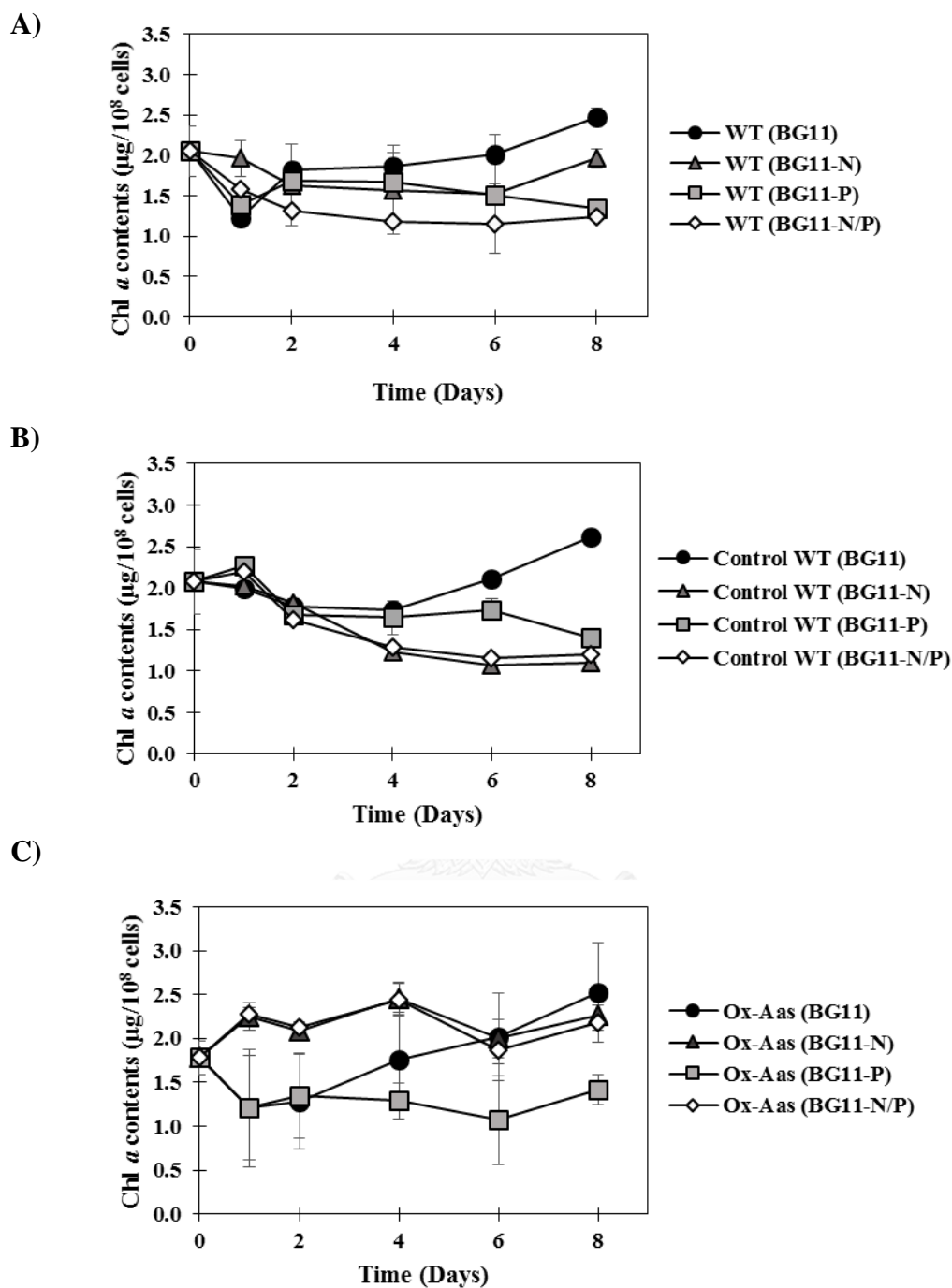


B)

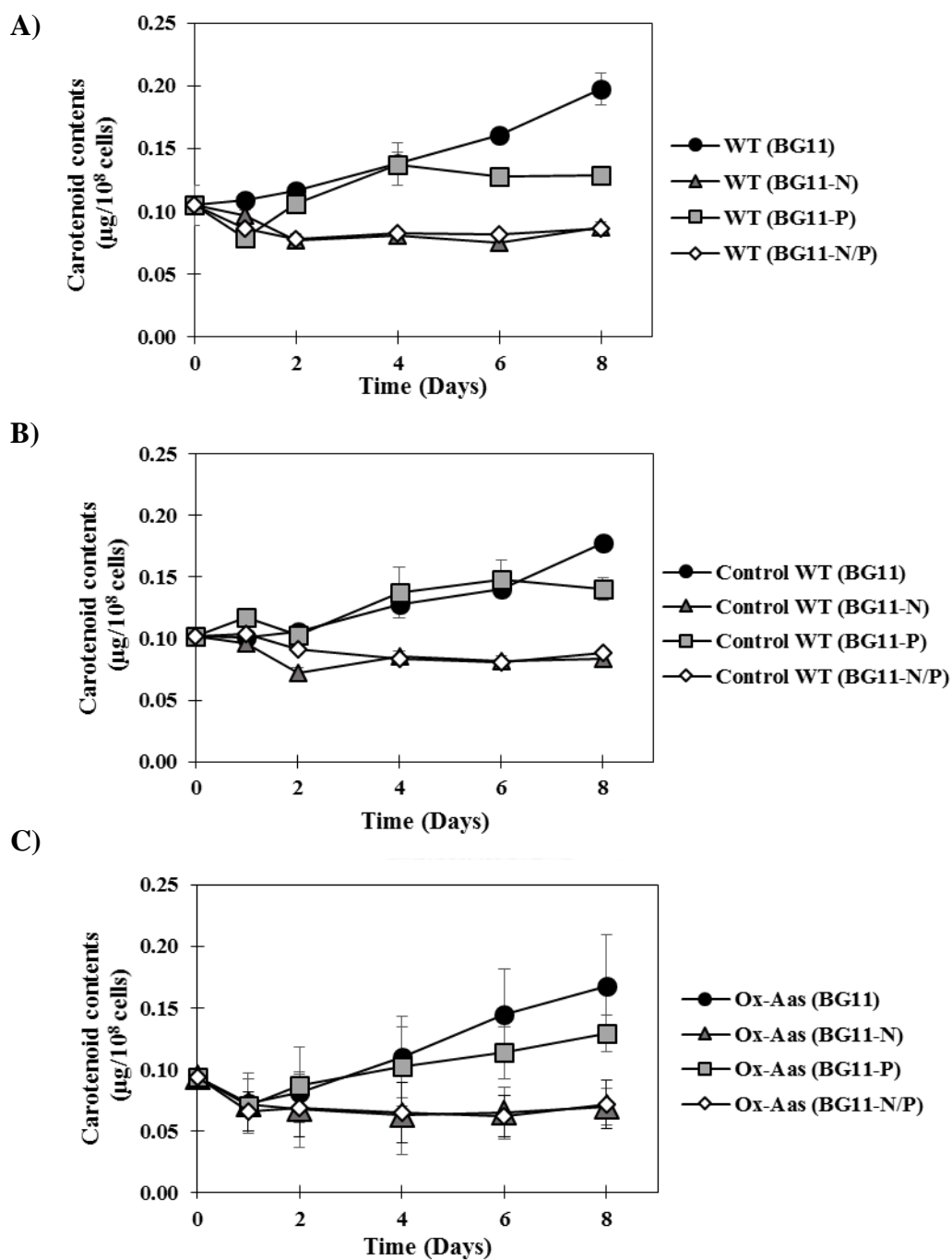


**Figure 3.12** Chlorophyll *a* (A) and carotenoid contents (B) of WT, Control WT and Ox-Aas strains grown for 15 days of cultivation. Data represented as Mean  $\pm$  S.D, (n=3).

In Figure 3.14A, the carotenoid content of WT cell under normal BG<sub>11</sub> medium was increased during treatment along 8 days. After treating with BG<sub>11</sub>-N and BG<sub>11</sub>-N/P conditions, those carotenoid contents of WT were significantly decreased when compared with those under normal BG<sub>11</sub> condition. In contrast, P-deprived condition did not effect on carotenoid accumulation in 1-4 days of treatment whereas after 4 day-treatment shown the constant level of the carotenoid contents until 8 days of treatment. However, the carotenoid level of WT cells under BG<sub>11</sub>-P condition at day 6-8 of treatment was less than that under normal BG<sub>11</sub> condition. In Figure 3.14B, the carotenoid contents of Control WT cells under both normal BG<sub>11</sub> and BG<sub>11</sub>-P conditions were increased during treatments. After a treatment with BG<sub>11</sub>-N medium, the carotenoid content of Control WT was significantly decreased when compared with that normal condition. Interestingly, after 4 day-treatment under BG<sub>11</sub>-N/P condition, the carotenoid content in Control WT cells was also decreased as similar level as in BG<sub>11</sub>-N condition. In Figure 3.14C, the increased levels of carotenoid accumulation of Ox-Aas strain were observed under normal BG<sub>11</sub> and BG<sub>11</sub>-P conditions. After Ox-Aas cells were treated with BG<sub>11</sub>-N and BG<sub>11</sub>-N/P conditions, the carotenoid contents in the cell were clearly decreased when compared with those under normal condition along 8 days of treatment.



**Figure 3.13** Chlorophyll *a* contents of WT (A), Control WT (B) and Ox-Aas (C) strains grown for 8 days of cultivation under normal BG<sub>11</sub> condition (BG11), N deprived condition (BG11-N), P deprived condition (BG11-P), and N/P deprived condition (BG11-N/P). Data represented as Mean  $\pm$  S.D. (n=3).

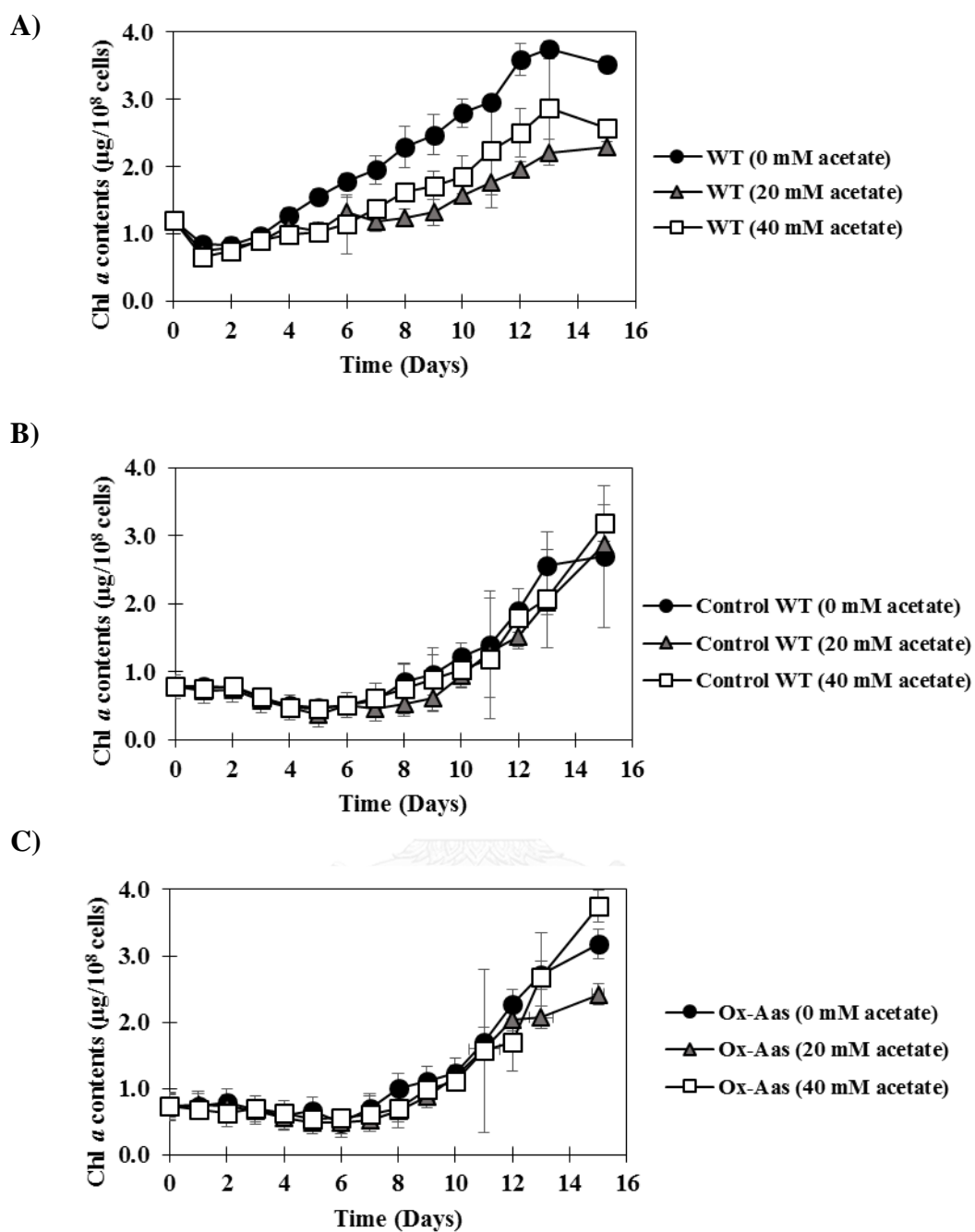


**Figure 3.14** Carotenoid contents of WT (A), Control WT (B) and Ox-Aas (C) strains grown for 8 days of cultivation under normal BG11 condition (BG11), N deprived condition (BG11-N), P deprived condition (BG11-P), and N/P deprived condition (BG11-N/P). Data represented as Mean  $\pm$  S.D, (n=3).

### 3.3.3 Intracellular pigment contents under acetate addition

After those WT, Control WT and Ox-Aas cells were cultivated in long term acetate treatment (including 0 mM, 20 mM and 40 mM concentrations of acetate, respectively) added in normal BG<sub>11</sub> medium. The Chl *a* and carotenoid contents were determined and shown in Figures 3.15 and 3.16, respectively.

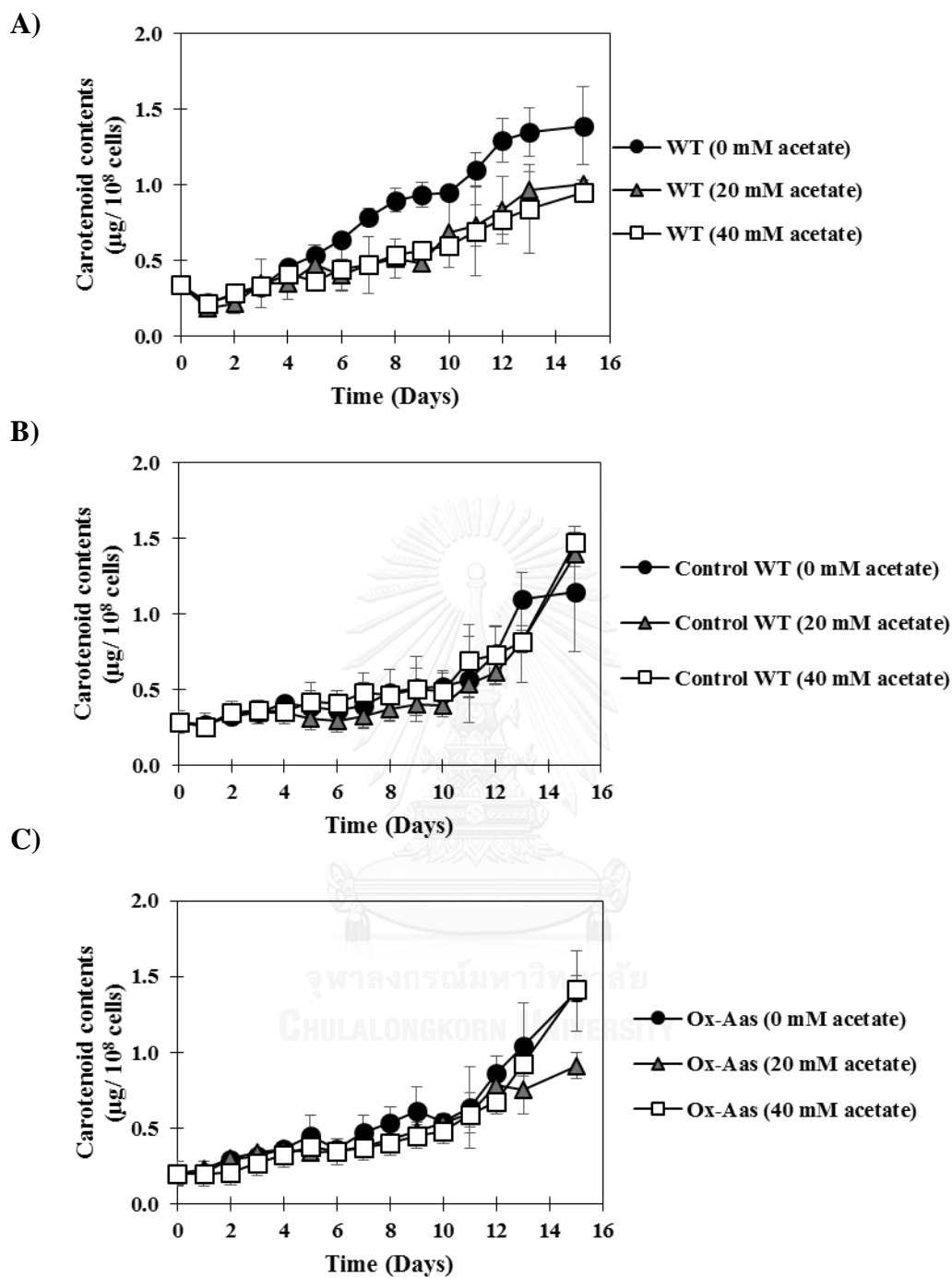
In Figure 15A, the Chl *a* content of WT cells was increased during cultivation time (15 days) under normal condition (at 0 mM acetate). When the amount of acetate were increased at 20 mM and 40 mM of acetate additions, the Chl *a* content of WT cells was significantly increased but lower than that under normal 0 mM acetate condition. In Figure 3.15B, the Chl *a* content of Control WT cells under 0, 20 and 40 mM acetate additions were decreased in first 2-8 days of cultivation whereas the increased levels were observed during 8-15 days of cultivation. In Figure 15C, their Chl *a* content of Ox-Aas cells was increased during cultivation time under all conditions. At 20 mM and 40 mM of acetate additions, their Chl *a* content of Ox-Aas cells was not different at all growth stages. All results demonstrated that those Chl *a* contents of Control WT and Ox-Aas strains were not significantly different in all growth of stages.



**Figure 3.15** Chlorophyll *a* contents of WT (A), Control WT (B) and Ox-Aas (C) strains grown for 15 days of cultivation under the normal BG<sub>11</sub> condition (0 mM) and BG<sub>11</sub> containing various concentrations of acetate (20 mM and 40 mM, respectively). Data represented as Mean  $\pm$  S.D, (n=3).



In Figure 3.16A, the carotenoid content of WT cells was increased during cultivation time under all conditions studied. The acetate additions at 20 mM and 40 mM apparently decreased the carotenoid accumulation when compared to that under normal condition at 0 mM acetate. The similar levels of carotenoids were found under acetate additions at 20 mM and 40 mM concentrations. In Figure 3.16B, the carotenoid contents of Control WT cells were increased during cultivation time under all conditions. The supplementation of acetate at both 20 mM and 40 mM did not affect on the carotenoid contents of Control WT cells. The carotenoid contents of Control WT strain were stable at first 1-8 days of cultivation and gradually increased after 8-12 days, and sharply increased after 12 day of cultivation. In Figure 3.16C, Ox-Aas cells showed a gradual increase in day 1-10 of cultivation and obviously increased after 10 days. When the amount of acetate were increased at 20 mM and 40 mM of acetate addition, the carotenoid contents of Ox-Aas cells were not different at all growth stages when compared with that under normal condition.



**Figure 3.16** Carotenoid contents of WT (A), Control WT (B) and Ox-Aas (C) strains grown for 15 days of cultivation under the normal BG<sub>11</sub> condition (0 mM) and BG<sub>11</sub> containing various concentrations of acetate (20 mM and 40 mM, respectively). Data represented as Mean  $\pm$  S.D, (n=3).

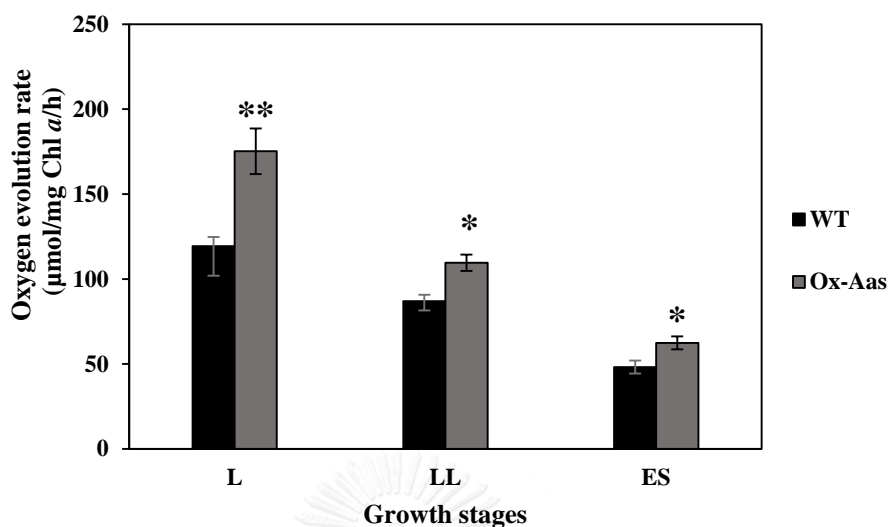
### **3.5 Oxygen evolution rate of *Synechocystis* cells**

#### **3.5.1 Oxygen evolution rate under normal BG<sub>11</sub> condition**

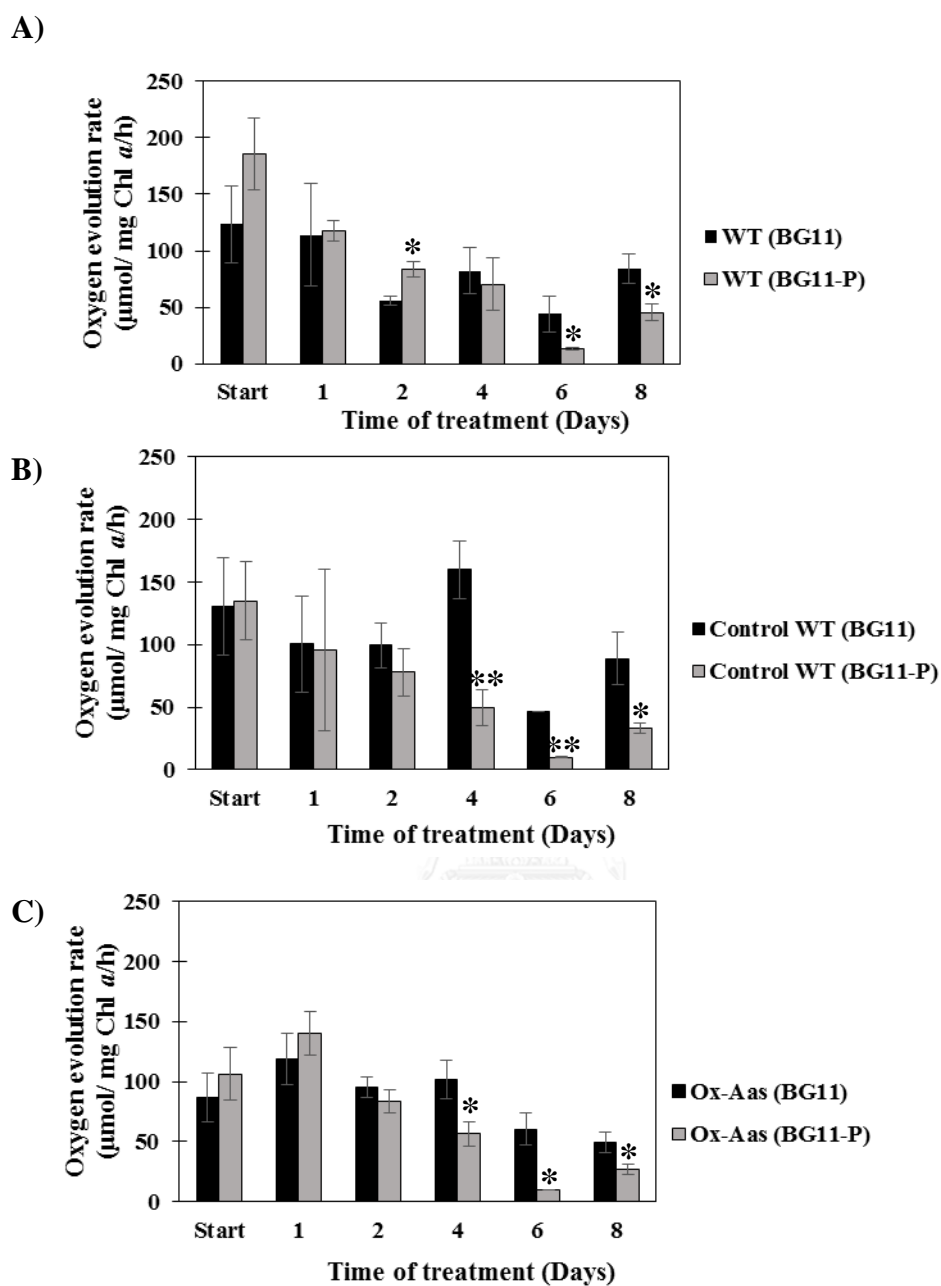
The oxygen evolution rate was detected during cell cultivation including log phase (L-phase), late-log phase (LL-phase) and early stationary phase (ES-phase), respectively. In Figure 3.17, oxygen evolution rate of Ox-Aas cells exhibited higher than WT of about 1.4 fold of L-phase, 1.2 fold of LL-phase and 1.2 fold of ES-phase, respectively.

#### **3.5.2 Oxygen evolution rate under phosphorus-deprived condition**

In Figure 3.18, the oxygen evolution rates of WT, Control WT and Ox-Aas cells were detected during treatment with phosphorus deprivation (BG<sub>11</sub>-P) compared with normal condition (BG<sub>11</sub>). In Figure 3.18A, the oxygen evolution rate of WT under BG<sub>11</sub>-P medium was not significantly different when compared with normal in first 2 days of treatment. After 4 day-treatment of BG<sub>11</sub>-P medium, the oxygen evolution rate of WT exhibited lower than normal condition which represented during late-log and early stationary phase of the cells growth. In Figure 3.18B, the oxygen evolution rate of Control WT cells under BG<sub>11</sub>-P medium was not different when compared with its treatment under normal condition. The significant decreases of Control WT-oxygen evolution rate were observed after 4 day-treatment. In Figure 3.18C, the oxygen evolution rate of Ox-Aas cells under BG<sub>11</sub>-P treatment was not different in first 2 day-treatment when compared with normal condition whereas the decreases on their oxygen evolution rate were shown after 4 day-treatment.



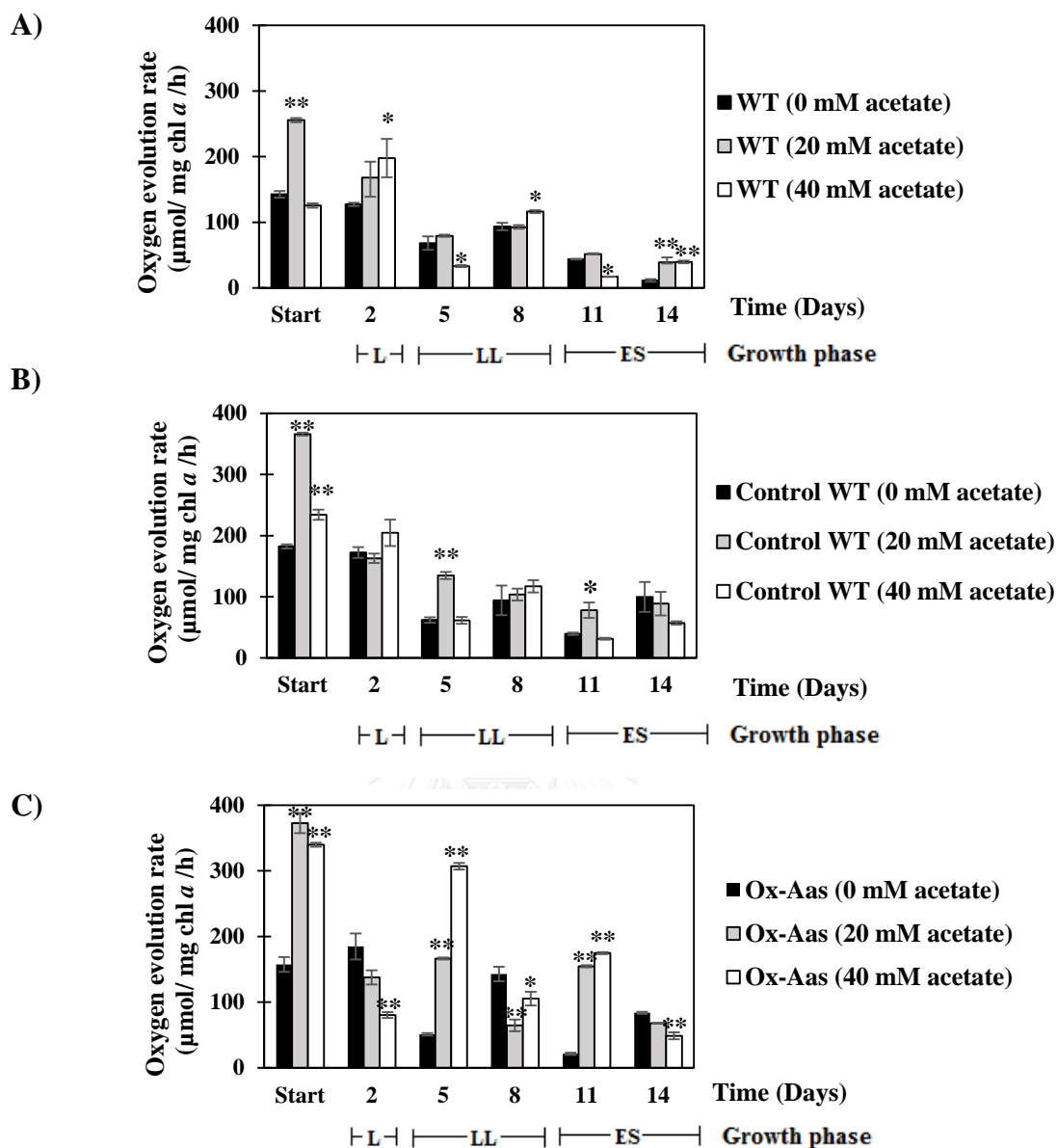
**Figure 3.17** Oxygen evolution rates of WT and Ox-Aas in each growth stage: log phase (L), late-log phase (LL) and early stationary phase (ES) of both WT and Ox-Aas strains. Data represented as Mean  $\pm$ S.D, (n=3). Asterisks represent statistical significance between oxygen evolution rate of WT and Ox-Aas strains (\* =  $p < 0.05$ , \*\* =  $p < 0.01$ ).



**Figure 3.18** Oxygen evolution rates of WT (A), Control WT (B) and Ox-Aas (C) cells after adaptation to phosphorus-deprived BG11 medium (BG11-P) compared with normal condition (BG11). Data represented as Mean  $\pm$  S.D, (n=3). Asterisks represent statistical significance between oxygen evolution rate of cells under P-deprived condition and normal condition (\* =  $p < 0.05$ , \*\* =  $p < 0.01$ ).

### 3.5.3 Oxygen evolution rate under acetate addition

In Figure 3.19, the oxygen evolution rate of WT, Control WT and Ox-Aas cells were detected during treatment with various concentrations of acetate. In Figure 3.19A, the oxygen evolution rate of WT cells under normal condition was reduced during 15 days of cultivation. The oxygen evolution rate of WT cells under 20 mM acetate addition was highest during L-phase of growth when compared with its cultivation under normal condition whereas the 40 mM acetate addition decreased WT cell O<sub>2</sub> evolution rate. In Figure 3.19B, the oxygen evolution rate of Control WT cells under normal condition was decreased along 15 days of cultivation. The oxygen rate of Control WT cells under 20 mM acetate addition was highest during log phase of growth when compared with those of normal condition and 40 mM acetate condition. The efficiency of photosynthesis of Control WT strain was not significantly different with WT. In Figure 3.19C, the oxygen evolution rates of Ox-Aas cells under both 20 mM and 40 mM acetate additions were higher than those rates under normal condition. The photosynthetic efficiency of Ox-Aas strain exhibited higher than those of WT and Control WT cells.



**Figure 3.19** Oxygen evolution rates of WT (A), Control WT (B) and Ox-Aas (C) cells grown for 15 days of cultivation under the normal BG<sub>11</sub> medium (0 mM acetate) and various acetate addition at 20 mM and 40 mM concentrations, respectively. Data represented as Mean  $\pm$  S.D, (n=3). Asterisks represent statistical significance between oxygen evolution rate of cells under acetate addition and normal condition (\* =  $p < 0.05$ , \*\* =  $p < 0.01$ ).

### **3.6 Sudan Black staining of *Synechocystis* cells**

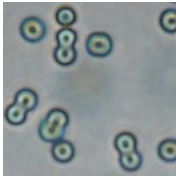
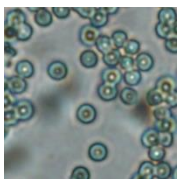
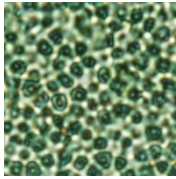
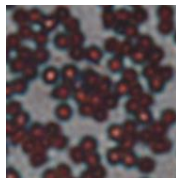
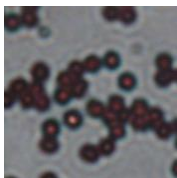
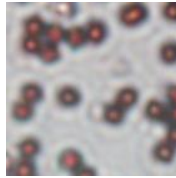
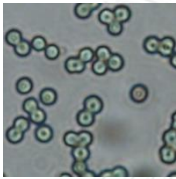
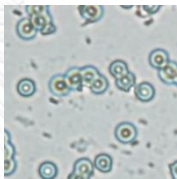
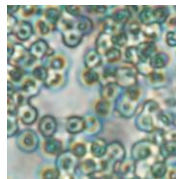
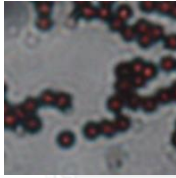
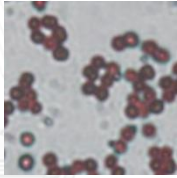
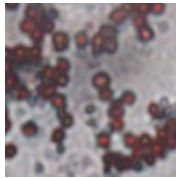
#### **3.6.1 Total lipid screening by Sudan Black staining of *Synechocystis* cells under normal condition**

The most polar lipids in *Synechocystis* cells are membrane lipid. The polar lipids of the cells in each growth stage were stained by Sudan Black B staining and detected under the light microscopy. In Figure 3.20, the visual images showed the stained-membrane in black color. Both WT and Ox-Aas strains showed no differences on stained cell morphology in all growth stages (L, LL and ES phages, respectively) under normal BG<sub>11</sub> medium condition.

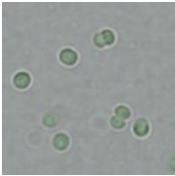
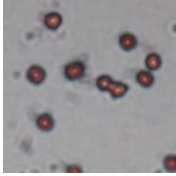
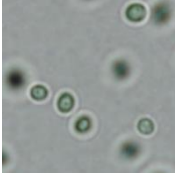
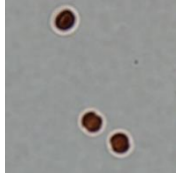
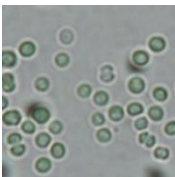
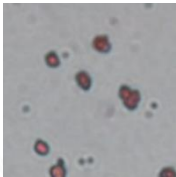
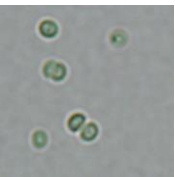
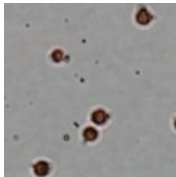
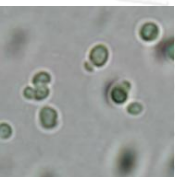
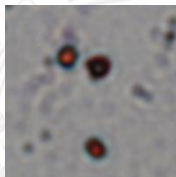
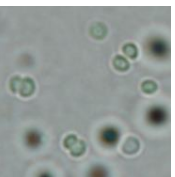
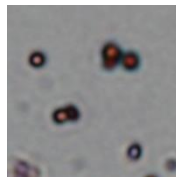
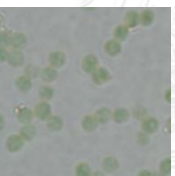
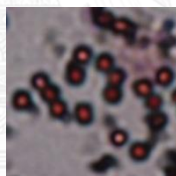
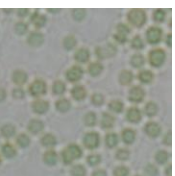

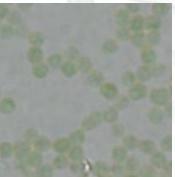
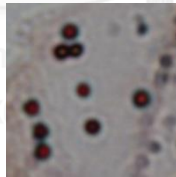
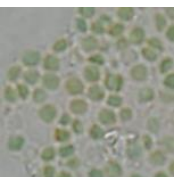

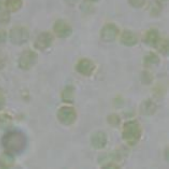

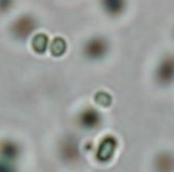
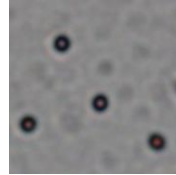
#### **3.6.2 Total lipid screening by Sudan Black B staining of *Synechocystis* cells under phosphorus-deprived condition**

In Figure 3.21, the polar lipids of WT, Control WT and Ox-Aas cells after adapted under P-deprived BG<sub>11</sub> medium (BG<sub>11</sub>-P), were stained by Sudan Black B staining and detected under the light microscopy. The visual images of WT cells treated under BG<sub>11</sub>-P conditions of all growth stages (L, LL, ES phages) were not different when compared with its cultivation under normal condition. The visual images of Control WT cells treated under BG<sub>11</sub>-P conditions of all growth stages (L, LL, ES phages) were not different when compared with its normal condition. Neither the visual images of Ox-Aas cells treated under BG<sub>11</sub>-P conditions of all growth stages (L, LL, ES phages) were observed when compared with normal condition.

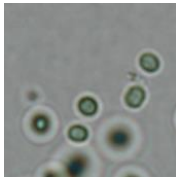
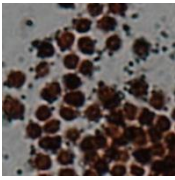
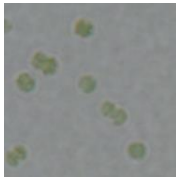
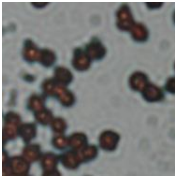
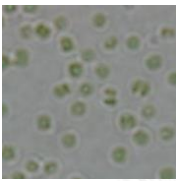
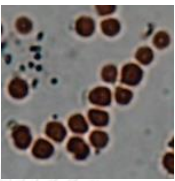
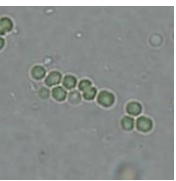
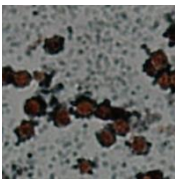
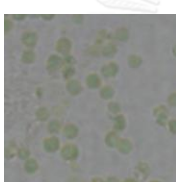
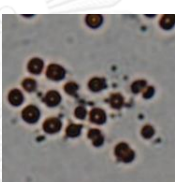
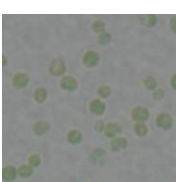
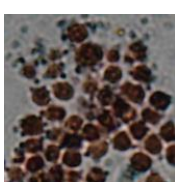
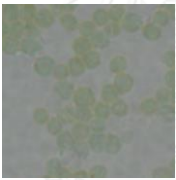
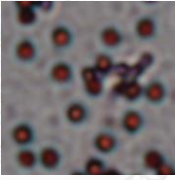
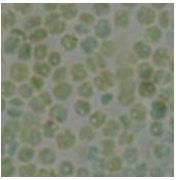
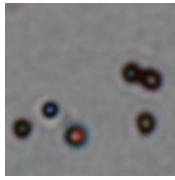
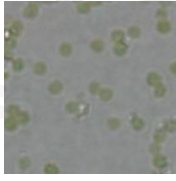
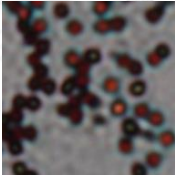
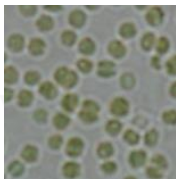
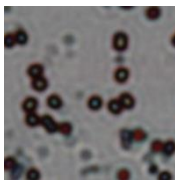
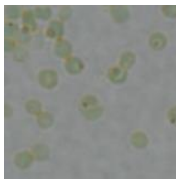
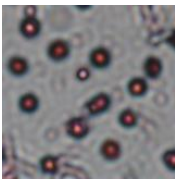
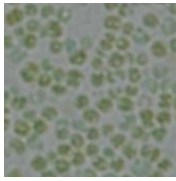
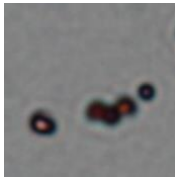


Strain	Growth stages		
	Log phase	Late-log phase	Early stationary phase
<b>WT</b>			
Normal cells			
Stained cells			
<b>Ox-Aas</b>			
Normal cells			
Stained cells			

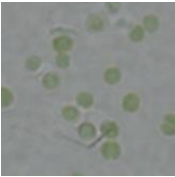
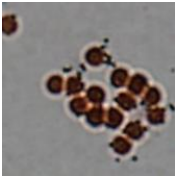
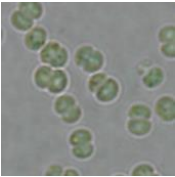
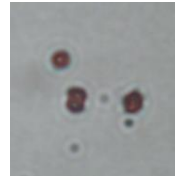
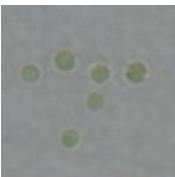
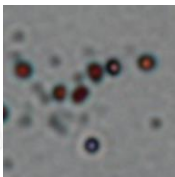
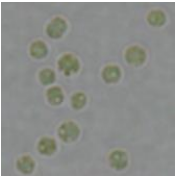
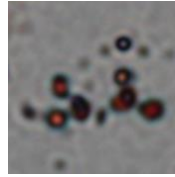
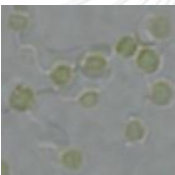
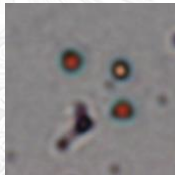
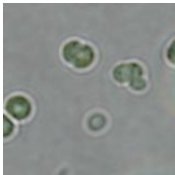
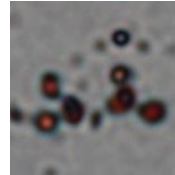
**Figure 3.20** Microscopic images of Sudan Black B stained cells including WT and Ox-Aas strains under normal condition. Cells were stained by Sudan Black B solution and visualized under light microscope with a magnification of 100x.

Days	Strain	Conditions			
		Normal BG <sub>11</sub> medium		BG <sub>11</sub> -P	
		Normal cells	Stained cells	Normal cells	Stained cells
Start	WT				
	Control WT				
	Ox-Aas				
2	WT				
	Control WT				
	Ox-Aas				

**Figure 3.21** Microscopic images of Sudan Black B stained cells including WT, Control WT and Ox-Aas strains under normal BG<sub>11</sub> medium and phosphorus-deprived condition (BG<sub>11</sub>-P). Cells were stained by Sudan Black B solution and visualized under light microscope with a magnification of 100x.

Days	Strain	Conditions			
		Normal BG <sub>11</sub> medium		BG <sub>11</sub> -P	
		Normal cells	Stained cells	Normal cells	Stained cells
4	WT				
	Control WT				
	Ox-Aas				
6	WT				
	Control WT				
	Ox-Aas				

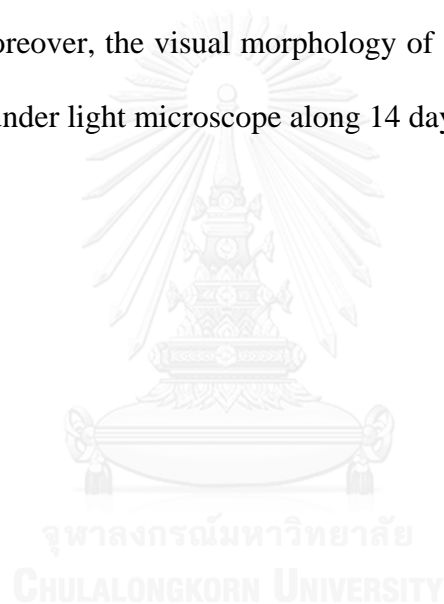
**Figure 3.21** (Continued) Microscopic images of Sudan Black B stained cells including WT, Control and Ox-Aas strains under normal BG<sub>11</sub> medium and phosphorus-deprived condition (BG<sub>11</sub>-P). Cells were stained by Sudan Black B solution and visualized under light microscope with a magnification of 100x.

Days	Strain	Conditions			
		Normal BG <sub>11</sub> medium		BG <sub>11</sub> -P	
		Normal cells	Stained cells	Normal cells	Stained cells
8	WT				
	Control WT				
	Ox-Aas				

**Figure 3.21** (Continued) Microscopic images of Sudan Black B stained cells including WT, Control and Ox-Aas strains under normal BG<sub>11</sub> medium and phosphorus-deprived condition (BG<sub>11</sub>-P). Cells were stained by Sudan Black B solution and visualized under light microscope with a magnification of 100x.

### **3.6.3 Total lipid screening by Sudan Black staining of *Synechocystis* sp. cells under acetate addition**

In Figure 3.22, the polar lipid staining of WT, Control WT and Ox-Aas cells during adapting with various concentrations of acetate in normal BG<sub>11</sub> medium were detected under the light microscopy. The visual images of those of WT, Control WT and Ox-Aas cells treated under 20 mM and 40 mM acetate conditions of all growth stages (L, LL, ES phages) were not different when compared with its cultivation under normal condition. Moreover, the visual morphology of stained cells was not changed by visual inspection under light microscope along 14 days of treatment.



Days	Strain	Conditions					
		0 mM acetate		20 mM acetate		40 mM acetate	
		Normal cells	Stained cells	Normal cells	Stained cells	Normal cells	Stained cells
Start	WT						
	Control WT						
	Ox-Aas						
2	WT						
	Control WT						
	Ox-Aas						

**Figure 3.22** Microscopic images of Sudan Black B stained cells including WT, Control and Ox-Aas strains under normal BG<sub>11</sub> medium (0 mM acetate) and acetate addition conditions including 20 mM and 40 mM of acetate. Cells were stained by Sudan Black B solution and visualized under light microscope with a magnification of 100x.

Days	Strain	Conditions					
		0 mM acetate		20 mM acetate		40 mM acetate	
		Normal cells	Stained cells	Normal cells	Stained cells	Normal cells	Stained cells
5	WT						
	Control WT						
	Ox-Aas						
8	WT						
	Control WT						
	Ox-Aas						

**Figure 3.22** (Continued) Microscopic images of Sudan Black B stained cells including WT, Control and Ox-Aas strains under normal BG<sub>11</sub> medium (0 mM acetate) and acetate addition conditions including 20 mM and 40 mM of acetate. Cells were stained by Sudan Black B solution and visualized under light microscope with a magnification of 100x.

Days	Strain	Conditions					
		0 mM acetate		20 mM acetate		40 mM acetate	
		Normal cells	Stained cells	Normal cells	Stained cells	Normal cells	Stained cells
11	WT						
	Control WT						
	Ox-Aas						
14	WT						
	Control WT						
	Ox-Aas						

**Figure 3.22** (Continued) Microscopic images of Sudan Black B stained cells including WT, Control and Ox-Aas strains under normal BG<sub>11</sub> medium (0 mM acetate) and acetate addition conditions including 20 mM and 40 mM of acetate. Cells were stained by Sudan Black B solution and visualized under light microscope with a magnification of 100x.



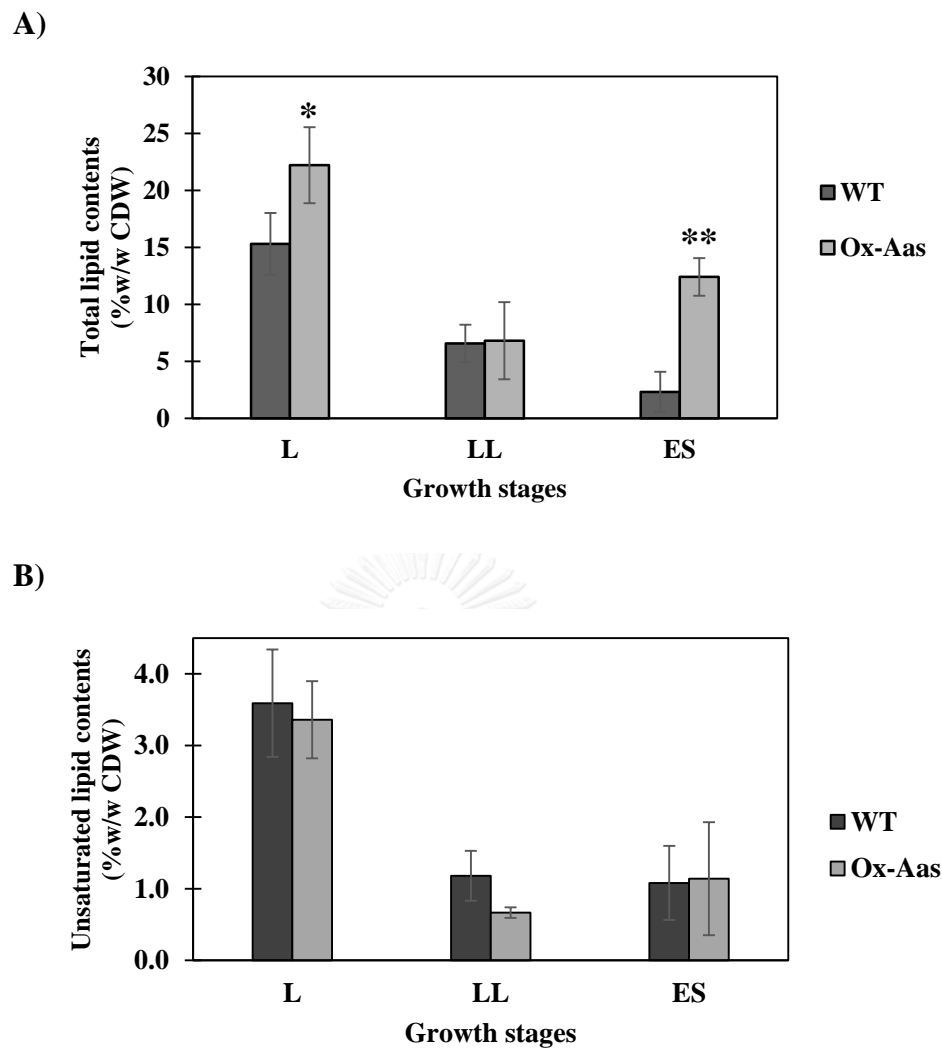
### **3.7 Total lipid and unsaturated lipid contents**

#### **3.7.1 Total lipid contents of *Synechocystis* sp. PCC 6803 cells under normal condition**

In Figure 3.23A, the total lipid contents of cells grown in each growth stage were determined by dichromate oxidation reaction. The total lipid contents of Ox-Aas cells was 1.5 fold higher than WT under log phase of growth. At late-log phase, the indifferences on total lipid contents of both WT and Ox-Aas strains were observed. At early stationary phase, total lipid contents of Ox-Aas cells exhibited 5 fold higher than WT.

#### **3.7.2 Total unsaturated lipid contents under normal condition**

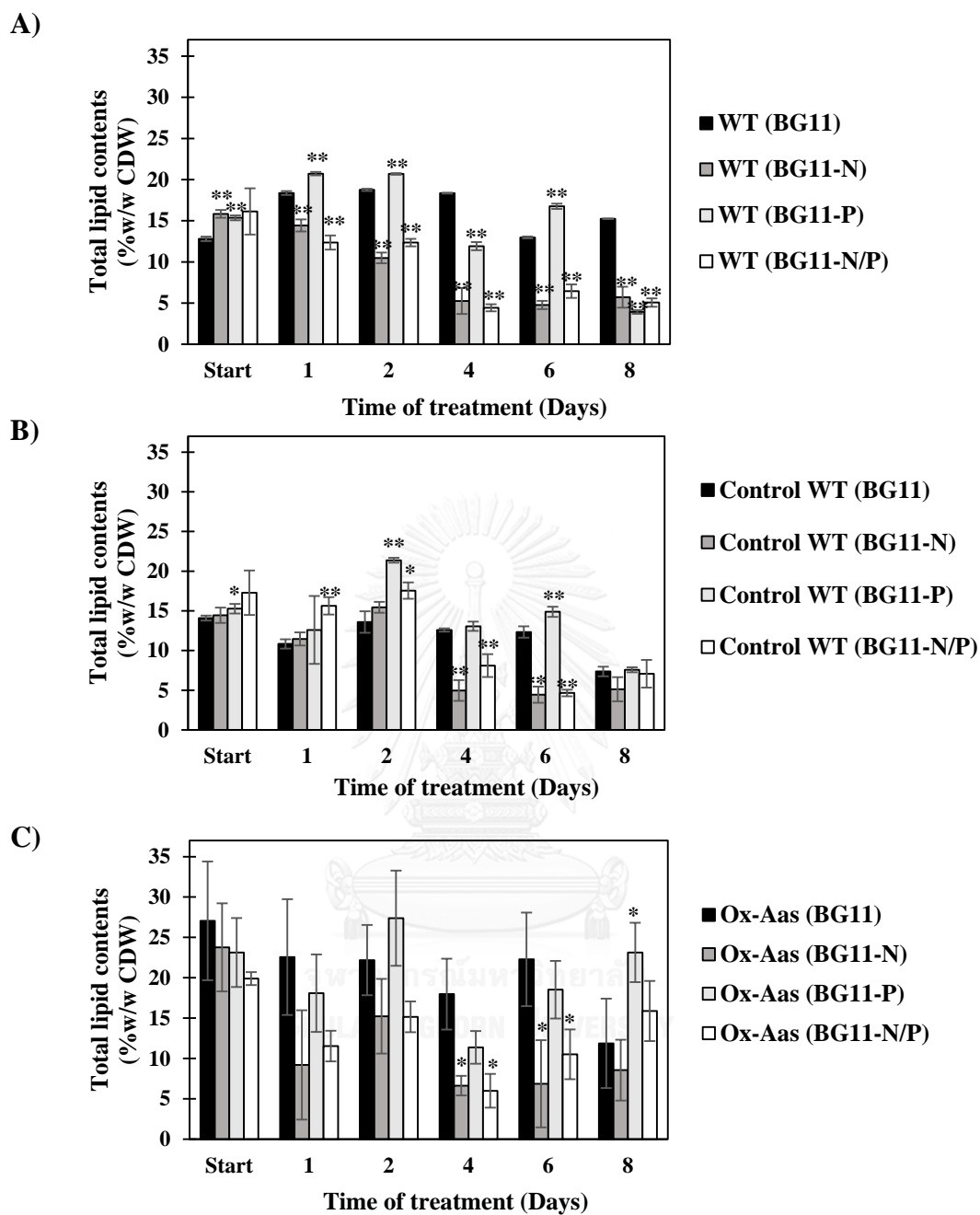
In Figure 3.23B, the total unsaturated lipid contents of cells grown in each growth stage were determined by colorimetric sulfo-phospho vanillin reaction. The unsaturated lipid contents in both WT and Ox-Aas strains were not different in all growth stages (L, LL and ES phases, respectively). The highest amount of total unsaturated lipid was found in both WT and Ox-Aas cells under log phase of growth.



**Figure 3.23** Total lipid (A) and total unsaturated lipid (B) contents of WT and Ox-Aas strains grown in each growth stage of log (L), late-log (LL) and early stationary (ES) phases, respectively in normal BG<sub>11</sub> condition. Data represented as Mean ± S.D, (n=3). Asterisks represent statistical significance between the total lipid (A) contents and total unsaturated (B) lipid contents of WT cells and Ox-Aas under normal condition (\* =  $p < 0.05$ , \*\* =  $p < 0.01$ ).

### 3.7.3 Total lipid contents under various nutrient deprived conditions

The total lipid contents in WT, Control WT and Ox-Aas cells under nutrient-deprived condition including nitrogen-deprived BG<sub>11</sub> medium (BG<sub>11</sub>-N), phosphorus-deprived BG<sub>11</sub> medium (BG<sub>11</sub>-P) and nitrogen and phosphorus-deprived BG<sub>11</sub> medium (BG<sub>11</sub>-N/P) were shown in Figure 3.24. The total lipids in WT cells exhibited highest content during 1-2 days of treatment. After WT cells were adapted under BG<sub>11</sub>-N condition, the total lipid contents in WT cells exhibited highest level at the start of treatment and later 1.2 fold decrease was observed when compared to it under normal condition at day 2 of treatment. Under BG<sub>11</sub>-P treatment, WT strain accumulated high level of total lipids during 1-2 days of treatment whereas when BG<sub>11</sub>-N/P-treated WT cells accumulated their total lipids in a significantly decrease during 1 to 8 days of treatment. Under normal condition, the insignificant changes of total lipid of Control WT were observed at day 1-6 of treatment and decreased at day 8 of treatment. After Control WT was treated under N-deprivation, the total lipid content of the Control WT cell was not changed at 1-2 days of treatment whereas when the cells were adapted with P-limitation, their lipid content exhibited highest amount at day 2 of treatment with 1.6 fold increase compared to normal condition. The total lipids in Control WT cells showed highest content when adapted under BG<sub>11</sub>-N/P condition at the start treatment with 1.3 fold higher than Control WT under normal condition. Under the normal condition, the total lipid content of Ox-Aas gave the highest level at the start of treatment. When Ox-Aas cells were adapted under the BG<sub>11</sub>-N condition, the profile of total lipid content was decreased along 8 days of treatment whereas BG<sub>11</sub>-P-treated Ox-Aas cells showed the increased lipid amount as similar as that treated under normal BG<sub>11</sub> condition at start of treatment.

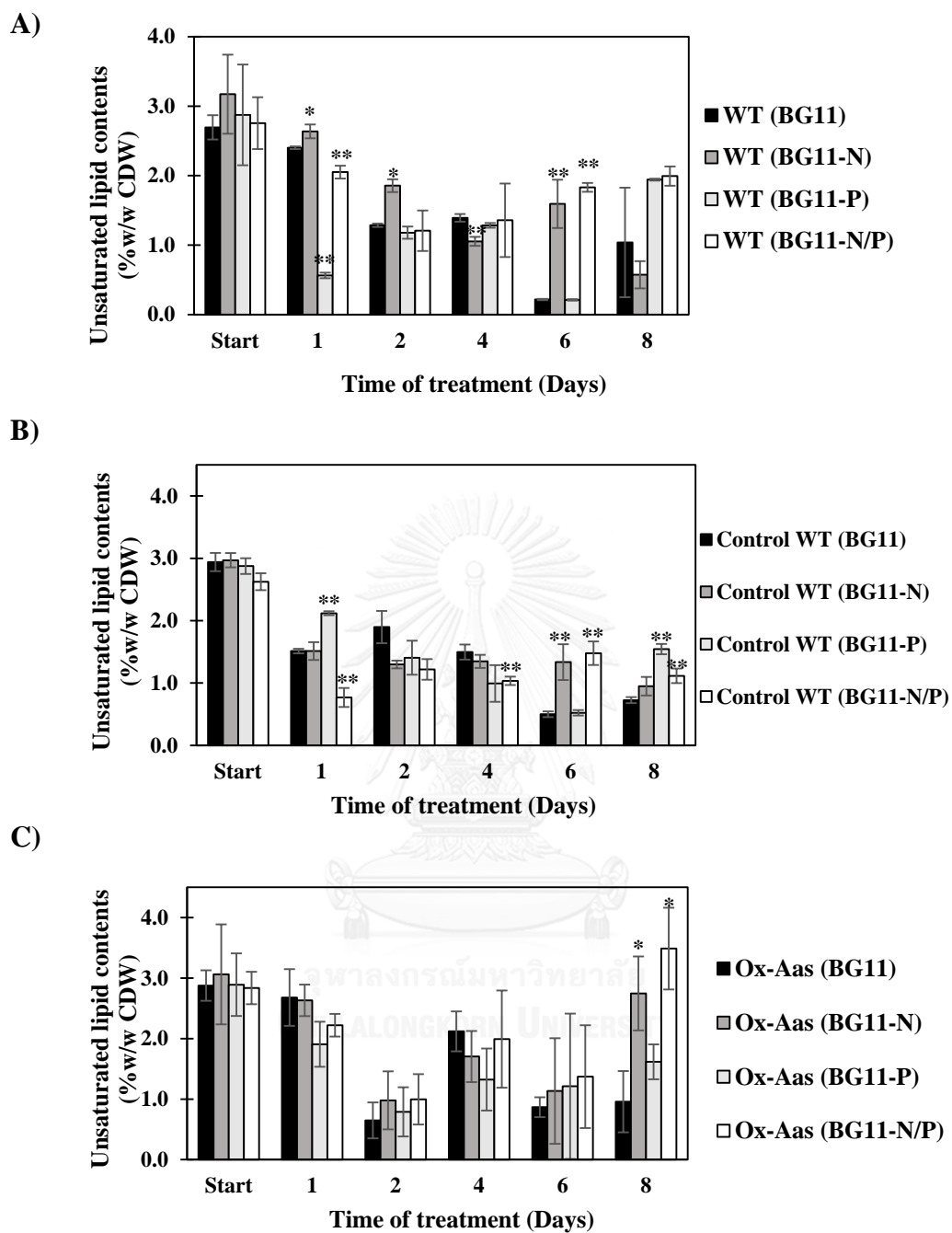


**Figure 3.24** Total lipid contents of WT (A), Control (B) and Ox-Aas (C) strains after treatment under normal BG<sub>11</sub> condition (BG11), N deprived condition (BG11-N), P deprived condition (BG11-P), and N/P deprived condition (BG11-N/P) condition. Data represented as Mean  $\pm$  S.D, (n=3). Asterisks represent statistical significance between the lipid contents of cells under nutrient deprived conditions and its level under normal condition (\* =  $p < 0.05$ , \*\* =  $p < 0.01$ ).

Under BG<sub>11</sub>-N/P condition, the total lipid contents in Ox-Aas cells showed highest level at day 2 of treatment. The results shown that P-deprived BG<sub>11</sub> condition could enhance lipid accumulations in the cells of all strains.

#### **3.7.4 Total unsaturated lipid contents under various nutrient deprived conditions**

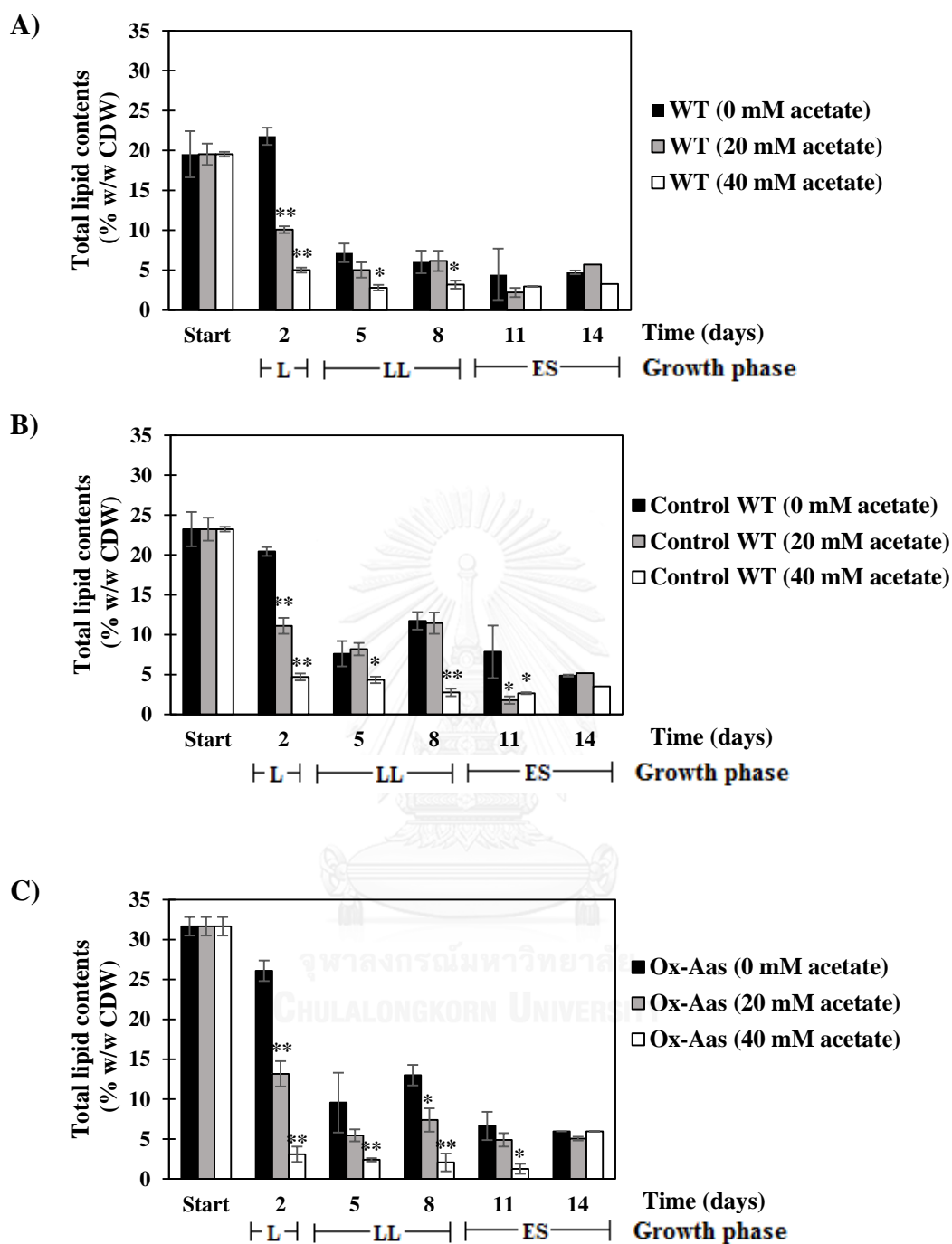
The total unsaturated lipid contents in WT, Control WT and Ox-Aas cells under nutrient deprived condition including nitrogen-deprived BG<sub>11</sub> medium (BG<sub>11</sub> -N), phosphorus-deprived BG<sub>11</sub> medium (BG<sub>11</sub> -P) and nitrogen and phosphorus-deprived BG<sub>11</sub> medium (BG<sub>11</sub> -N/P) were shown in Figure 3.25. Under normal condition, the unsaturated lipid contents of WT cells showed the highest level at start day of treatment and later decreased along 8 days of treatment. Under BG<sub>11</sub>-N condition, the unsaturated lipid contents of WT cells were increased higher than those under normal condition. After WT cells were adapted under BG<sub>11</sub>-P condition, the unsaturated lipid contents of WT cells were decrease after 1-6 days of treatment. The BG<sub>11</sub>-N/P condition affected on the increase of unsaturated lipid contents when compared to normal condition. In Figure 3.25B, the Control WT cells showed the higher induction under BG<sub>11</sub>-P and BG<sub>11</sub>-N/P conditions when compared to those under normal conditions. The total unsaturated lipid of Ox-Aas cells shown in Figure 3.25C. Under both BG<sub>11</sub>-N and BG<sub>11</sub>-N/P conditions, the unsaturated lipid levels of Ox-Aas was not different at 1-6 days of treatment and later showed increases of unsaturated lipid contents under 8 days of treatment compared to its under normal condition. After Ox-Aas cells were adapted with BG<sub>11</sub>-P, their total unsaturated lipid was insignificantly different from its level under normal condition.



**Figure 3.25** Unsaturated lipid contents of WT (A), Control (B) and Ox-Aas (C) strains after treatment under normal BG<sub>11</sub> condition (BG11), N deprived condition (BG11-N), P deprived condition (BG11-P), and N/ P deprived condition (BG11-N/P) condition. Data represented as Mean  $\pm$  S.D, (n=3). Asterisks represent statistical significance between the unsaturated lipid contents of cells under nutrient deprived conditions and its level under normal condition (\* =  $p < 0.05$ , \*\* =  $p < 0.01$ ).

### 3.7.5 Total lipid contents of the cells under the acetate addition

The total lipid contents in WT, Control WT and Ox-Aas cells under the various concentrations of acetate (0 mM and 40 mM acetate) were shown in Figure 3.26. The tendency of total lipid contents of WT strains showed a decrease when the concentration of acetate was increased from 0 to 40 mM acetate addition. In Figure 3.26B, the total lipid of Control WT cells showed the highest content at the start of log phase of growth and later its accumulation was tended to decrease. These Control WT cells showed significantly decrease under LL-phase of growth when compared with that under normal condition. Results showed that acetate addition with all concentrations studied did not affect on the lipid levels of Control WT cells under ES-phase of cell growth. In Figure 3.26C, the total lipid contents of Ox-Aas cells were decreased from the start of treating until ES-phase of growth when the concentrations of acetate were increased.

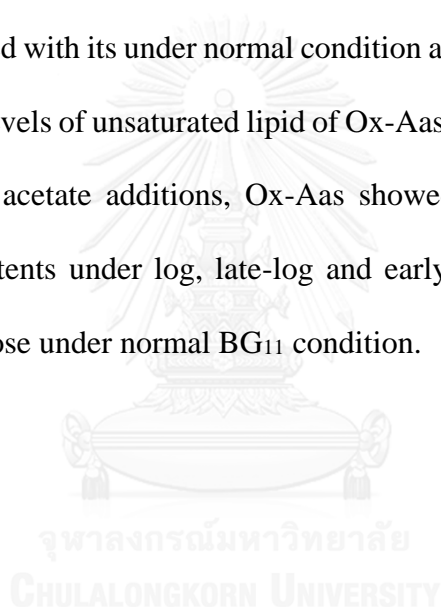


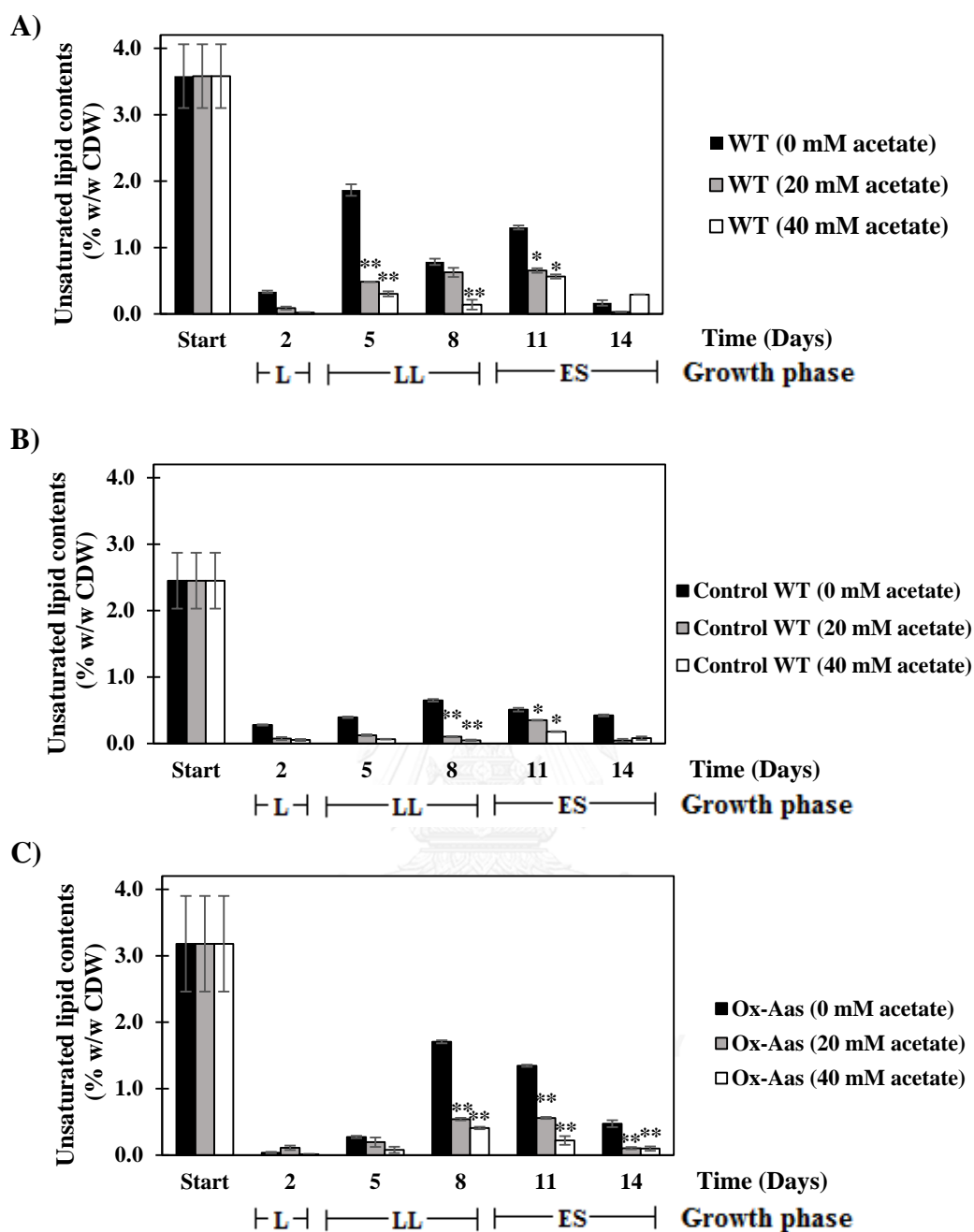
**Figure 3.26** Total lipid contents of WT (A), Control WT (B) and Ox-Aas (C) strains after treating with various concentrations of acetate in BG<sub>11</sub> medium (0 mM, 20 mM and 40 mM acetate). Data represented as Mean  $\pm$  S.D, (n=3). Asterisks represent statistical significance between the lipid contents of cells under various concentrations of acetate addition and its level under normal condition (\* =  $p < 0.05$ , \*\* =  $p < 0.01$ ).



### 3.7.6 Total unsaturated lipid contents under acetate addition

The total unsaturated lipid contents in WT, Control WT and Ox-Aas cells under the various concentrations of acetate (20 mM and 40 mM acetate) were shown in Figure 3.27. After WT cells were treated with 20 mM and 40 mM of acetate, the unsaturated lipid of WT showed a clear decrease of the unsaturated lipid contents under all growth phases when compared to those under normal BG<sub>11</sub> condition. The total unsaturated lipid contents of Control WT tended to decrease after treating with higher levels of acetate when compared with its under normal condition along days of treatment (Figure 3.27B). The highest levels of unsaturated lipid of Ox-Aas cells was observed at the start of log phase. Under acetate additions, Ox-Aas showed obviously the decreases of unsaturated lipid contents under log, late-log and early stationary phases of growth when compared to those under normal BG<sub>11</sub> condition.





**Figure 3.27** Total unsaturated lipid contents of WT (A), Control WT (B) and Ox-Aas (C) strains after treating with various concentrations of acetate in BG<sub>11</sub> medium (0 mM, 20 mM and 40 mM acetate). Data represented as Mean  $\pm$  S.D, (n=3). Asterisks represent statistical significance between the unsaturated lipid contents of cells under various concentrations of acetate and its level under normal condition (\* =  $p < 0.05$ , \*\* =  $p < 0.01$ ).

### 3.8 The expression levels of genes related to fatty acid biosynthesis

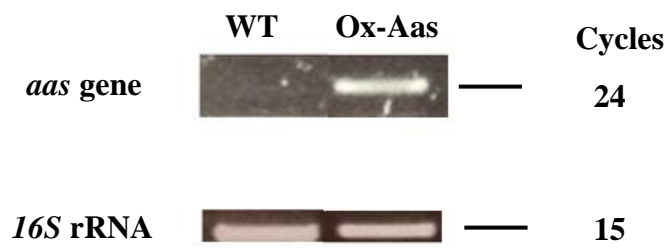
#### 3.8.1 The expression levels of *aas* transcript under normal condition

The expression levels of *aas* transcript of both WT and Ox-Aas strains were analyzed by reverse transcription PCR (RT-PCR) method. The expression levels of *aas* and *16S* rRNA gene in each strain were shown in Figure 3.28A. The transcript level of *aas* gene in Ox-Aas strain was exhibited of about 10 fold higher than WT under normal condition. The expression levels of genes including *phaA*, *accA*, *aas* and *plsX* of WT and Ox-Aas strains under normal condition were presented in Figure 3.29. The results shown that the transcript levels of *phaA*, *aas* and *plsX* genes in Ox-Aas strain were higher than those of WT whereas the expression level of *accA* transcript was lower than WT under normal BG<sub>11</sub> condition.

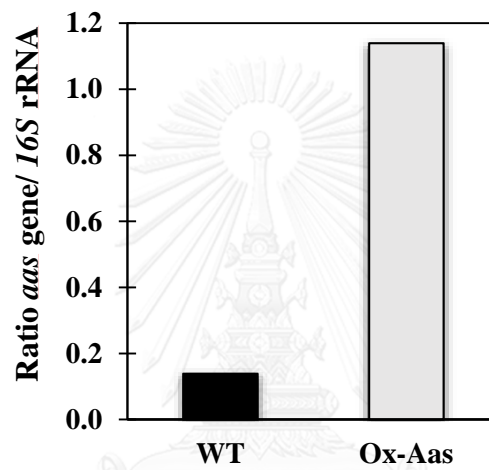
#### 3.8.2 The expression levels of related genes under phosphorus-deprived condition

The transcript levels of *accA*, *aas*, *plsX*, *phaA* and *16S* rRNA genes were shown in Figure 3.30. After WT cells were adapted under phosphorus-deprived (BG<sub>11</sub>-P) condition, the transcript levels of *accA*, *aas* and *plsX* genes were increased of about 1.8, 2, and 4 fold higher than those of WT under normal condition (BG<sub>11</sub>), respectively, whereas *phaA* transcript was down-regulated of about 1.1 fold decrease. After Ox-Aas cells were adapted under BG<sub>11</sub>-P condition, the transcript levels of *accA*, *phaA*, *aas* and *plsX* genes were of about 2, 1.5, 1.2 and 3.3 fold decreases compared with those of Ox-Aas under normal condition, respectively. The transcript levels of *phaA*, *aas* and *plsX* genes of Ox-Aas strain exhibited higher than those of WT whereas the expression level of *accA* gene was 3 fold-decrease.

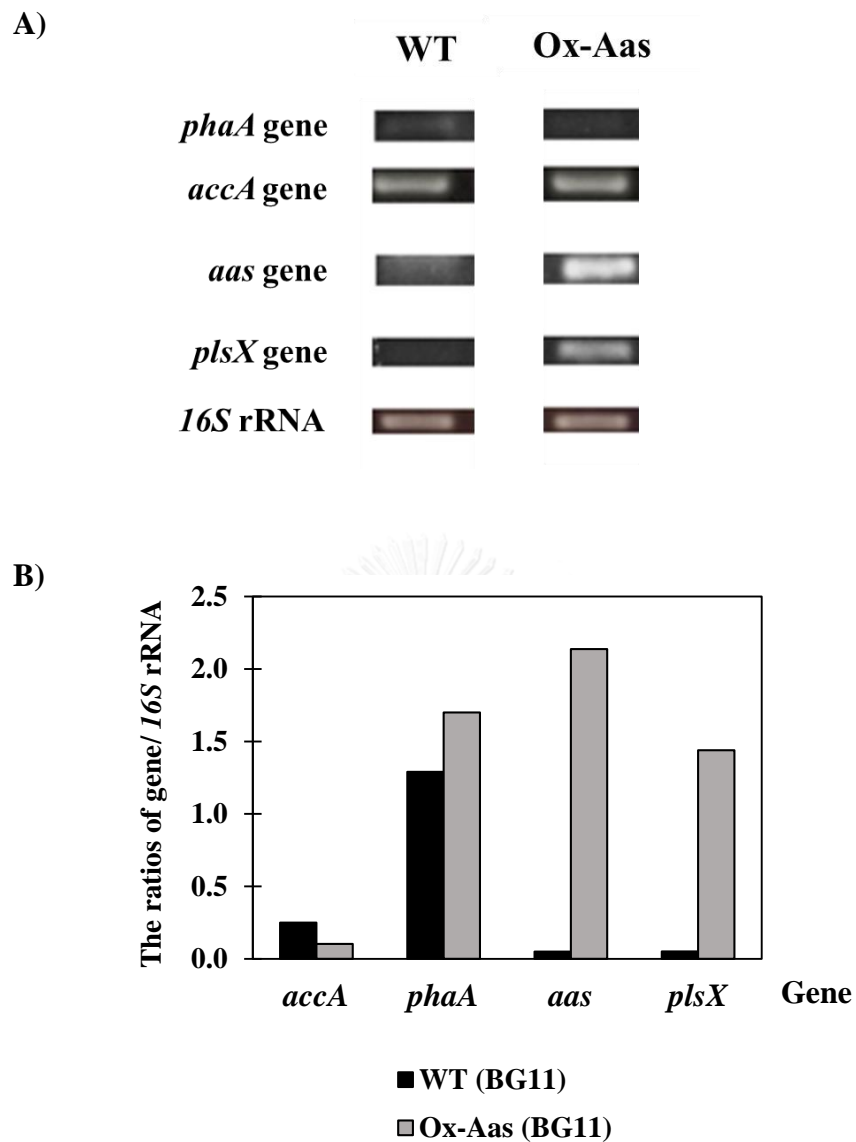
A)



B)



**Figure 3.28** RT-PCR products of *16S* rRNA and *aas* transcripts (A) in both strains under the normal BG<sub>11</sub> medium. The intensity ratio (B) of *aas*/*16S* rRNA transcripts analyzed by GelQuant.NET program.

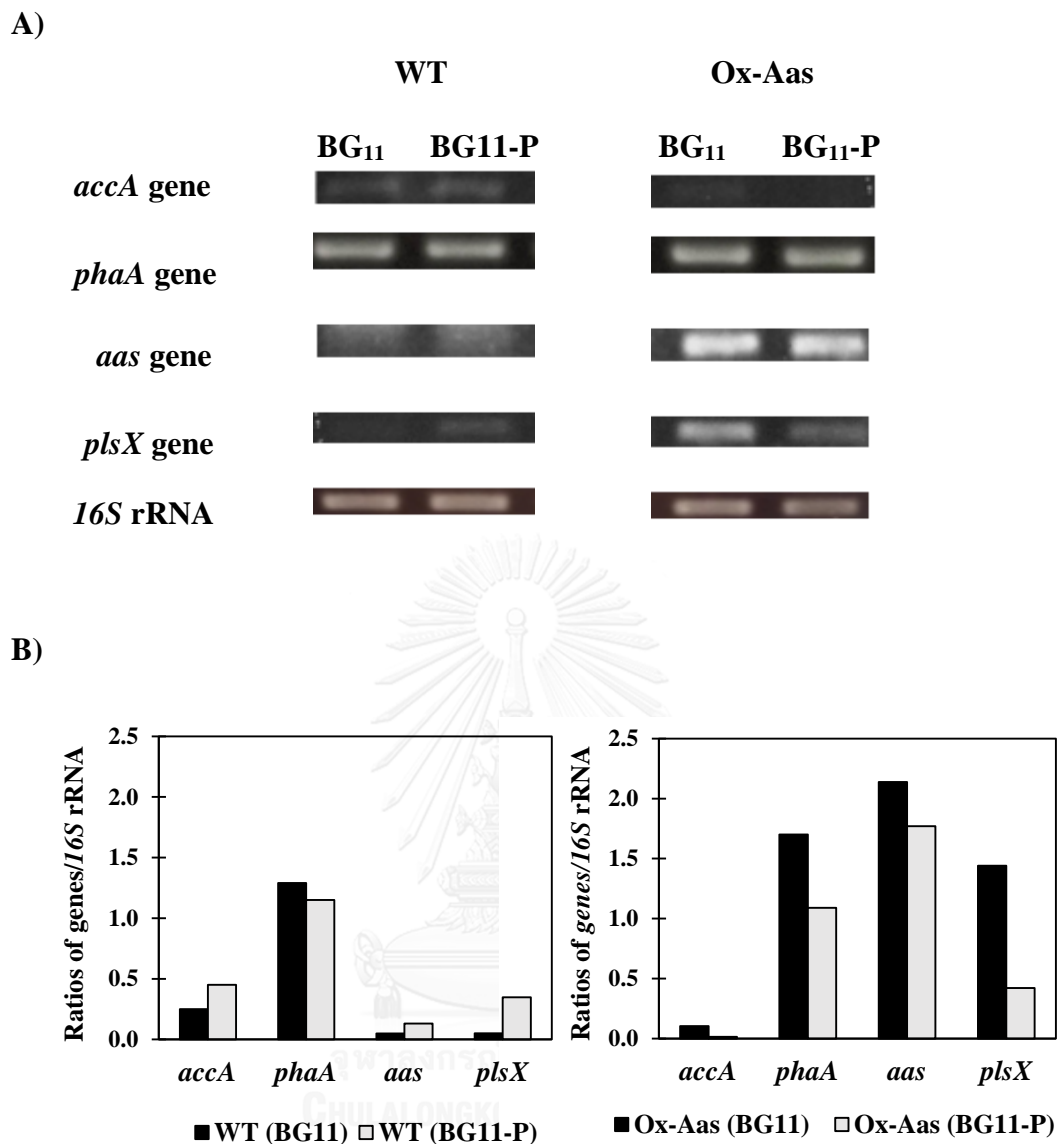


**Figure 3.29** The transcript levels (A) of *phaA*, *accA*, *aas*, *plsX* and *16S* rRNA genes of WT and Ox-Aas strains after adapted under the normal (BG<sub>11</sub>) condition. The intensity ratios (B) of *accA/16S* rRNA, *phaA/16S* rRNA, *aas/16S* rRNA and *plsX/16S* rRNA analyzed by GelQuant.NET program.

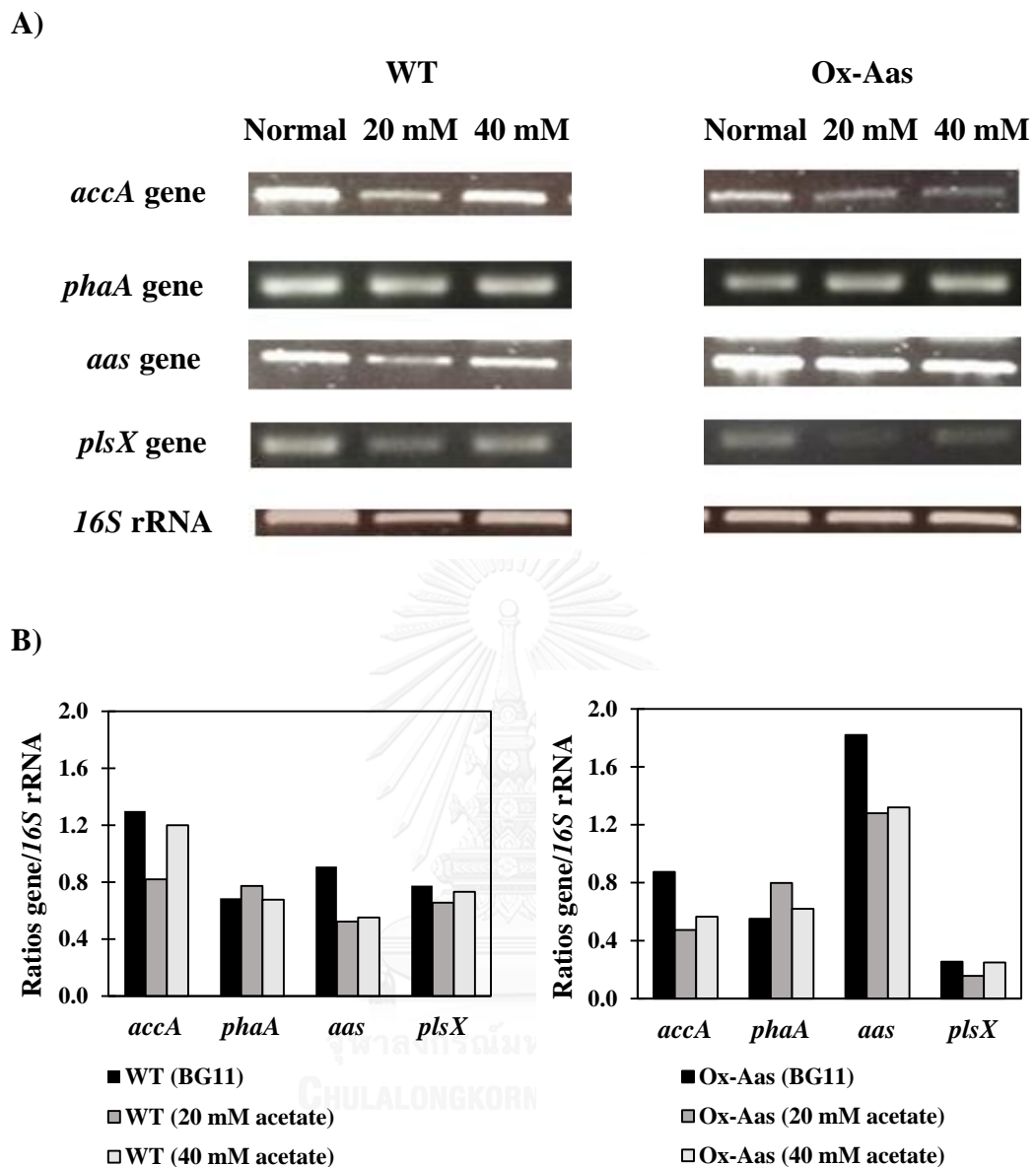
Under BG<sub>11</sub>-P condition, the transcript levels of *accA* and *phaA* genes of Ox-Aas strain were decreased of about 2 and 1.1 fold lower than those of WT, respectively, whereas the expression levels of *aas* and *plsX* transcripts were increased of about 8.5 and 4 fold higher than those of WT, respectively.

### 3.8.3 The expression levels of related genes under acetate addition

The transcript amounts of *accA*, *aas*, *plsX*, *phaA* and *16S* rRNA genes were shown in Figure 3.31. Under normal condition during log-phase of cell growth, the transcript levels of *phaA*, *accA* and *plsX* genes of Ox-Aas strain were 0.85, 0.69 and 0.75 fold lower than WT, respectively, whereas the expression level of *aas* gene was 2 fold higher than WT. Under acetate addition conditions, the transcript patterns of *accA*, *plsX* and *aas* genes of both WT and Ox-Aas strains were not apparently different between 20 and 40 mM acetate conditions. The results suggested that when the concentration of acetate was increased, the transcript levels of all gene transcripts studied were decreased. However, Ox-Aas strain accumulated higher level of *aas* transcript than that of WT. Results were corresponded to the determination of lipid contents in the cells that the acetate addition could not enhance lipid accumulation when the amount of acetate in medium was increased.



**Figure 3.30** The transcript levels (A) of *phaA*, *accA*, *aas*, *plsX* and *16S* rRNA genes of WT and Ox-Aas strains after adapted under the normal (BG<sub>11</sub>) and phosphorus-depleted medium (BG<sub>11</sub>-P) conditions. The intensity ratios (B) of *accA*/*16S* rRNA, *phaA*/*16S* rRNA, *aas*/*16S* rRNA and *plsX*/*16S* rRNA analyzed by GelQuant.NET program.



**Figure 3.31** The transcript levels (A) of *phaA*, *accA*, *aas*, *plsX* and *16S* rRNA genes of WT and Ox-Aas under the BG<sub>11</sub> normal (Normal) and the nutrient modified conditions (20 mM and 40 mM acetate) during log-phase of cell growth. The intensity ratios (B) of *accA/16S* rRNA, *phaA/16S* rRNA, *aas/16S* rRNA and *plsX/16S* rRNA transcripts analyzed by GelQuant.NET program.



## CHAPTER IV

### DISCUSSION

In this study, we employed the bioinformatics to demonstrate that the multiple sequence alignment of amino acid sequences of AAS proteins from *Arabidopsis thaliana*, *Synechocystis* sp. PCC 6803 and *Synechococcus* sp. PCC 7942 presented two highly conserved sequence motifs which corresponded to acyl-ACP synthetase in previous study. Kaczmarzyk and Fulda (2009) reported that AAS of *Synechocystis* sp. PCC 6803 and *Synechococcus* sp. PCC 7942 showed three putative specific residues that absolutely conserved in the group of acyl-ACP synthetase proteins which correlated to AAE15 from *Arabidopsis thaliana* (Koo *et al.*, 2005). In cyanobacterium *Synechocystis* sp. PCC 6803, the annotated amino acid sequences of *aas* gene were shown as long-chain fatty acid CoA ligase or acyl-CoA synthetase and predicted as fatty acid-activating enzyme. The conserved motifs within those amino acid sequences can be identified as AMP-binding proteins which was highly degree of similarity to certain AMP-binding proteins of *Arabidopsis thaliana*. One of this member group was designated as acyl-ACP synthetase or AAE15 encoded by *at4g14070* gene located in chloroplast. The function of acyl-ACP synthetase enzymatic activity is to incorporate exogenous elongated fatty acids into fatty acyl-ACP (Koo *et al.*, 2005). The mutants of unicellular *Escherichia coli* and *Saccharomyces cerevisiae* (yeast) with the deletion of acyl-ACP synthetase showed that acyl-ACP synthetase enzyme did not utilize exogenous fatty acids (Knoll *et al.*, 1995; Overath *et al.*, 1969). The genome sequence of cyanobacterium *Synechocystis* sp. PCC 6803 shows only one protein which predicted as fatty acid activation enzyme. This protein is acyl-acyl carrier protein synthetase

encoded by *slr1609* or *aas* gene (Kaczmarzyk and Fulda, 2010). Its nucleotide sequences are available in Cyanobase database.

In this study, we constructed *Synechocystis* with *aas*-overexpressing (Ox-Aas) strain and demonstrated total lipid contents of cells compared with WT. The pEERM 1 vector was used in this study. This vector is a series of integrative vectors which used for transgenic overexpression in the genome by carried all genetic parts including inserted gene which needed for integration and expression. The differential series of pEERM vectors depended on insertion sites in the genome, with either the strong native *psbA2* promoter or the nickel inducible *nrsB* promoter which used for diving expression of inserted gene (Englund *et al.*, 2015). In this research, pEERM vector contains the region of upstream and downstream of *psbA2* gene which used for homologous recombination, *PsbA2* promoter, multiple cloning sites including *XbaI*, *PstI* and *SpeI*, terminators and antibiotic chloramphenicol cassettes. All of these regions were integrated into the open-reading frame of *psbA2* and then used *psbA2* promoter to drive gene expression. The deletion of native *psbA2* gene was occurred by double homologous recombination. The *psbA2* gene encodes the D1 protein involved in photosynthesis system II (PSII). The PSII of higher plants, algae and cyanobacteria is prone to light-induced oxidative damages and D1 protein is the primary target of that damage. Thus, D1 protein can be constantly degraded and re-synthesized in multiple steps called PSII repair cycle (Aro *et al.*, 1993; Baena-Gonzalez and Aro, 2002; Nixon *et al.*, 2010). In cyanobacteria, D1 protein encodes by *psbA1*, *psbA2* and *psbA3* gene and the transcript levels of each gene depended on the environment (Mulo *et al.*, 2009). When *psbA2* is deleted, *psbA3* gene can be compensated. Therefore, the changed phenotype has not been reported (Mohamed and Jansson, 1989) from the use of the site.

However, we found that the obtained Ox-Aas strain was crossed over by single recombination of all successive clones while the Control WT strain was crossed over by double recombination. A single recombination was occurred to integrate the complete plasmid at the target site (Figure 3.4B) whereas double recombination was occurred by replacing the native gene between two sites of recombination (Figure 3.4C). The type of recombination depends on site and length of sequences including flanking region, DNA fragment of insertion and cyanobacterial strains, such as the homologous recombinant of *Synechosystis* sp. PCC 6803 requires the shortest flanking homologous targets sequence at least 300 bp (Domain *et al.*, 2004) whereas *Nostoc punctiforme* strain ATCC29133 (PCC 73102) requires about 700 bp (Cohen *et al.*, 1998). Labarre and coworkers (1989) found that single integrative crossover occurred rarely in *Synechosystis* sp. PCC 6803, they also suggested that this recombination occurred via non-reciprocal exchange (gene conversion) rather than a double recombination (Labarre *et al.*, 1989). However, Ox-Aas in this study was successfully constructed by single recombination mechanism.

We also demonstrated that the growth of WT cells was higher than those of both *aas*-overexpressing (Ox-Aas) and Control WT cells. However, Ox-Aas cell growth was higher than Control WT whereas the pigment contents including chlorophyll *a* and carotenoid of both Ox-Aas and Control WT exhibited lower amount than WT after log phase (4 days) of growth stages. The oxygen evolution rate which represented as the photosynthetic efficiency of Ox-Aas was higher than WT during all growth phases. This result indicates that engineered Ox-Aas strain could grow normally with the normal efficiency of photosynthesis. There are many previous reports working with engineering strains with genes related to photosynthesis. Recently, Sardre and

coworkers (2012) found that the growth profiles of a knockout mutant lacking 4-hydroxybenzoate solanesyltransferase (encoded by *slr0926* gene related to ubiquinone biosynthesis, a central role in energy transformation process in cyanobacteria) was higher than that of the mutant cell carrying an empty T415 vector (Sadre *et al.*, 2012). As corresponding as the other research reported that the growth patterns of three mutants (CB, CK and PAL) of light-harvesting complex which cultivated under normal BG<sub>11</sub> medium containing 10 µg/ml of antibiotics (chloramphenicol or kanamycin) were slightly lower than *Synechocystis* sp. PCC 6803 WT during cultivation times (16 days) whereas chlorophyll *a* of WT (2.10 and 2.48 µg/10<sup>8</sup> cells) gave higher than those of mutant strains (1.47 and 1.71 µg/10<sup>8</sup> cells of CB, 2.40 and 1.67 µg/10<sup>8</sup> cells of CK) at exponential and stationary phases (after 24 and 120 hours of cultivation, respectively). The normal *in vivo* oxygen evolution rate of cyanobacterial WT cells with ranging of about 60-200 µmol/ mg Chl *a*/h depending on the mutagenic cells and the intensity of light for cultivation (Page *et al.*, 2012). The levels of those pigments in that research were consistent to our results in this study. Moreover, Ruffing and Jones (2012) shown the growth curve of *Synechococcus* sp. PCC 7002 and *S. elongatus* PCC 7942 strains with genes knockout of the FAA-recycling acyl-ACP synthetase/long-chain-fatty acid CoA ligase (*aas/fabD*) and the FAA-recycling acyl-ACP synthetase/long-chain-fatty acid CoA ligase/*E.coli* thioesterase (*aas/tesA*) were slightly lower than their WT under the normal BG<sub>11</sub> medium (Ruffing and Jones, 2012). In addition, the antibiotics in the cultured medium effected on growths of algae, cyanobacterial and bacterial cells also depended on theirs concentrations (Van der Grinten *et al.*, 2010). In bacterium *Escherichia coli* cells, the growth rate was inhibited by antibiotic chloramphenicol (50% at 1.8 µM Cm) as well as protein synthesis which was inhibited by antibiotic

(Harvey and Koch, 1980). The concentration of 1.0-6.0  $\mu\text{g/ml}$  Cm gradually decreased the growth of the nitrogen-fixing cyanobacterium *Nostoc muscorum* (Pattanaik and Singh, 1988).

On the other hand, our finding from nitrogen-starvation (-N) effect on cell growth of all WT, Control WT and Ox-Aas strains showed a slight decrease after 4 day-treatment whereas the pigment contents of cells under this condition was decreased after 24 hour of treatment than these under normal condition. The nutrient starvations including phosphorus (-P), nitrogen (-N) and both phosphorus and nitrogen (-N/P) nutrients affected on growth of cyanobacterial cells as well as in microalgae and algae (Garibay-Hernandez *et al.*, 2013; Harke and Gobler, 2013). The previous research reported that the growth and pigment contents of *Synechococcus* sp. PCC 7002 cells were decreased after 24 hours-treatment with nitrogen-depleted (-N) medium and then they did not grow photoautotrophically in N-depleting condition (Davies *et al.*, 2014). This was due to their inhibitory effect to degrade the light-harvesting phycobilisomes as source of nitrogen (Grundel *et al.*, 2012). The data shown that chlorophyll *a* content was not increased after treating with N-limitation condition and it seemed to lower than normal condition (Davies *et al.*, 2014) and this N-depleted condition apparently induced the reduction of chlorophyll *a* concentrations during treated times (Juergens *et al.*, 2015). In this study, the phosphorus-deprived (-P) condition slightly decreased cell growth of both WT and Ox-Aas strains after 4 day-treatment. However, it was reported previously that algal blooming was found in natural water containing a low concentration of phosphorus (P) area with a few  $\mu\text{g/L}$  amount (Schopf *et al.*, 1996). The experimental data of previous reports showed the affinity values of either nitrogen or phosphorus of many cyanobacteria were higher than many other photosynthetic

microalgae (Mur *et al.*, 1999). As they had a specific affinity with phosphorus, they could store phosphorus that enough for two to four cell divisions (Schopf *et al.*, 1996) which led them gaining higher cell density and growth. In this study, the phosphorus deprivation also affected on chlorophyll *a* reduction in both WT and Ox-Aas strains whereas it showed a slight decrease on the carotenoid accumulation in both strains. It is coincident with a previous report that P-limitation effected to the pigments by an obvious reduction of chlorophyll *a* contents but slightly affected to carotenoid reduction in *Microcystis aeruginosa* PCC 7806 (Yang *et al.*, 2013). Moreover, the oxygen evolution rate was changed during cultivation under the nutrient deprivations. The oxygen evolution of a unicellular algae *Chlamydomonas reinhardtii* which cultivated under N-depleting demonstrated lower level when compared with WT (Juergens *et al.*, 2015). On the other hand, our study revealed that acetate supplementation which various concentrations influenced on cell growth and pigments of WT, Ox-Aas and Control WT strains with a slight reduction whereas the oxygen evolution rates of all studied strains were not changed in corresponding to the levels of acetate concentrations in the medium. It was contrast with the previous study that growth curve of *Synechocystis* WT was increased when sodium acetate was increased to 20 mM in normal BG<sub>11</sub> medium (Guifang *et al.*, 2002). In *Chlamydomonas reinhardtii* cells, acetate concentrations had no influence on their growth rate, respiration, PS II efficiency and chlorophyll content whereas the oxygen evolution rate tended to decrease against the increase of acetate concentration (0, 3.7, 7.4, 14.7 and 29.4 mM, respectively) (Heifetz *et al.*, 2000). In this study, the decreases of growth and pigment contents of engineered strains might be caused by the disruption of *psbA<sub>2</sub>* gene in Control WT and the overexpressing of *aas* gene in Ox-Aas strain besides the effect of

antibiotic chloramphenicol which added into medium during cultivation of these strains.

On the other hand, although the Sudan Black staining method could not distinguish the differences of lipids between WT and Ox-Aas strains which cultivated under all condition studied, the polar lipids located on *Synechocystis* membranes were visually observed under microscope. Sudan Black B staining is slightly basic dye which used for screening total polar lipids with acidic group of phospholipid compounds in tissues sections and cells (Burdon, 1946). The most of polar lipids presented in thylakoid membranes of cyanobacteria (Quintana *et al.*, 2011).

We also demonstrated the higher level of total lipids in Ox-Aas strain than WT at log and early stationary phases whereas the total unsaturated lipid content was not significantly when compared with WT under normal condition. Strikingly, our finding indicated the higher amount of lipid content than earlier study which reported the lipid accumulation of *Synechocystis* cells which was still limited to about 15% w/w CDW (Sheng *et al.*, 2011). The data suggested that Ox-Aas which successfully constructed in this study effectively enhanced about 1.5 to 5-fold increase of lipid accumulation (22-25.5% w/w CDW) in *Synechocystis* cells under normal BG<sub>11</sub> medium by growth phases-dependent regulation. The levels of unsaturated lipid of both WT and Ox-Aas strains were not different in all growth phases. The Ox-Aas strain did not influence on unsaturated lipid production in *Synechocystis* cells. In contrast with the previous finding of the AAS effect on unsaturated fatty acid production, which reported that *Synechocystis* cells with *Aas*-deletion gene could enhance the level of unsaturated lipids (Kaczmarzyk and Fulda, 2010). That was due to the source of free fatty acids, substrates for AAS activity which were mainly released from membrane degradation

(Kaczmarzyk and Fulda, 2010). Mustardy *et al.* (1996) suggested that the fatty acid desaturation of membrane lipids took place in the thylakoid membranes. Thus, it is interesting that Ox-Aas strains could enhance the total lipid accumulation whereas the level of unsaturated lipids was not different when compared with WT (Mustardy *et al.*, 1996).

After we studied about the effect of the nutrient deprivations including -N, -P and both -N/P, it was found that the optimum condition of this study was phosphorus deprivation at log phases of growth which obviously enhanced the total lipid contents in *Synechocystis* cell of both WT and Ox-Aas strains by 1.2-fold increase of total lipids. The higher induction of unsaturated lipids was presented under BG<sub>11</sub>-N and BG<sub>11</sub>-N/P conditions. Changing environmental conditions caused changes in lipid composition which led to effect on photosynthetic yield and efficiency (Li *et al.*, 2012; Philipps *et al.*, 2011). In other report, the autophototrophic growth with nitrogen deprivation was the optimum condition for polyhydroxybutyrate (PHB) production at mid-stationary phase while the lipid was decreased (from 14.1 to 11.2 % lipid) in *Synechocystis* sp. PCC 6803 (Monshupanee and Incharoensakdi, 2014). The total lipid contents of non-nitrogen fixing marine cyanobacterium *Oscillatoria willei* BDU 130511 cells were decreased under nitrogen deprivation stress (Saha *et al.*, 2003). Moreover, the recent research reported that phosphorus (P) deficiency condition resulted in increased lipid content in *Synechocystis* sp PCC 6803 after 7 day-treatment when compared with those under BG<sub>11</sub>-N and normal BG<sub>11</sub> conditions. Coincidentally, unsaturated lipid content was enhanced after adapting under N and P deprived conditions (Singh and Mallick, 2014). Due to the fact that the protein synthesis under nitrogen deficiency was inhibited by unavailability of N source. Thus, it turned to other biosynthesis including carbohydrate



or lipid rather than protein synthesis (Richardson *et al.*, 1969). When the nitrogen pool was decreased, the amino acid synthesis was also decreased which influenced to excess of NADPH in the cells (Van Wegen *et al.*, 2001). However, NADPH acts as a reducing compound that plays the important role in two steps of reduction process of fatty acid synthesis (Hutchings, 2005). Furthermore, nitrogen limitation could cause the increase of oleic acid by increasing the activity of stearyl-ACP desaturase in *Botryococcus braunii* (Choi *et al.*, 2010). P-deficiency potentially enhanced lipid accumulation by increasing the reducing compounds (Konopka and Schnur, 1981). In this study, we found that the total lipid and unsaturated lipid accumulations tended to decrease when acetate concentrations were increased up to 40 mM in all WT, Control WT and Ox-Aas strains. This is caused by acetate which acted as carbon source for acetyl-CoA necessary in metabolic pathways including TCA cycle, PHB, fatty acid and lipid synthetic pathways. That acetate will be converted to acetyl-CoA via acetyl-CoA synthetase. The previous study reported that *Synechocystis* sp. PCC 6803 when treated with 20 mM acetate apparently enhanced PHB accumulation up to 11.0 % of dried cell weight instead of lipid enhancement (Guifang *et al.*, 2002). However, acetate could also flow to acetyl-CoA and passes many steps to fatty acid synthesis II (FAS II) in order to synthesize the fatty acyl-ACP, an intermediate compounds for lipid synthesis. Moreover, Acyl-ACP also controls fatty acid synthesis by acting as a feedback metabolites allosterically which inhibits the rate-limiting step, acetyl-CoA carboxylase (encoded by *AccBACD*) enzymatic activity. Moreover, acyl-ACP likely inhibits two enzymes inside FAS process including  $\beta$ -ketoacyl synthase I (encoded by *fabH*) and trans-2-enoyl-ACP reductase (FabI encoded by *fabI*) (Heath and Rock, 1996).

In this research, the transcripts of *accA*, *aas*, *plsX*, *phaA* and 16S rRNA genes were observed and used for explaining of metabolic pathways. Under normal condition, the expression levels of *aas* and *plsX* genes of Ox-Aas strain was obviously higher than WT whereas the transcript level of *accA* was decreased when compared with WT. This result may be supported from the previous study that fatty acyl-CoA, the products of AAS activity acted as a substrate for many pathways including alkene/alkane production, lipid synthesis and also reversion to acetyl-CoA (Gao *et al.*, 2012; Quintana *et al.*, 2011; Wang *et al.*, 2013). The expression levels of *phaA* encoding PHA-specific beta-ketothiolase of both WT and Ox-Aas were not different under normal condition. Interestingly, after treating WT with P-deficient medium, *accA*, *aas*, and *plsX* transcripts were up-regulated whereas the expression level of *phaA* was slightly decreased. In Ox-Aas strain, the decrease of *accA* transcript was significantly decreased. The significant increases were seen with *phaA*, *aas* and *plsX* transcripts under normal condition whereas all gene transcripts studied of Ox-Aas was decreased by BG<sub>11</sub>-P condition. On the other hand, lack of nitrogen is the resulting of excess NADPH, reducing compounds, thus, this condition potentially induced fatty acid synthesis pathway (Heath *et al.*, 2002). Moreover, fatty acyl-ACP is the substrate of membrane lipid biosynthesis and the first enzyme of this pathway is phosphate acyltransferase (encoded by *plsX*) (Zhang and Rock, 2008). Under acetate additions, we found that not only the level of lipids was decreased, but the expression levels of *accA*, *aas* and *plsX* transcripts of both strains were also decreased. Whereas, *phaA* transcribes of both strains were slightly increased when 20 mM of acetate presence in the medium. Guifang *et al.* (2002) reported that 20 mM acetate in normal BG<sub>11</sub> conditions availably enhanced PHB accumulation of *Synechocystis* WT (Guifang *et al.*,

2002). From this work, the result suggested that *Synechocystis* with *aas*-overexpressing genes (Ox-Aas) effectively enhanced lipid accumulation in the cell. However, naturally producing lipid contents in living cells are limited by biochemical homeostasis mechanism.



## CHAPTER V

### CONCLUSION

In this study, the *aas*- overexpressing (Ox-Aas) strain of *Synechocystis* sp. PCC 6803 was successfully constructed by single recombination mechanism. Cell growth and intracellular pigment contents of Ox-Aas were slightly lower than wild type (WT) whereas the oxygen evolution rate of Ox-Aas was higher than WT. In addition, the total lipid content of Ox-Aas strain was significantly higher than wild type whereas the unsaturated lipid contents were not different. The highest lipid content of Ox-Aas was accumulated during log phase of growth about 22.2 %w/w CDW which was higher than WT with 15.3 %w/w CDW. Moreover, the transcript levels of *aas* gene of Ox-Aas strain was 10 fold higher than WT at log phase of growth when grown in normal BG<sub>11</sub> medium. On the other hand, P-deprived condition potentially induced the accumulation of total lipid in Ox-Aas strain up to 1.5 fold (about 27.3 %w/w CDW) higher than wild type at log phase of cell growth. In contrast, the acetate supplementation (up to 40 mM concentration) decreased total lipids and unsaturated lipid accumulations in both WT and Ox-Aas strains. From the amino acid sequence alignment and phylogenetic tree, the acyl-ACP synthetase protein of *Synechocystis* is the member of AMP-binding group which contains the specific amino acid residues related to acyl-ACP synthetases. Although, AAS play a role in fatty acid recycling process, overexpression of *aas*-gene of *Synechocystis* apparently enhanced lipid levels in the cells. Moreover, the transcript levels of *accA* which is the rate-limiting step of fatty acid biosynthesis of Ox-Aas strain tended to decrease when the expression levels of *aas* gene was increased. Altogether, the *aas*- overexpressing strain of *Synechocystis* sp. PCC 6803 effectively enhanced total lipid contents, which could be further increased under phosphorus-deprived condition.

## REFERENCES

- Anand, J. and Arumugam, M. (2015). "Enhanced lipid accumulation and biomass yield of *Scenedesmus quadricauda* under nitrogen starved condition." *Bioresource Technology* 188: 190-194.
- Andre, C., Haslam, R. P. and Shanklin, J. (2012). "Feedback regulation of plastidic acetyl-CoA carboxylase by 18:1-acyl carrier protein in *Brassica napus*." *Proceedings of the National Academy of Sciences of the United States of America* 109(25): 10107-10112.
- Aro, E.-M., Virgin, I. and Andersson, B. (1993). "Photoinhibition of photosystem II. Inactivation, protein damage and turnover." *Biochimica et Biophysica Acta (BBA) - Bioenergetics* 1143(2): 113-134.
- Awai, K., Watanabe, H., Benning, C. and Nishida, I. (2007). "Digalactosyldiacylglycerol is required for better photosynthetic growth of *Synechocystis* sp. PCC 6803 under phosphate limitation." *Plant & Cell Physiology* 48(11): 1517-1523.
- Baena-Gonzalez, E. and Aro, E. M. (2002). "Biogenesis, assembly and turnover of photosystem II units." *Philosophical Transactions of the Royal Society of London. Series B: Biological Sciences* 357(1426): 1451-1459; discussion 1459-1460.
- Balogi, Z., Török, Z., Balogh, G., Jósavay, K., Shigapova, N., Vierling, E., Vígh, L. and Horváth, I. (2005). "'Heat shock lipid' in cyanobacteria during heat/light-acclimation." *Archives of Biochemistry and Biophysics* 436(2): 346-354.

- Barnes, E. M. and Wakil, S. J. (1968). "Studies on the mechanism of fatty acid synthesis: XIX. Preparation and general properties of palmityl thioesterase." *Journal of Biological Chemistry* 243(11): 2955-2962.
- Bonner, W. M. and Bloch, K. (1972). "Purification and properties of fatty acyl thioesterase I from *Escherichia coli*." *Journal of Biological Chemistry* 247(10): 3123-3133.
- Burdon, L. K. (1946). "Fatty material in bacteria and fungi revealed by staining dried, fixed slide." *Journal of Bacteriology* 52: 665-678.
- Cai, T., Ge, X., Park, S. Y. and Li, Y. (2013). "Comparison of *Synechocystis* sp. PCC 6803 and *Nannochloropsis salina* for lipid production using artificial seawater and nutrients from anaerobic digestion effluent." *Bioresource Technology* 144: 255-260.
- Chamovitz, D., Sandmann, G., and Hirschberg, J. (1993). "Molecular and biochemical characterization of herbicide-resistant mutants of cyanobacteria reveals that phytoene desaturation is a rate-limiting step in carotenoids biosynthesis." *Journal of Biological Chemistry* 268: 17348-17353.
- Cheng, Y.-S., Zheng, Y. and VanderGheynst, J. S. (2011). "Rapid quantitative analysis of lipids using a colorimetric method in a microplate format." *Lipids* 46(1): 95-103.
- Choi, G.-G., Kim, B.-H., Ahn, C.-Y. and Oh, H.-M. (2010). "Effect of nitrogen limitation on oleic acid biosynthesis in *Botryococcus braunii*." *Journal of Applied Phycology* 23(6): 1031-1037.

- Cohen, M. F., Meeks, J. C., Cai, Y. A. and Wolk, C. P. (1998). Transposon mutagenesis of heterocyst-forming filamentous cyanobacteria. San Diego, Academic Press Incorporation.
- Davies, F. K., Work, V. H., Beliaev, A. S. and Posewitz, M. C. (2014). "Engineering limonene and bisabolene production in wild type and a glycogen-deficient mutant of *Synechococcus* sp. PCC 7002." Frontiers in Bioengineering and Biotechnology 2: 21.
- Davis, M. S. and Cronan, J. E., Jr. (2001). "Inhibition of *Escherichia coli* acetyl coenzyme A carboxylase by acyl-acyl carrier protein." Journal of Bacteriology 183(4): 1499-1503.
- Davis, M. S., Solbiati, J. and Cronan, J. E., Jr. (2000). "Overproduction of acetyl-CoA carboxylase activity increases the rate of fatty acid biosynthesis in *Escherichia coli*." Journal of Biological Chemistry 275(37): 28593-28598.
- Domain, F., Houot, L., Chauvat, F. and Cassier-Chauvat, C. (2004). "Function and regulation of the cyanobacterial genes *lexA*, *recA* and *ruvB*: LexA is critical to the survival of cells facing inorganic carbon starvation." Molecular Microbiology 53(1): 65-80.
- Englund, E., Andersen-Ranberg, J., Miao, R., Hamberger, B. and Lindberg, P. (2015). "Metabolic engineering of *Synechocystis* sp. PCC 6803 for production of the plant diterpenoid manoyl oxide." ACS Synthetic Biology 4(12): 1270-1278.
- Fales, F. W. (1971). "Evaluation of a spectrophotometric method for determination of total fecal lipid." Clinical Chemistry 17(1103-1107).
- Fisher, A. B. and Jain, M. (2001). Phospholipases: Degradation of phospholipids in membranes and emulsions. eLS, John Wiley & Sons, Ltd.

- Fuhrmann, E., Gathmann, S., Rupprecht, E., Golecki, J. and Schneider, D. (2009). "Thylakoid membrane reduction affects the photosystem stoichiometry in the cyanobacterium *Synechocystis* sp. PCC 6803." *Plant Physiology* 149(2): 735-744.
- Fuszard, A. M., Ow, Y. S., Gan, S. C., Noirel, J., Ternan, G. N., McMullan, G., Biggs, A. C., Reardon, F. K. and Wright, C. P. (2013). "The quantitative proteomic response of *Synechocystis* sp. PCC 6803 to phosphate acclimation." *Aquatic Biosystems* 9: 5.
- Gao, Q., Wang, W., Zhao, H. and Lu, X. (2012). "Effects of fatty acid activation on photosynthetic production of fatty acid-based biofuels in *Synechocystis* sp. PCC 6803." *Biotechnology for Biofuels* 5(1): 1-9.
- Garibay-Hernandez, A., Vazquez-Duhalt, R., Serrano-Carreón, L. and Martínez, A. (2013). "Nitrogen limitation in *Neochloris oleoabundans*: a reassessment of its effect on cell growth and biochemical composition." *Applied Biochemistry and Biotechnology* 171(7): 1775-1791.
- Grigorieva, G. and Shestakov, S. (1982). "Transformation in the cyanobacterium *Synechocystis* sp. PCC 6803." *FEMS Microbiology Letters* 13: 367-370.
- Grundel, M., Scheunemann, R., Lockau, W. and Zilliges, Y. (2012). "Impaired glycogen synthesis causes metabolic overflow reactions and affects stress responses in the cyanobacterium *Synechocystis* sp. PCC 6803." *Microbiology* 158(Pt 12): 3032-3043.
- Guifang, W., Tian, B., Zhongyao, S. and Qingyu, W. (2002). "Sodium acetate stimulates PHB biosynthesis in *Synechocystis* sp. PCC 6803." *Tsinghua Science and Technology*, 7.



- Harke, M. J. and Gobler, C. J. (2013). "Global transcriptional responses of the toxic cyanobacterium, *Microcystis aeruginosa*, to nitrogen stress, phosphorus stress, and growth on organic matter." *PloS One* 8(7): e69834.
- Harvey, J. R. and Koch, L. A. (1980). "How partially inhibitory concentrations of chloramphenicol affect the growth of *Escherichia coli*." *Antimicrobial Agents and Chemotherapy* 18: 323-337.
- Heath, J. R., Jackowski, S. and Rock, O. C. (2002). "Fatty acid and phospholipid metabolism in prokaryotes." *Biochemistry of Lipids, Lipoproteins and Membranes*: 59-96.
- Heath, J. R. and Rock, O. C. (1996). "Inhibition of beta-ketoacyl-acyl carrier protein synthase III (FabH) by acyl-acyl carrier protein in *Escherichia coli*." *The Journal of Biological Chemistry* 271: 10996-11000.
- Heifetz, B. P., Forster, B., Osmond, B. C., Giles, J. L. and Boynton, E. J. (2000). "Effects of acetate on facultative autotrophy in *Chlamydomonas reinhardtii* assessed by photosynthetic measurements and stable isotope analyses." *Plant Physiology* 122: 1439-1445.
- Hutchings, D. (2005). "Fatty acid synthesis and the oxidative pentose phosphate pathway in developing embryos of oilseed rape (*Brassica napus* L.)." *Journal of Experimental Botany* 56(412): 577-585.
- Ikeuchi, M. and Tabata, S. (2001). "*Synechocystis* sp. PCC 6803 — a useful tool in the study of the genetics of cyanobacteria." *Photosynthesis Research* 70(1): 73-83.
- Jantaro, S., Mäenpää, P., Mulo, P. and Incharoensakdi, A. (2003). "Content and biosynthesis of polyamines in salt and osmotically stressed cells of *Synechocystis* sp. PCC 6803." *FEMS Microbiology Letters* 228(1): 129-135.

- Jaworski, J. G. and Stumpf, P. K. (1974). "Fat metabolism in higher plants. Properties of a soluble stearyl-acyl carrier protein desaturase from maturing *Carthamus tinctorius*." *Archives of Biochemistry and Biophysics* 162(1): 158-165.
- Juergens, M. T., Deshpande, R. R., Lucker, B. F., Park, J. J., Wang, H., Gargouri, M., Holguin, F. O., Disbrow, B., Schaub, T., Skepper, J. N., Kramer, D. M., Gang, D. R., Hicks, L. M. and Shachar-Hill, Y. (2015). "The regulation of photosynthetic structure and function during nitrogen deprivation in *Chlamydomonas reinhardtii*." *Plant Physiology* 167(2): 558-573.
- Kaczmarzyk, D. and Fulda, M. (2010). "Fatty acid activation in cyanobacteria mediated by acyl-acyl carrier protein synthetase enables fatty acid recycling." *Plant Physiology* 152.
- Kaneko, T., Sato, S., Kotani, H., Tanaka, A., Asamizu, E., Nakamura, Y., Miyajima, N., Hirosawa, M., Sugiura, M. and Sasamoto, S. (1996). "Sequence analysis of the genome of the unicellular cyanobacterium *Synechocystis* sp. strain PCC 6803. II. Sequence determination of the entire genome and assignment of potential protein-coding regions." *DNA Research* 3 109-136.
- Kaneko, T. and Tabata, S. (1997). "Complete genome structure of the unicellular cyanobacterium *Synechocystis* sp. PCC 6803." *Plant Cell Physiology* 38: 1171-1176.
- Khozin-Goldberg, I. and Cohen, Z. (2006). "The effect of phosphate starvation on the lipid and fatty acid composition of the fresh water eustigmatophyte *Monodus subterraneus*." *Phytochemistry* 67(7): 696-701.

Knoll, L. J., Schall, O. F., Suzuki, I., Gokel, G. W. and Gordon, J. I. (1995).

"Comparison of the reactivity of tetradecenoic acids, a triacsin, and unsaturated oximes with four purified *Saccharomyces cerevisiae* fatty acid activation proteins." *The Journal of Biological Chemistry* 270: 20090-20097.

Konopka, A. and Schnur, M. (1981). "Biochemical composition and photosynthetic carbon metabolism of nutrient limited cultures of *Merismopedia tenuissima* (Cyanophyceae) 1." *Journal of Phycology* 17(2): 118-122.

Koo, A. J., Fulda, M., Browse, J. and Ohlrogge, J. B. (2005). "Identification of a plastid acyl-acyl carrier protein synthetase in *Arabidopsis* and its role in the activation and elongation of exogenous fatty acids." *Plant Journal* 44(4): 620-632.

Labarre, J., Chauvat, F. and Thuriaux, P. (1989). "Insertional mutagenesis by random cloning of antibiotic resistance genes into the genome of the cyanobacterium *Synechocystis* strain PCC 6803." *Journal of Bacteriology* 171: 3449-3457.

Li, X., Moellering, E. R., Liu, B., Johnny, C., Fedewa, M., Sears, B. B., Kuo, M. H. and Benning, C. (2012). "A galactoglycerolipid lipase is required for triacylglycerol accumulation and survival following nitrogen deprivation in *Chlamydomonas reinhardtii*." *The Plant Cell* 24(11): 4670-4686.

Liberton, M., Howard Berg, R., Heuser, J., Roth, R. and Pakrasi, B. H. (2006).

"Ultrastructure of the membrane systems in the unicellular cyanobacterium *Synechocystis* sp. strain PCC 6803." *Protoplasma* 227(2): 129-138.

Los, D. A., Zorina, A., Sinetova, M., Kryazhov, S., Mironov, K. and Zinchenko, V. V. (2010). "Stress sensors and signal transducers in cyanobacteria." *Sensors (Basel)* 10(3): 2386-2415.

- Maslova, I. P., Mouradyan, E. A., Lapina, S. S., Klyachko-Gurvich, G. L. and Los, D. A. (2004). "Lipid fatty acid composition and thermophilicity of cyanobacteria." *Russian Journal of Plant Physiology* 51(3): 353-360.
- Meene, A. M. L., Hohmann-Marriott, M. F., Vermaas, W. F. J. and Roberson, R. W. (2006). "The three-dimensional structure of the cyanobacterium *Synechocystis* sp. PCC 6803." *Archives of Microbiology* 184(5): 259-270.
- Mohamed, A. and Jansson, C. (1989). "Influence of light on accumulation of photosynthesis-specific transcripts in the cyanobacterium *Synechocystis* 6803." *Plant Molecular Biology* 13(6): 693-700.
- Monshupanee, T. and Incharoensakdi, A. (2014). "Enhanced accumulation of glycogen, lipids and polyhydroxybutyrate under optimal nutrients and light intensities in the cyanobacterium *Synechocystis* sp. PCC 6803." *Journal of Applied Microbiology* 116(4): 830-838.
- Montgomery, B. L. (2014). "The regulation of light sensing and light-harvesting impacts the use of cyanobacteria as biotechnology platforms." *Frontiers in Bioengineering and Biotechnology* 2: 22.
- Moran, R. a. P., D. (1980). "Chlorophyll determination in intact tissues using N, N-dimethylformamide." *Plant Physiology* 65: 478-479.
- Mulo, P., Sicora, C. and Aro, E. M. (2009). "Cyanobacterial *psbA* gene family: optimization of oxygenic photosynthesis." *Cellular and Molecular Life Sciences* 66(23): 3697-3710.

- Mur, L. R., Skulberg, O. M. and Utkilen, H. (1999). Cyanobacteria and the environment. Toxic cyanobacteria in water *A guide to their public health consequences, monitoring and management*, E & FN Spon, World Health Organization 41-112.
- Murata, N. and Nishida, I. (1987). *Lipids of blue-green algae (cyanobacteria)*. Orlando, Academic Press Incorporation.
- Mustardy, L., Los, A. D., Gombos, Z. and Murata, N. (1996). "Immunocytochemical localization of acyl-lipid desaturases in cyanobacterial cells: Evidence that both thylakoid membranes and cytoplasmic membranes are sites of lipid desaturation." *Plant Biology* 93: 10524-10527.
- Nelson, D. V. and Cox, M. M. (2008). *Lehninger Principles of Biochemistry* New York: W.H. , Freeman and Company.
- Nixon, P. J., Michoux, F., Yu, J., Boehm, M. and Komenda, J. (2010). "Recent advances in understanding the assembly and repair of photosystem II." *Annals of Botany* 106(1): 1-16.
- Olie, J. and Potts, M. (1986). "Purification and biochemical analysis of the cytoplasmic membrane from the desiccation-tolerant cyanobacterium *Nostoc commune* UTEX 584." *Applied and Environmental Microbiology* 52: 706-710.
- Otsuka, H. (1961). "Changes of lipid and carbohydrate contents in *Chlorella* cells during the sulfur starvation, as studied by the technique of synchronous culture." *Journal of General and Applied Microbiology* 7(1): 72-77.
- Overath, P., Pauli, G. and Schairer, H. U. (1969). "Fatty acid degradation in *Escherichia coli*." *European Journal of Biochemistry* 7(4): 559-574.

- Padham, A. K., Hopkins, M. T., Wang, T. W., McNamara, L. M., Lo, M., Richardson, L. G., Smith, M. D., Taylor, C. A. and Thompson, J. E. (2007). "Characterization of a plastid triacylglycerol lipase from *Arabidopsis*." *Plant Physiology* 143(3): 1372-1384.
- Page, L. E., Liberton, M. and Pakrasi, H. B. (2012). "Reduction of photoautotrophic productivity in the cyanobacterium *Synechocystis* sp. strain PCC 6803 by phycobilisome antenna truncation." *Applied and Environmental Microbiology* 78(17): 6349-6351.
- Pattanaik, U. and Singh, P. K. (1988). "Antibiotic effects on growth and heterocyst differentiation of the cyanobacterium *Nostoc muscorum*." *Acta Microbiologica Hungarica* 35(2): 81-88.
- Philipps, G., Happe, T. and Hemschemeier, A. (2011). "Nitrogen deprivation results in photosynthetic hydrogen production in *Chlamydomonas reinhardtii*." *Planta* 235(4): 729-745.
- Quintana, N., Van der Kooy, F., Van de Rhee, M. D., Voshol, G. P. and Verpoorte, R. (2011). "Renewable energy from cyanobacteria: energy production optimization by metabolic pathway engineering." *Applied Microbiology and Biotechnology* 91(3): 471-490.
- Ramanan, R., Kim, B. H., Cho, D. H., Ko, S. R., Oh, H. M. and Kim, H. S. (2013). "Lipid droplet synthesis is limited by acetate availability in starchless mutant of *Chlamydomonas reinhardtii*." *FEBS Letters* 587(4): 370-377.

- Ray, T. K. and Cronan, J. E. J. (1976). "Activation of long chain fatty acids with acyl carrier protein: Demonstration of a new enzyme, acyl-acyl carrier protein synthetase, in *Escherichia coli*." *Proceedings of the National Academy of Sciences of the United States of America* 73: 4374-4378.
- Reistetter, E. N., Krumhardt, K., Callnan, K., Roache-Johnson, K., Saunders, J. K., Moore, L. R. and Rocap, G. (2013). "Effects of phosphorus starvation versus limitation on the marine cyanobacterium *Prochlorococcus* MED4 II: gene expression." *Environmental Microbiology* 15(7): 2129-2143.
- Reitan, K. I., Rainuzzo, J. R. and Olsen, Y. (1994). "Influence of lipid composition of live feed on growth, survival and pigmentation of turbot larvae." *Aquaculture International* 2(1): 33-48.
- Richardson, B., Orcutt, D. M., Schwertner, H. A., Martinez, C. L. and Wickline, H. E. (1969). "Effects of nitrogen limitation on the growth and composition of unicellular algae in continuous culture." *Applied Microbiology* 18(2): 245-250.
- Ritter, D. and Yopp, J. H. (1993). "Plasma membrane lipid composition of the halophilic cyanobacterium *Aphanothece halophytica*." *Archives of Microbiology* 159(5): 435-439.
- Ruffing, A. M. and Jones, H. D. (2012). "Physiological effects of free fatty acid production in genetically engineered *Synechococcus elongatus* PCC 7942." *Biotechnology and Bioengineering* 109(9): 2190-2199.
- Sadre, R., Pfaff, C. and Buchkremer, S. (2012). "Plastoquinone-9 biosynthesis in cyanobacteria differs from that in plants and involves a novel 4-hydroxybenzoate solanesyltransferase." *Biochemical Journal* 442(3): 621-629.

- Saha, K. S., Uma, L. and Subramanian, G. (2003). "Nitrogen stress induced changes in the marine cyanobacterium *Oscillatoria willei* BDU 130511." *FEMS Microbiology Ecology* 45(3): 263-272.
- Schopf, J. W., A.K.S.K., P., Nienow, J. A. and V.N.R., R. (1996). Cyanobacteria, pioneers of the early earth. *Contributions in Phycology*, Berlin publishers. 112: 13-32.
- Sheng, J., Vannela, R. and Rittmann, B. E. (2011). "Evaluation of methods to extract and quantify lipids from *Synechocystis* PCC 6803." *Bioresource Technology* 102(2): 1697-1703.
- Singh, K. D. and Mallick, N. (2014). "Accumulation potential of lipids and analysis of fatty acid profile of few microalgal species for biodiesel feedstock." *Journal of Microbiology and Biotechnology Research* 4: 37-44.
- Valenzuela, J., Carlson, R. P., Gerlach, R., Cooksey, K., Peyton, B. M., Bothner, B. and Fields, M. W. (2013). "Nutrient resupplementation arrests bio-oil accumulation in *Phaeodactylum tricornutum*." *Applied Microbiology and Biotechnology* 97(15): 7049-7059.
- Van der Grinten, E., Pikkemaat, M. G., van den Brandhof, E.-J., Stroomberg, G. J. and Kraak, M. H. S. (2010). "Comparing the sensitivity of algal, cyanobacterial and bacterial bioassays to different groups of antibiotics." *Chemosphere* 80(1): 1-6.
- Van Mooy, B. A., Fredricks, H. F., Pedler, B. E., Dyhrman, S. T., Karl, D. M., Koblizek, M., Lomas, M. W., Mincer, T. J., Moore, L. R., Moutin, T., Rappe, M. S. and Webb, E. A. (2009). "Phytoplankton in the ocean use non-phosphorus lipids in response to phosphorus scarcity." *Nature* 458(7234): 69-72.



- Van Mooy, B. A., Rocap, G., Fredricks, H. F., Evans, C. T. and Devol, A. H. (2006). "Sulfolipids dramatically decrease phosphorus demand by picocyanobacteria in oligotrophic marine environments." *Proceedings of the National Academy of Sciences of the United States of America* 103(23): 8607-8612.
- Van Wagenen, J., Miller, T. W., Hobbs, S., Hook, P., Crowe, B. and Huesemann, M. (2012). "Effects of light and temperature on fatty acid production in *Nannochloropsis Salina*." *Energies* 5(12): 731-740.
- Van Wegen, R. J., Lee, S. Y. and Middelberg, A. P. (2001). "Metabolic and kinetic analysis of poly(3-hydroxybutyrate) production by recombinant *Escherichia coli*." *Biotechnology and Bioengineering* 74(1): 70-80.
- Vincent, F. W. (2009). Planktonic and attached: Cyanobacteria. *Plankton of inland waters*. Canada, Laval University.
- Vothknecht, U. C. and Westhoff, P. (2001). "Biogenesis and origin of thylakoid membranes." *Biochimica et Biophysica Acta (BBA) - Molecular Cell Research* 1541(1-2): 91-101.
- Wada, H. and Murata, N. (1990). "Temperature-induced changes in the fatty acid composition of the cyanobacterium, *Synechocystis* PCC 6803." *Plant Biology* 92: 1062-1069.
- Wang, W., Liu, X. and Lu, X. (2013). "Engineering cyanobacteria to improve photosynthetic production of alka(e)nes." *Biotechnology for Biofuels* 6: 69.
- Wang, Z. T., Ullrich, N., Joo, S., Waffenschmidt, S. and Goodenough, U. (2009). "Algal lipid bodies: stress induction, purification, and biochemical characterization in wild-type and starchless *Chlamydomonas reinhardtii*." *Eukaryotic Cell* 8(12): 1856-1868.

- Weier, D., Müller, C., Gaspers, C. and Frentzen, M. (2005). "Characterisation of acyltransferases from *Synechocystis* sp. PCC 6803." *Biochemical and Biophysical Research Communications* 334(4): 1127-1134.
- Yang, Z., Kong, F., Shi, X., Yu, Y. and Zhang, M. (2013). "UV-B radiation and phosphorus limitation interact to affect the growth, pigment content, and photosynthesis of the toxic cyanobacterium *Microcystis aeruginosa*." *Journal of Applied Phycology* 26(4): 1669-1674.
- Yu, Y., You, L., Liu, D., Hollinshead, W., Tang, Y. J. and Zhang, F. (2013). "Development of *Synechocystis* sp. PCC 6803 as a phototrophic cell factory." *Marine Drugs* 11(8): 2894-2916.
- Zhang, Y. M. and Rock, C. O. (2008). "Membrane lipid homeostasis in bacteria." *Nature Reviews Microbiology* 6: 222-233.

**APPENDICE**



จุฬาลงกรณ์มหาวิทยาลัย  
CHULALONGKORN UNIVERSITY

## APPENDIX A

Normal medium (BG<sub>11</sub>), volume 1 Liter (Rippka *et al.*, 1979)

Standard BG<sub>11</sub> medium

Chemical compounds	Stock (1L)	Liquid medium	Solid medium
CaCl <sub>2</sub> .2H <sub>2</sub> O	36 g	1 ml	1 ml
Citric acid	6 g	1 ml	1 ml
EDTA	1 g	1 ml	1 ml
Ferric ammonium citrate	6 g	1 ml	1 ml
K <sub>2</sub> HPO <sub>4</sub>	30 g	1 ml	1 ml
MgSO <sub>4</sub> .7H <sub>2</sub> O	75 g	1 ml	1 ml
NaCO <sub>3</sub>	20 g	1 ml	1 ml
NaNO <sub>3</sub>	150 g	10 ml	10 ml
1000x Trace element*		1 ml	1 ml
1M HEPES-NaOH	238.3 g	10 ml	10 ml
30% Na <sub>2</sub> S <sub>2</sub> O.5H <sub>2</sub> O	300 g	-	10 ml
Distilled water	-	To 1000 ml	To 1000 ml
Agar	-	-	15 g

\*1000x trace element (1000 mL)

H <sub>3</sub> BO <sub>3</sub>	2.86 g	Na <sub>2</sub> MoO <sub>4</sub> .2H <sub>2</sub> O	0.390 g
MnCl <sub>2</sub> .4H <sub>2</sub> O	1.81 g	CuSO <sub>4</sub> .5H <sub>2</sub> O	0.080 g
ZnSO <sub>4</sub> .7H <sub>2</sub> O	0.221 g	Co (NO <sub>3</sub> ) <sub>2</sub> .6H <sub>2</sub> O	0.049 g

### **Nutrient modifications**

Nitrogen modification from normal medium (BG<sub>11</sub>)

- Without NaNO<sub>3</sub> from BG<sub>11</sub> medium
- Ferric ammonium citrate was replaced by FeSO<sub>4</sub> 6 g/liter

Phosphorus modification from normal medium (BG<sub>11</sub>)

- Without K<sub>2</sub>HPO<sub>4</sub> from BG<sub>11</sub> medium

Nitrogen and phosphorus modification from normal medium (BG<sub>11</sub>)

- Without NaNO<sub>3</sub> and K<sub>2</sub>HPO<sub>4</sub> from BG<sub>11</sub> medium

### **Acetate addition**

20 mM acetate addition

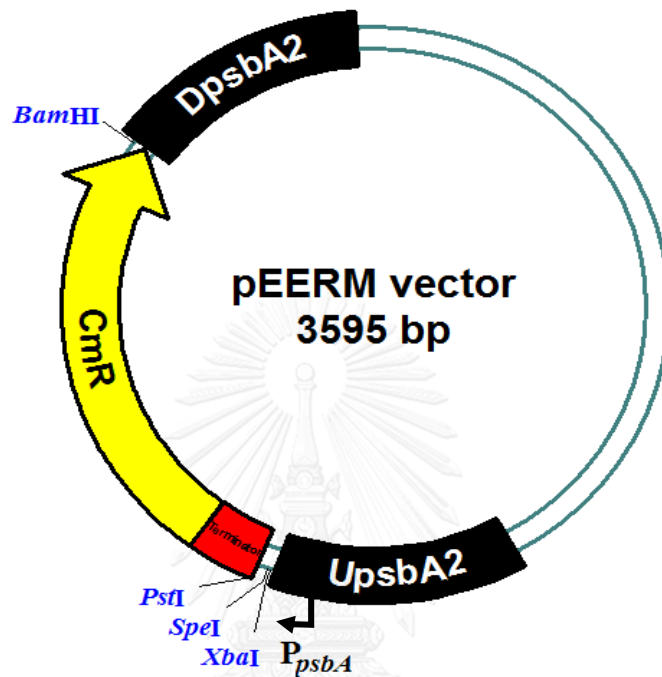
- Added potassium acetate 1.96 g/L into normal BG<sub>11</sub> medium

40 mM acetate addition

- Added potassium acetate 3.92 g/L into normal BG<sub>11</sub> medium

## APPENDIX B

pEERM vector



pEERM vector was used for overexpression gene in *Synechocystis* PCC 6803 which created for using integration into *Synechocystis* genome at *psbA2* gene encodes D1 protein which involves in photosystem II (PSII). The physical map of pEERM vector containing strong promoter (*P<sub>psbA</sub>*), selective chloramphenicol antibiotic resistance cassette gene and multiple cloning sites of *Xba*I, *Spe*I and *Pst*I. The size of pEERM vector is 3,595 bp.

**APPENDIX C**

## LB Medium (1 liter)

Chemical compounds	Liquid medium	Solid medium
Bacto tryptone	10 g	10 g
Yeast extract	5 g	5 g
NaCl	10 g	10 g
Agar	-	15 g

Adjusted distilled water to a total volume of 1 liter. The medium was sterilized by autoclaving at 121 °C for 15 minutes.

**APPENDIX D****TAE buffer**

Working solution

1 X 0.04 M Tris-acetate

0.01 M EDTA

Concentrated stock solution (1 liter)

50: 242 g Tris base

57.1 mL glacial acetic acid

100 mL 0.5 M EDTA (pH 8.0)



## APPENDIX E

### Preparation of agarose gel electrophoresis and quantification

1. 0.5 TAE electrophoresis buffer (100 mL) was prepared.
2. 1.5 g of agarose powder was added into the TAE buffer.
3. The mixture was dissolved by microwave.
4. The comb was placed in a suitable position of the tray.
5. Agarose gel solution was poured onto tray and left it for completely set then, the comb was carefully removed.
6. The gel was placed into electrophoresis tank.
7. 6x of loading dye was added into each sample before loaded into the slot well.
8. The lid of gel tank was closed and the electrical status was adjusted to 400 volts.
9. The electric current was turned off and the gel was taken to the bowl for stained with ethidium bromide (a stock solution of 1 mg/mL adjusting final concentration to 0.5 $\mu$ g/mL) and later destained with water for 10 min.
10. The stained gel was placed into UV-light machine to quantify their bands.

**APPENDIX F**

## Sudan black B solution

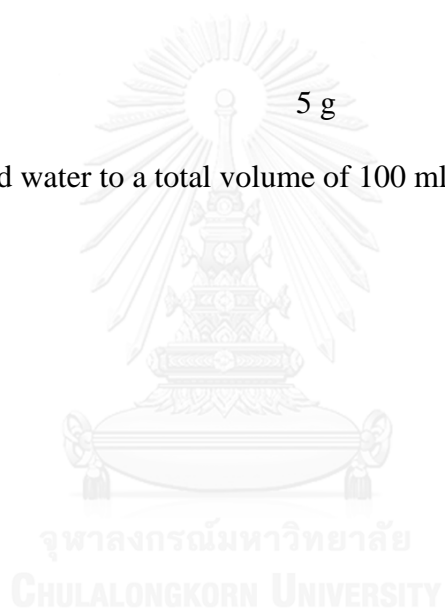
Sudan black B 3 g

Added 70 % ethanol to a total volume of 100 ml

## -Safranin O solution

Safranin O 5 g

Added distilled water to a total volume of 100 ml



**APPENDIX G**

## Vanillin-phosphoric acid reagent

Vanillin 100 ml

Vanillin 2 mg

Added distilled water to a total volume of 100 ml

17% phosphoric acid 100 ml

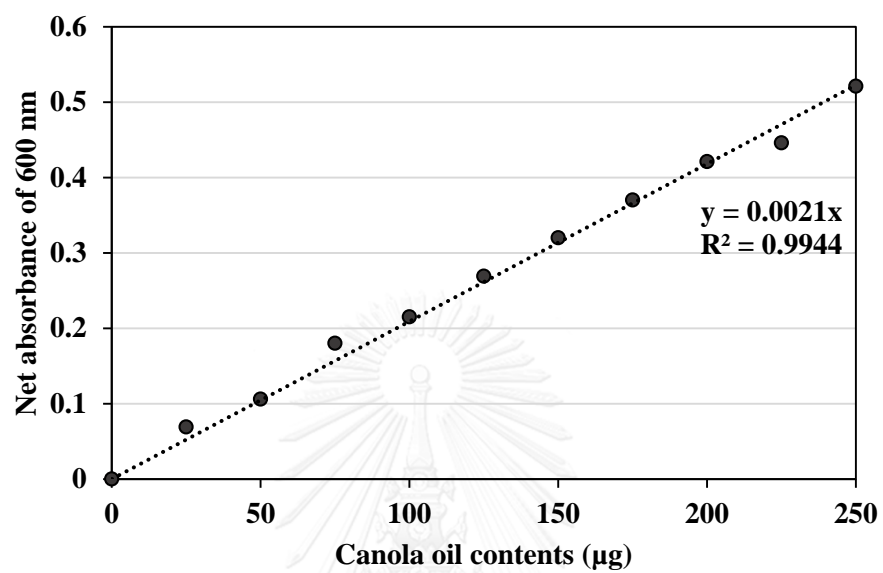
Phosphoric acid 17 ml

Added distilled water to a total volume of 100 ml

The mixture volume added 0.2 mg vanillin per ml 17 % phosphoric acid

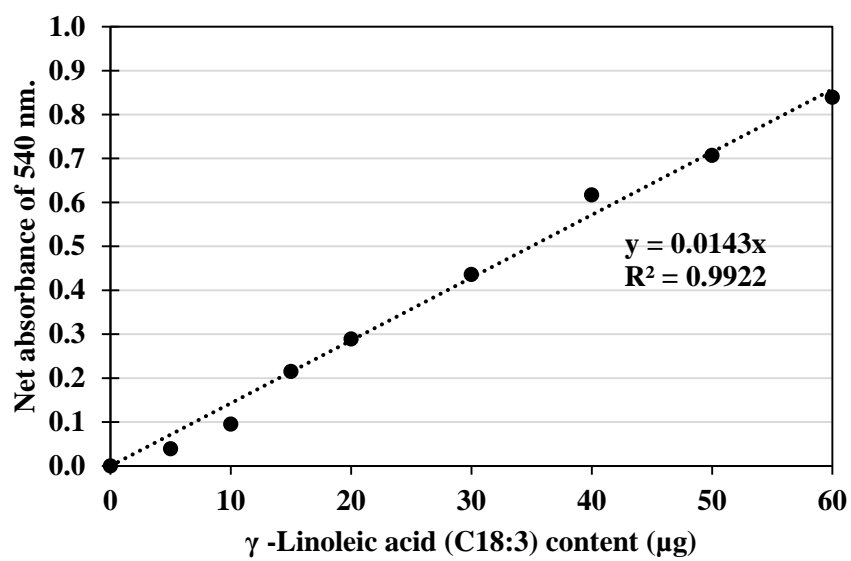
## APPENDIX H

Standard curve for total lipid content used canola oil as commercial standard



## APPENDIX I

Standard curve for total unsaturated lipid content used  $\gamma$ -Linoleic acid (C18:3)  
as commercial standard



## VITA

Miss Kamonchanock Eungrasamee was born on January 28, 1991 in Bangkok, Thailand. She has been a scholarship student, Development and Promotion of Science and Technology Talents Project (DPST), Royal Thai Government scholarship since 2009. She graduated a Bachelor of Science degree in Chemistry with second class honors, Faculty of Science from Silpakorn University, Thailand in 2012. She had started to study the Master of Science degree in Biochemistry, Faculty of Science from Chulalongkorn University since 2013. During studying for her Master's degree, she joined the research group at Ångström Laboratories, Department of Chemistry, Uppsala University, Sweden, and did her research for almost 6 months (10 May to 31 Oct 2015) supported by her scholarship's foundation.

### Proceeding:

Kamonchanock Eungrasamee, Peter Linblad, Aran Incharoensakdi and Saowarath Jantaro (2015). Total lipid and unsaturated lipid contents in cyanobacterium *Synechocystis* sp. PCC 6803 with overexpressing Aas gene. The 27th Annual Meeting of the Thai Society for Biotechnology and International Conference (TSB 2015), 17-20 November 2015, Mandarin Hotel Bangkok by Centre Point, Bangkok, Thailand.